Single Digital-Photo Correction for a GIS Application

and Error Analysis

by

Limei Ran

Thesis submitted to the Faculty of the

Virginia Polytechnic Institute and State University

in partial fulfillment of the requirements for the degree of

Master of Science

in

Geography

APPROVED:

Laurence W. Carstensen, Chairman

Paul V. Bolstad

James B. Campbell

July, 1992

Blacksburg, Virginia

Single Digital-Photo Correction for a GIS Application

and Error Analysis

by

Limei Ran

Laurence W. Carstensen, Chairman

Geography

(ABSTRACT)

Single digital-photo correction using the collinearity condition equations for a GIS application was investigated by control and test data from digital photos and USGS 1:24,000 topographic maps and by USGS 7.5-minute DEMs of two study areas, Prentiss, North Carolina and Blacksburg, Virginia. The collinearity equations were used to remove geometric errors caused by image tilt and relief displacement. In addition to the study of geometric error in uncorrected and corrected digital photos, the impact of error in ground control points and error in DEM data on the accuracy of rectification was analyzed in terms of errors in point position, line length, and polygon area. Computer programs for single digital-photo correction using the collinearity equations and for impact analysis of errors in ground control and DEM data were developed.

Point errors in uncorrected photos were tested by the affine transformation from UTM to photo coordinates by control points. Estimated error for the Prentiss photo was 14.599 meters and that for the Blacksburg photo was 11.252 meters. Due the poor distribution of control and test points, estimated errors in uncorrected photos were underestimated. Estimated error for the corrected photo of the Prentiss area was 11.397 meters and that for the Blacksburg area was 7.071 meters. Geometric errors in corrected digital photos were clearly not significantly greater than 12.192 meters. Error removed for the Blacksburg photo was significantly greater than zero and that for the Prentiss photo was not significantly greater than zero. Estimated removed errors were also underestimated.

Errors in point position, line length, and polygon area of corrected digital photos were positively related to error in ground control points for photo orientation and error in DEM data for registration. The accuracy of ground control points has greater impact on point position and polygon area, and the accuracy of DEM data has greater impact on line length. The point position error, line length change, and polygon area change caused by random error within ± 15 meters in ground control points were within 4 meters, 0.12% and 0.3% and those caused by random error within ± 10 meters in DEM data of test features were within 2 meters, 0.11% and 0.0065%. It is both practical and accurate to use ground control points obtained from USGS 7.5-minute topographic maps and USGS 7.5-minute DEMs for single digital-photo correction by the collinearity equations for most GIS applications with spatial data layers obtained from USGS 1:24,000 topographic maps or smaller-scale maps for areas such as those studied here.

Acknowledgements

I would like to thank Dr. Laurence W. Carstensen and Dr. James B. Campbell for their advice, recommendations, and assistance. I wish to thank Dr. Paul V. Bolstad for his advice and comments, for supplying the photos, maps and DEM data which are basic data sources for this study, and for aiding me with the use of ERDAS software.

Special appreciation goes to my husband, Mr. Huiqi Li and my parents and sisters, whose spiritual support were invaluable through my graduate study.

Table of Contents

INTRODUCTION **1**

1.1 Background 1

1.2 Objective 6

LITERATURE REVIEW OF SINGLE DIGITAL-PHOTO RESECTION **8**

2.1 Introduction 8

2.2 Errors in Digital Photographic Coordinates 10

2.3 Single-Photo Resection and Correction 17

2.4 Accuracy Assessment 25

METHODOLOGY **27**

3.1 Hypotheses and Assumptions 27

3.2 Study Areas and Data Sources 28

3.3 Methodology 31

3.3.1 Obtaining Control and Test Data 31

3.3.2 Testing Errors in Uncorrected Photos 33

3.3.3 Single Digital Photo Resection and Correction 34

3.3.4 Testing Errors in Corrected Photos 37
3.3.5 The Impact of Ground Control and the DEM on the Correction 38

RESULTS **43**
4.1 Control and Test Data 43
4.2 Errors in Uncorrected Photos 50
4.3 Space Resection and Errors in Corrected Photos 57
4.4 Degree of Error Caused by Errors in Ground Control and DEM data 66

CONCLUSIONS AND RECOMMENDATIONS **82**
5.1 Conclusions 82
5.2 Recommendations for Further Study 84
5.3 Recommendations for Applications of the Study 86

BIBLIOGRAPHY **87**

ADDITIONAL DATA TABLES AND FIGURES **90**

SOURCE CODE FOR SINGLE DIGITAL PHOTO CORRECTION USING THE COLLINEARITY EQUATIONS **108**

Vita **139**

List of Illustrations

Figure 2.1. Principal Point and Fiducial Center 12

Figure 2.2. Relief Displacement 13

Figure 2.3. Photo Rotation ω, ϕ and κ 14

Figure 2.4. Collinearity Condition 15

Figure 3.1. Flow Chart for Single Digital-Photo Resection and Correction 36

Figure 3.2. Flow Chart for the Impact of Ground Control and DEM on the Correction . . . 40

Figure 4.1. Plotting Point Distance Offsets versus Errors in Ground Control Points and Point Elevation, Prentiss, N.C. 68

Figure 4.2. Plotting Point Distance Offsets versus Errors in Ground Control Points and Point Elevation, Blacksburg, Va. 70

Figure 4.3. Plotting Line Length Change Percentages versus Errors in Ground Control Points and Line Elevations, Prentiss, N.C. 73

Figure 4.4. Plotting Line Length Change Percentages versus Errors in Ground Control Points and Line Elevations, Blacksburg, Va. 75

Figure 4.5. Plotting Polygon Area Change Percentages versus Errors in Ground Control Points and Polygon Elevations, Prentiss, N.C. 78

Figure 4.6. Plotting Polygon Area Change Percentages versus Errors in Ground Control Points and Polygon Elevations, Blacksburg, Va. 80

Figure A.1. Control Point Distribution, Prentiss, N.C. 95

Figure A.2. Test Point Distribution, Prentiss, N.C. 96

Figure A.3. Control Point Distribution, Blacksburg, Va. 97

Figure A.4. Test Point Distribution, Blacksburg, Va. 98

Figure A.5. Vector Errors of Computed Test Points by Affine Transformation, Prentiss, N.C. 99

Figure A.6. Vector Errors of Computed Test Points by Affine Transformation, Blacksburg, Va. 100

Figure A.7. Vector Errors of Computed Test Points by the Collinearity Equations, Prentiss, N.C. 101

Figure A.8. Vector Errors of Computed Test Points by the Collinearity Equations, Blacksburg, Va. 102

List of Tables

Table 4.1. Affine Transformation of Eight Tic Points from Digitizer Table to UTM Coordinates, Prentiss, N.C. 45

Table 4.2. Residuals of the Affine Transformation of Eight Tic Points from Digitizer Table to UTM coordinates, Prentiss, N.C. 46

Table 4.3. Affine Transformation of Eight Tic Points from Digitizer Table to UTM Coordinates, Blacksburg, Va. 47

Table 4.4. Residuals of the Affine Transformation of Eight Tic Points from Digitizer Table to UTM coordinates, Blacksburg, Va. 48

Table 4.5. Affine Transformation of Control Points from UTM to Scaled Photo Coordinates, Prentiss, N.C. 52

Table 4.6. Affine Transformation Residuals of Control and Test Points from UTM to Scaled Photo Coordinates, Prentiss, N.C. 53

Table 4.7. Affine Transformation of Control Points from UTM to Scaled Photo Coordinates, Blacksburg, Va. 54

Table 4.8. Affine Transformation Residuals of Control and Test Points from UTM to Scaled Photo Coordinates, Blacksburg, Va. 55

Table 4.9. Relief Displacement Estimation 58

Table 4.10. Space Resection 60

Table 4.11. Space Resection Residuals of Control and Test Points from UTM to Scaled Photo Coordinates, Prentiss, N.C. 61

Table 4.12. Space Resection Residuals of Control and Test Points from UTM to Scaled Photo Coordinates, Blacksburg, Va. 63

Table 4.13. Errors Removed Using the Collinearity Condition Equations 64

Table 4.14. Linear Regression Analyses of Point Distance Offsets, Prentiss, N.C. 69

Table 4.15. Linear Regression Analyses of Point Distance Offsets, Blacksburg, Va. 71

Table 4.16. Linear Regression Analyses of Line Length Change Percentages, Prentiss, N.C. . 74

Table 4.17. Linear Regression Analyses of Line Length Change Percentages, Blacksburg, Va. 76

Table 4.18. Linear Regression Analyses of Polygon Area Change Percentages, Prentiss, N.C. 79

Table 4.19. Linear Regression Analyses of Polygon Area Change Percentages, Blacksburg, Va. 81

Table A.1. Control Points, Prentiss, N.C. 91

Table A.2. Test Points, Prentiss, N.C. 92

Table A.3. Control Points, Blacksburg, Va. 93

Table A.4. Test Points, Blacksburg, Va. 94

Table A.5. Test Line and Polygon 103

Table A.6. Point, Line and Polygon Errors Caused by Errors in Ground Control Points and DEM Data, Prentiss, N.C. 104

Table A.7. Point, Line and Polygon Errors Caused by Errors in Ground Control Points and DEM Data, Blacksburg, Va. 106

Chapter 1

INTRODUCTION

1.1 Background

An emerging trend in geographic information system applications is the use of multiple systems and diverse data sets in a single study (Piwowar et al., 1990). In GIS applications, geographic data can come from different data sources. In addition to maps, the major data sources are remotely sensed data, such as aerial photographs and satellite images in pictorial and digital forms. Recent work has emphasized the integration of remotely sensed data from image analysis systems (IAS) with other digital spatial data from geographic information systems (GIS). The integration facilitates image classification, change detection, visual spatial data acquisition, spatial data analysis and decision making in regional planning and environmental analysis (Brouwer et al., 1990). The integration of these technologies will inevitably lead to a synergistic approach to spatial data handling in environmental analyses (Ehlers et al., 1989). To date research on IAS/GIS integration has been in three areas: generating thematic data in GIS from image data, increasing the "realism" of

cartographic representation (e.g., visualization), and using GIS data as auxiliary knowledge to improve image analysis (Ehlers et al., 1989).

Until recently, research has focused on the integration of satellite image data with GIS data, mainly due to availability of high resolution satellite data in digital format, such as SPOT's High Resolution Visible (HRV) sensor and Landsat's Thematic Mapper (TM), large aerial coverage and increased capabilities of computers. However, the integration of digital aerial photographs with GIS data to provide thematic data is becoming popular, particularly when spatial data analysis is needed for a small area because aerial photography is one of the most valued sources in providing spatial data for small areas and has some advantages compared with satellite images (Hudson, 1991). For three kinds of information: content, position, and elevation, some satellite data, such as that from SPOT, can provide positional and elevation information with sufficient accuracy (Naithani, 1990). But, the content aspect of a present-day satellite image, including SPOT, is insufficient for many analyses. Many cultural features such as buildings, roads, railroads and detailed land information can not be obtained from present-day electro-optical sensors due to insufficient ground resolution. Those detailed features must be extracted from other source materials. Aerial photography has the highest potential for this extraction because of high resolution. Moreover, aerial photography can be flown at desired scale and time to suit special requirements and provide most up-to-date information (Naithani, 1990). Obviously, photogrammetry has great promise in GIS applications for small areas by providing more sufficient and current spatial information.

With the rapid development of science and technology, photogrammetry has passed through both conventional and modern phases in this century. Conventional photogrammetry is characterized by using analog instruments to correct photos geometrically and extract information. While conventional photogrammetry has been used in different fields for a long time; modern photogrammetry is moving towards fully analytical techniques and digital image processing. It is especially applicable to resource management, environmental analysis, and spatial data analysis systems such as GIS. With the aid of computers, micro-electronics, and powerful software, more accurate and precise measurements can be made on the photographs by using analytical plotters

or digital image processing methods (Brouwer 1990, Hudson 1991, Warner 1990, and Torlegard 1988). Moreover, the introduction of the personal computer to modern photogrammetry makes aerial photo orientation and data computation more accessible, efficient, and economical, especially for spatial analysis of a small area. Therefore, aerial photographs become an even more important and accurate data source in spatial data systems.

Digital photogrammetry is based on images stored pixel-wise as greyvalues in a computer memory, as opposed to previous forms of photogrammetry in which photographs or other physical images were placed in photogrammetric instruments for observations (Torlegard, 1988). The processing and storage methods of the digital aerial photograph are similar to methods used for satellite images. Digital photogrammetric systems must be compatible with satellite image processing. Therefore, photogrammetric developments have broad implication for integration of remote sensing and GIS. Integration of digital photogrammetric systems and GIS will greatly benefit natural resource management, environmental analysis, and local and global resource monitoring.

Research and applications such as digital photo correction, three-dimensional visualization, image processing and user interfaces (Ehlers et al 1989) have been completed separately in moving toward a fully digital photogrammetric system. In different functions of digital photogrammetry, digital photo correction is critically important. Because it is the first phase in digital processing, its accuracy affects the following processes in spatial data analysis systems, such as IAS/GIS. Final analytical results are significantly influenced by cumulative effects of errors with the confidence in decisions based on erroneous results greatly decreased.

Geometric correction of a digital photo involves a mathematical model. The mathematical model comprises two parts, functional and statistical, which complement each other. The better the correction model describes the image geometry, the smaller the statistical errors will be. Typical ground control, which makes use of relationships between object space (the ground) and image space, is needed in the mathematical model.

Many methods in modern photogrammetry are based on geometry of photographs extended with parameters for film shrinkage, lens distortion and atmospheric refraction, such as collinearity and coplanarity conditions. Single photo resection is based on the collinearity condition. Therefore, mathematical models are more accurate than analog instruments and could be developed to a higher degree of fidelity to reality, i.e. with less approximation. In analytical photogrammetry, corrected single photo coordinates are measured in mono- and stereocomparators based on six orientation elements calculated from the collinearity equations. In digital photogrammetry, single photos are stored in computers in digital form obtained by scanning photos or digital recorders in sensor platforms. They can then be corrected in computers based on projection geometries. New computer hardware development moves photogrammetry toward fully automatic digital aerial photo processing. The current situation clearly indicates that we are at an early stage of development of fully digital photogrammetric systems.

In cartographic study, image tilt and relief displacement are generally considered major error sources. The degree of relief displacement presented in images depends on sensor platform height and relief conditions in image area. The lower the platform and the greater the relief, the higher the relief displacement will be. For satellite images, due to very high platforms, relief displacement may not be specifically considered in the correction function. That is the reason many satellite image corrections employ polynomial functions which correct images well when terrains are uniform or smooth. But for aerial digital photos, the same polynomial correction may not satisfy positional accuracy requirements due to high relief displacement. To achieve such accuracy, it is necessary to correct image data for relief displacement by using the collinearity equations which incorporate a digital elevation model (DEM) for photo correction (Ehlers et al 1989 and Trotter 1991). Relief displacement is important not only in digital aerial photo correction but also in some low-satellite image correction (Koency 1979), when a DEM is available. Unfortunately, sufficiently accurate DEMs rarely exist, primarily because of their high cost of production (Trotter 1991). Therefore, the DEM requirement considerably limits image data's automated incorporation into GIS, as positional accuracy is of critical importance to many users of GIS (Marble and Peuquet 1983). As

digital elevation data become increasingly available, routine correction of image data prior to thematic data extraction becomes feasible.

The first step in single digital photo correction using the collinearity equations is to compute the six elements of exterior orientation. This is done using control points from the photo and ground to solve linearized collinearity equations. The six elements establish the position of the sensor (camera) station in space at the time the photograph was taken. Then a rotation matrix is computed from the three angular exterior elements about the ground X, Y and Z axes to remove the effects of tip, tilt, and swing of the aircraft on the photo geometry. This leaves radial displacement due to differences in elevation as the remaining source of error in the planimetry. Correct image positions for ground features of interest are obtained by the collinearity equations using ground X, Y and Z coordinates, the rotation matrix, and the other three exterior elements (sensor's X, Y and Z coordinates in the ground coordinate system) (DeMars 1988). Obviously, the collinearity equations must incorporate DEM data for the X, Y and Z of the ground point to correct images geometrically. In comparison with polynomial models, the collinearity function is much more accurate. It is a real-time single image correction method which can be used not only in aerial photo correction but also in satellite image correction. Therefore, using the function to correct digital aerial photos to get accurate spatial data is practical, efficient, and economical for spatial data analysis in a small area when a suitable DEM is available.

Corrected digital photos can be digitized on a computer screen or automatically classified to obtain thematic layers used in a GIS. A prime function of GIS is to provide the means whereby information from a number of themes can be merged to provide an appropriate product in response to a particular user-specified enquiry (Trotter 1991). So there is often a registration problem in relating various thematic layers in analysis, i.e. coincident points on the overlays may not correspond to the same point on the ground. Location accuracy of rectified remotely sensed data or extracted thematic data layers can be no better than the data upon which the rectification is based (DeMars 1988). Errors in control points and the DEM decrease the accuracy of rectification. Therefore, before the spatial data from the digital aerial photo is used in analysis, its accuracy must be evalu-

ated if the spatial data are to be utilized in spatial data analysis with GIS data as a decision basis for resource management and environmental analysis.

1.2 Objective

Some research on the correction of single digital aerial photograph has been done in recent years (Gagnon et al 1990, Hood et al 1989, Helava 1987, DeMars 1988, and Veress and Youcai 1987). But previous work has not been directed toward GIS applications. Although the work has given some estimations about the accuracy of correction such as standard error of the correction model and vector error of test points, it has not given more detailed error analysis. Because the error level existing in the uncorrected photo varies, error being removed by employing the collinearity function must be estimated to understand the reliability and effectiveness of the function. Moreover, because errors in control points and the DEM are random, we can control it only in a certain range, not eliminate it. Errors always exist in control points and the DEM. Accuracy of the correction model is influenced by the accuracy of both control points and the DEM because the collinearity equations use control points to compute the six orientation elements and use the DEM to compute image positions of ground points. It is very important to estimate the error level remaining in the corrected photo, which is caused by errors in control points and DEM data. By analyzing relationships among errors remaining in the corrected photo, errors in control points, and errors in the DEM, accuracy and reliability of the corrected photo may be estimated from the accuracy of control points and the DEM. Based on the accuracy required from the photo, the accuracy requirement for control points and the DEM may also be estimated. This error analysis has significance for error control in control points and DEMs when spatial data in corrected photos are to be used with varied spatial data which have different accuracies.

The purpose of the thesis is to study the use of the collinearity equations for image rectification and thematic data extraction used in a GIS application with spatial data from USGS 1:24,000 or smaller scale maps, to assess errors removed and remaining by the correction, and to analyze the impact of errors in ground control and the DEM on rectification. There are five objectives for the study:

1. To document error in an uncorrected digital aerial photo,

2. to correct a digital photo to a planimetric map coordinate system by using the collinearity equations,

3. to estimate the accuracy of the corrected digital aerial photo,

4. to estimate error removed by the correction, and

5. to assess the degree of error caused by error in ground control points and error in DEM data and the impact of their errors on the accuracy of rectification.

Chapter 2

LITERATURE REVIEW OF SINGLE DIGITAL-PHOTO RESECTION

2.1 Introduction

In recent years, GIS has been used in varied fields for spatial data analysis, often for detailed environmental studies of small areas. The data sources for the GIS are diverse. There are two major sources of geographical data; topographical maps, such as USGS quad-maps, and remotely sensed data. In using a digital aerial photo, geometric correction and error analysis are the first important steps. The accuracy of the correction can limit the use of the spatial data extracted from the digital photo and influence the results of analysis. The need for these analyses was apparent from a study by Paul V. Bolstad in the School of Forestry and Wildlife Resources at Virginia Tech, involving analysis of the cumulative effects of landscape features on water quality across a stream order gradient. Geographic data developed from a combination of maps, aerial photographs and field surveys, and organized in a geographic information system (PC ARC/INFO software) required

accuracy assessment. The thematic data include catchment boundaries, landcover, landuse, terrain, road location and surface properties, structure location, soil properties, and stream positions and characteristics. The landuse/landcover layer will come from a digital aerial photo of the watershed. Therefore, the integration method and accuracy of the photo interpreted data are crucial for the evaluation of water quality. Accurate registration from the image to map coordinate systems is essential for the accuracy of the land information layer and will affect the accuracy of the final analytical result. The study of digital aerial photo correction and error analysis can help the integration of the data from other sources with the data extracted from the photo.

Photo correction is a procedure to correct errors in x and y coordinates of photo points. Errors in the photo come from different sources. Generally, only the errors caused by image tilt and relief displacement are considered major in aerial photo correction for mapping. When systematic errors are corrected, it is also called photo rectification in photogrammetry. Rectification is a process by which a tilted or oblique photograph is transformed into an equivalent vertical and unique-scale photograph taken from the same exposure station (Moffitt and Mikhail, 1980). Paper photos may be rectified either graphically or instrumentally. But digital aerial photos can be corrected geometrically by space resection. Space resection, which has been popularly used in analytical and digital photogrammetry, is the process by which the spatial position and orientation of a photograph is determined based on at least three control points in both image and on the ground (Moffitt and Mikhail, 1980). In space resection, the three-dimensional coordinates X_L, Y_L and Z_L of the exposure station in the ground coordinate system are computed in addition to the angular space orientation expressed by the orientation angles ω, ϕ, and κ (Figure 2.3). Using the six orientation elements and based on the collinearity condition of the exposure, the photo point, and the corresponding ground point, the collinearity equations can be established. The digital aerial photo can be rectified by using the equations point by point after the process of space resection. When necessary, film, atmosphere, and principal point errors may also be corrected by incorporating additional parameters in the equations or using continuous functions. In space resection, the accuracy of orientation computation is controlled by the accuracy of control points. In digital photograph

rectification, the accuracy of correction is determined by the accuracy of the DEM as well as the accuracy of the six orientation elements. Therefore, error analyses of the rectified photo, control points and DEM are crucial and significant for both digital photo correction and the uses of the spatial data from the corrected photo.

2.2 Errors in Digital Photographic Coordinates

An ideal aerial photograph is one which has been taken with a perfectly adjusted camera containing a distortion-free lens with the dimensionally-stable negative held flat in the focal plane, and in which the object space is a complete vacuum defined by three-dimensional cartesian coordinates (Moffitt and Mikhail, 1980). Moreover, photo coordinates are obtained by an error-free method. Since this ideal can never be realized, errors existing in the digital photo must be accounted for and corrected for further applications. Errors, which may be systematic or random, are discussed briefly as follows:

1. **Film and Platen Deformation.** If obtained directly from digital recorders in the sensor platform, the deformation does not exist in the digital photo. However, unlike satellite images, most aerial digital photos are obtained by scanning film photos. In this situation, the digital photo includes film and platen deformation, a function of the material, environment (such as temperature), aging and treatment (such as chemical processing). The effect may sometimes be complicated and troublesome since the deformation may be uniform, differential or irregular. This effect can be compensated by using correction equations (Ghosh, 1988) when high accuracy photo coordinates are required.

2. **Lens Distortions.** All lenses used today have measurable distortions and optical aberrations. Lens distortion can not only cause displacement of the image but also degrade the quality or

the sharpness, effects unfavorable to precise measurements. The camera calibration procedure determines the focal-length, the location of the principal point, and all distortion parameters. Therefore, lens distortions can be corrected by using a continuous function (details in Ghosh, 1988).

3. **Atmospheric Refraction**. On its path from the ground to the camera, a light ray passes through air with changing density, pressure, and temperature, causing a continuous bending of the ray due to refraction. Refraction is a function of the refractive index of the air at all the points along the ray path. The refractive index depends on temperature, pressure, and composition of the atmosphere (Ghosh, 1988). However it is almost impossible to determine all refractive indices along the ray path. So this type of distortion is generally rectified corresponding to the angular deviation of the ray path.

4. **Measurement Errors**. Measurement errors are related to the measuring instrument, such as photo scanners and comparators. They have no relation to systematic errors of the photograph. Each measuring instrument needs to be calibrated in order to minimize errors in the digital photo coordinates caused by it. Generally, this kind of error is not corrected due to the high accuracy of measuring instruments at present.

5. **Principal Point Displacement**. In photogrammetry, the principal point is the intersection of the perpendicular line from the interior perspective center to the plane of the photograph (Figure 2.1). Most of the analytical procedures, such as the collinearity equations, require photo coordinates with the principal point as the origin. Usually, the principal point can not be measured directly because it is not on the photograph. Therefore, photographic coordinates must be established in a system of reference, which is provided by the fiducial center. The coordinates of the principal point are derived from those of the fiducial center through using camera calibration data. The fiducial center and the principal point are usually considered to be identical in practice due to the small distance between the two points. This consideration can cause some systematic errors in the digital photo coordinates.

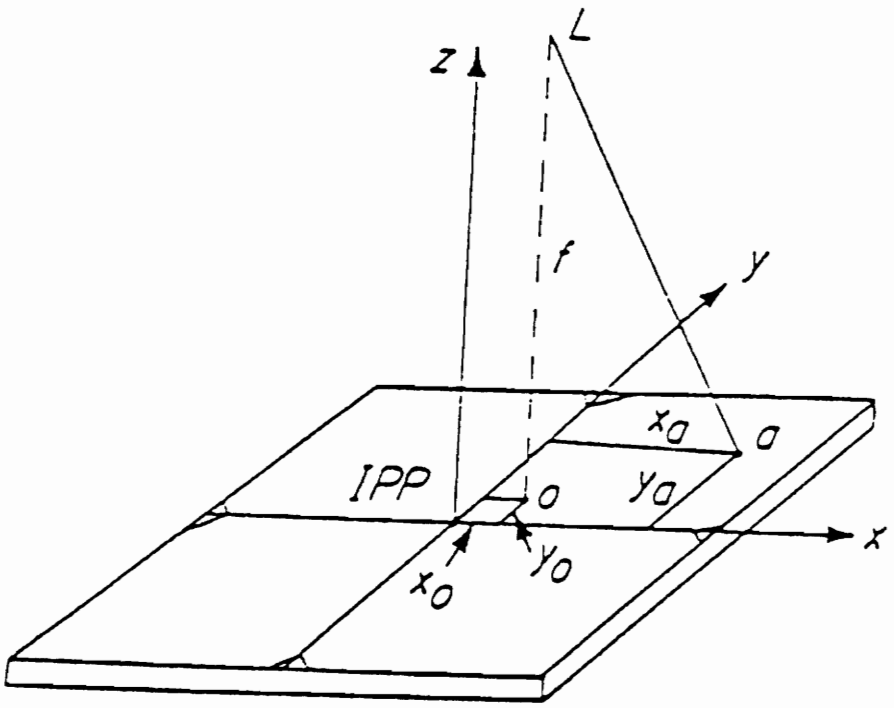

Figure 2.1. Principal Point and Fiducial Center: "L" is the interior perspective center; "O" is the principal point; and "a" is a image point (adapted from Moffitt and Mikhail, 1980).

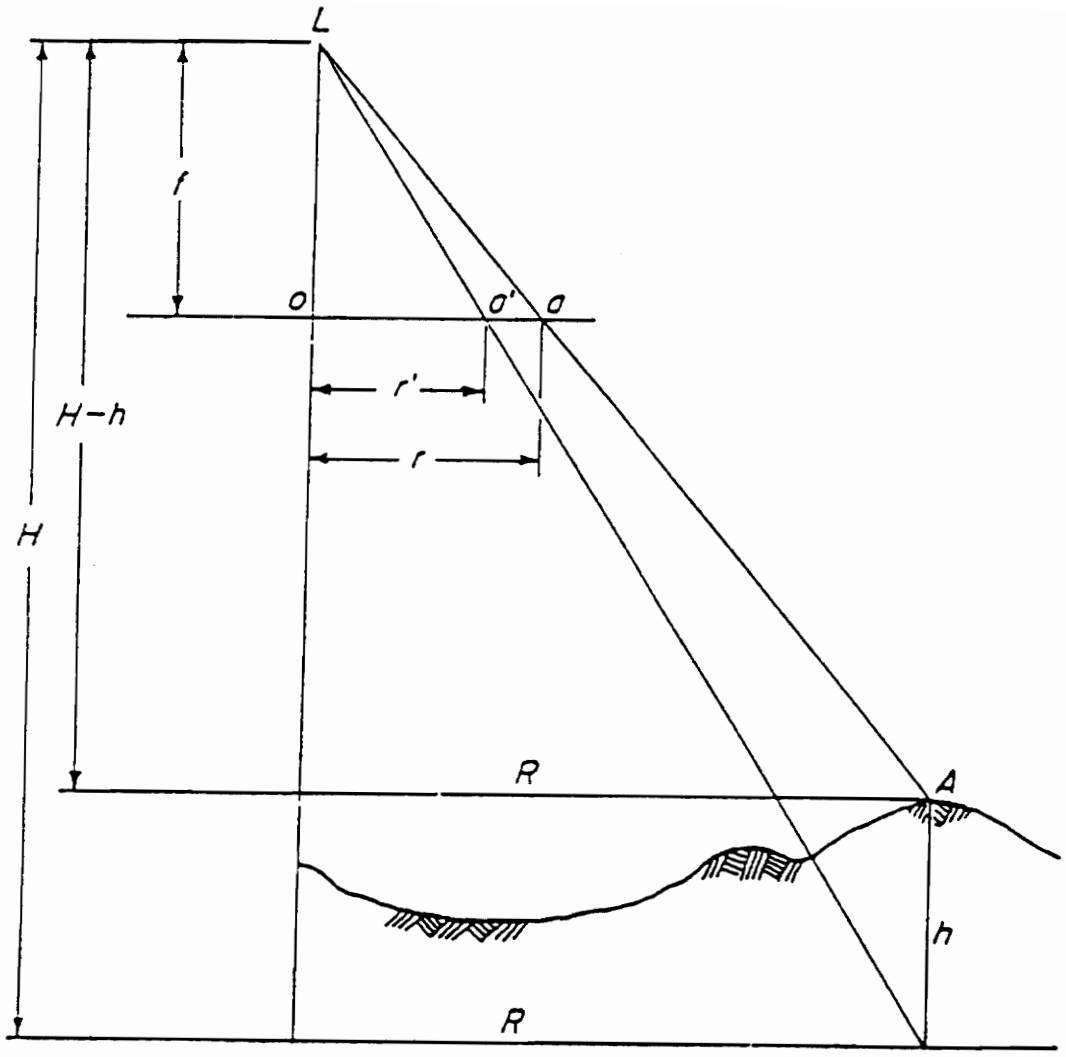

Figure 2.2. Relief Displacement: r-r' is the relief displacement of point 'a' on the image (adapted from Moffitt and Mikhail, 1980).

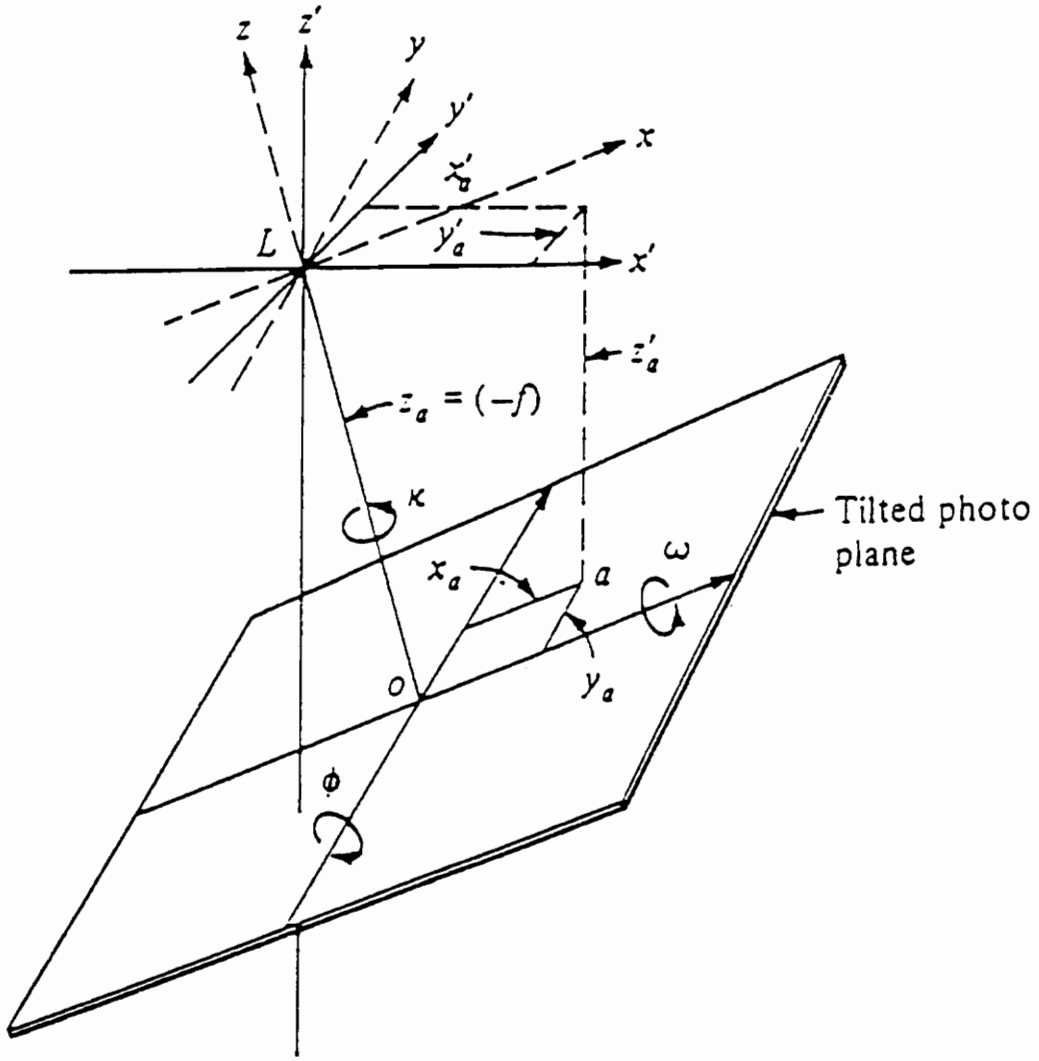

Figure 2.3. Photo Rotation ω, ϕ and κ: (adapted from Wolf, 1974).

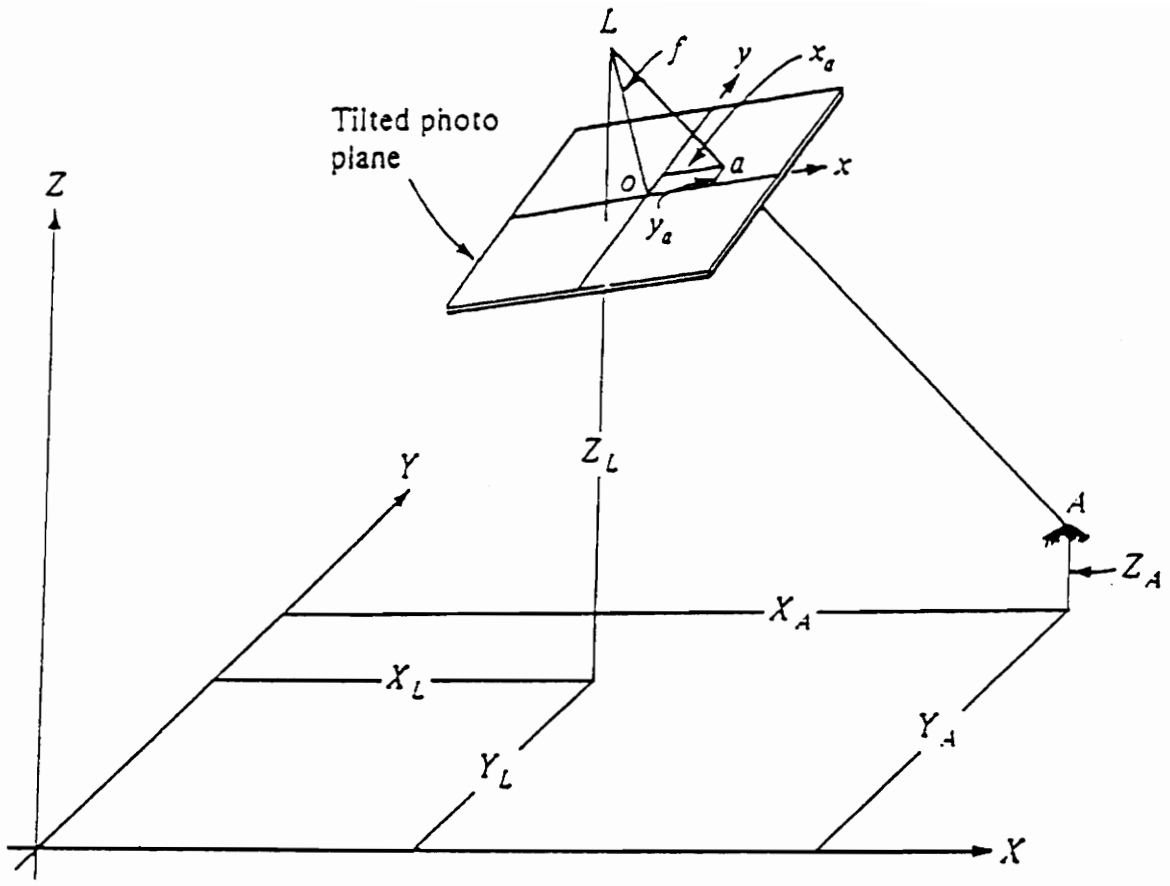

Figure 2.4. Collinearity Condition: "L", "a" and "A" lie on a line in space (adapted from Wolf, 1974).

6. **Earth Curvature**. The mathematical model for photo correction is a function between ground space defined by X, Y and Z and image space defined by x and y. In ground space, elevations are measured normal to the curved surface of the earth, and ground X and Y are defined on a plane coordinate system which is actually a curved surface. The error caused by earth curvature can be systematically removed. However, the error is very small in an aerial photo due to the low flying height of the airplane and small area coverage. It is only considered seriously in satellite images taken from high space sensors, such as NOAA Advanced Very High Resolution Radiometer (AVHRR).

7. **Image Motion**. Image motion can degrade image sharpness and displace image position. It has been considered one of the primary causes of errors in images. Image motion can be caused by vibration of camera processing and aircraft motion. The vibration caused by camera processing can be controlled by improving the quality of camera and has been discounted generally in aerial photo correction. The blurring, caused by the aircraft speed when the camera takes the photo in the effective exposure time, contributes an image error. But, the error can be compensated in regular photogrammetric cameras.

8. **Image Orientation**. Image orientation, also called image tilt, is expressed by tip, tilt, and swing (ω, ϕ and κ) caused by aircraft rotational motion (Figure 2.3). It is hard to control and often not readily known because it is determined by the aircraft attitude when the photograph was taken. Image tilt may cause considerable error in photographic coordinates. The error can be corrected by employing the rotation matrix computed from ω, ϕ and κ.

9. **Relief Displacement**. All points with elevations above or below the datum are displaced from their datum photograph positions (Figure 2.2). Relief displacement is always radial from the nadir as a function of elevation. The higher a point's elevation is, the larger the point's displacement will be. In a flat area, sometimes the error can be ignored. However, for any high elevation area the photo covers, the displacements of photographic coordinates can be considerably large. Because of changing terrain, displacement is irregular over the photo. There-

fore, it can not be adequately corrected by using systematic procedures. In modern photogrammetry, the collinearity condition equations, which depend on the interior perspective center, the photo point, and the ground point to lie on a line in space, are used to correct the displacement accurately.

2.3 Single-Photo Resection and Correction

Single photo resection includes single photo absolute orientation. It is also called space resection. It is used to compute the six exterior elements of a photo orientation for photo correction. It has been used in modern photogrammetry since the early 1960's. Harris et al. (1963) have given convenient equations for computing the orientation elements used in analytical photogrammetry. The three angular elements of orientation, ω, ϕ and κ, are the rotation angles of the axes of the photo measuring coordinate system relative to the ground coordinate system (Figure 2.3). The other three elements are X, Y and Z coordinates of the interior perspective center in the ground coordinate system (Figure 2.4). By knowing the six elements, the mathematical relationship between photo points and corresponding ground points can be established. Then, using the model, registration of coordinates from the image to ground or from the ground to image can be realized. Therefore, photo correction is achieved.

ω, ϕ and κ can be used to compute the rotation matrix for correcting errors caused by image tilt. The measured photographic coordinates with the fiducial center as the origin can be converted to a new photo coordinate system with the same origin by this matrix. The new photo coordinate system is parallel to the ground coordinate system. Moreover, the origin of the new photo coordinate system can be moved to the interior perspective center if the displacement of the principal point is known (Figure 2.3). In this case, the photo is absolutely on the focal plane of the camera (interior perspective center) and also parallel to the ground. All the points on the photo have the

same z coordinate as negative focal length and new x and y coordinates with the interior perspective center as the origin, through the rotation and origin transformation. The computation equation for the transformations for photo point "a" can be expressed in the following forms:

$$\begin{bmatrix} x_a - x_0 \\ y_a - y_0 \\ z_a \end{bmatrix} = \begin{bmatrix} m_{11} & m_{12} & m_{13} \\ m_{21} & m_{22} & m_{23} \\ m_{31} & m_{32} & m_{33} \end{bmatrix} \begin{bmatrix} x'_a \\ y'_a \\ z'_a \end{bmatrix} \qquad (2.1)$$

Where:

x_a *and* y_a — *x, y coordinates of point "a" with respect to the fiducial center*

x'_a *and* y'_a — *transformated x, y coordinates of point "a" with respect to the interior perspective center*

z'_a *and* z_a — *negative camera focal length* $(-f)$

x_0 *and* y_0 — *principal point coordinates*

m_{ij} — *rotation matrix values*

$$m_{11} = \cos\phi \cos\kappa$$

$$m_{12} = \sin\omega \sin\phi \cos\kappa + \cos\omega \sin\kappa$$

$$m_{13} = -\cos\omega \sin\phi \cos\kappa + \sin\omega \sin\kappa$$

$$m_{21} = -\cos\phi \sin\kappa$$

$$m_{22} = -\sin\omega \sin\phi \sin\kappa + \cos\omega \cos\kappa$$

$$m_{23} = \cos\omega \sin\phi \sin\kappa + \sin\omega \cos\kappa$$

$$m_{31} = \sin\phi$$

$$m_{32} = -\sin\omega\cos\phi$$

$$m_{33} = \cos\omega\cos\phi$$

Based on the ray path of photograph, the interior perspective center, the point defined by the transformed photo x′, y′ and z′, and the corresponding ground point must lie on a line in space (Figure 2.4). The collinearity condition equation is the space line equation which establishes the relationship between points in image and object spaces. By knowing the coordinates of the interior perspective center in the ground system, all points in the ground coordinate system can be transformed to the new photo coordinate system (x′, y′ and z′). In the same coordinate system, the collinearity condition equation can be established by using the coordinates of the interior perspective center, an image point and the corresponding ground point. The following equation is the collinearity condition equation for an image point - "a" and the ground point - "A" (Wolf, 1974):

$$\frac{x'_a - x_0}{X_A - X_L} = \frac{y'_a - y_0}{Y_A - Y_L} = \frac{z'_a}{Z_A - Z_L} \qquad (2.2)$$

In their reduced form:

$$x'_a - x_0 = \left(\frac{X_A - X_L}{Z_A - Z_L}\right) z'_a$$

$$y'_a - y_0 = \left(\frac{Y_A - Y_L}{Z_A - Z_L}\right) z'_a$$

$$z'_a = \left(\frac{Z_A - Z_L}{Z_A - Z_L}\right) z'_a \qquad (2.3)$$

Where:

X_A, Y_A and Z_A – X, Y and Z coordinates of point "A" in the ground system

X_L, Y_L *and* Z_L – *X, Y and Z coordinates of the interior perspective center in the ground system*

Substituting the reduced form into equation (2.1), the collinearity condition equation can be transformed to two equations which represent the relationships between measured photo coordinates and ground coordinates for all points on the photo. The collinearity equations for photo point "a" and corresponding ground point "A" are:

$$x_a - x_0 = -f\left[\frac{m_{11}(X_A - X_L) + m_{12}(Y_A - Y_L) + m_{13}(Z_A - Z_L)}{m_{31}(X_A - X_L) + m_{32}(Y_A - Y_L) + m_{33}(Z_A - Z_L)}\right] \quad (2.4)$$

$$y_a - y_0 = -f\left[\frac{m_{21}(X_A - X_L) + m_{22}(Y_A - Y_L) + m_{23}(Z_A - Z_L)}{m_{31}(X_A - X_L) + m_{32}(Y_A - Y_L) + m_{33}(Z_A - Z_L)}\right] \quad (2.5)$$

In a geometric transformation of coordinates between image and ground spaces using these equations, all unknown coefficients must be determined first. One method uses control points from both spaces to solve the system of equations. In space resection, there are six unknown variables, ω, ϕ, κ, X_L, Y_L *and* Z_L. Because each pair of control point (a, A) from photo and ground can produce two equations (eqs. (2.4) and (2.5)), at least 3 pairs of control points are needed to solve for six unknown variables. Usually more than three pairs of control points are used. This treatment allows the application of least squares for the use of redundant data and the minimization of random observational discrepancies. Afterward, these computed coefficients may be used to convert selected many other point coordinates or the whole photo from one space to the other. The transformation from ground to image spaces can be computed by utilizing equations (2.4) and (2.5).

The collinearity condition can take different forms in different applications. The forms expressed here are common in space resection and photo transformation from ground to image. Because the collinearity equations are non-linear, the equations are linearized using Taylor's expansion and only the first order terms are retained. Then an iterative system solving procedure is employed.

Before the collinearity equations are linearized, the equations need to be changed.

First, set:

$$\Delta X = (X_A - X_L) \quad \Delta Y = (Y_A - Y_L) \quad \Delta Z = (Z_A - Z_L)$$

$$q = m_{31}\Delta X + m_{32}\Delta Y + m_{33}\Delta Z$$

$$r = m_{11}\Delta X + m_{12}\Delta Y + m_{13}\Delta Z$$

$$s = m_{21}\Delta X + m_{22}\Delta Y + m_{23}\Delta Z$$

Then equations (2.4) and (2.5) can be expressed in the following form:

$$F_x = q(x_a - x_0) + rf \tag{2.6}$$

$$F_y = q(y_a - y_0) + sf \tag{2.7}$$

According to Taylor's theorem, equations (2.6) and (2.7) can be linearized and expressed as differential equations. The linearized and simplified collinearity equations are:

$$v_{x_a} = b_{11}d\omega + b_{12}d\phi + b_{13}d\kappa - b_{14}dX_L - b_{15}dY_L - b_{16}dZ_L + b_{14}dX_A + b_{15}dY_A + b_{16}dZ_A + J \tag{2.8}$$

$$v_{y_a} = b_{21}d\omega + b_{22}d\phi + b_{23}d\kappa - b_{24}dX_L - b_{25}dY_L - b_{26}dZ_L + b_{24}dX_A + b_{25}dY_A + b_{26}dZ_A + K \tag{2.9}$$

Where:

v_{x_a} *and* $.v_{y_a}$ — *corrections to measured photo coordinates* x_a *and* y_a

b_{1j} — *coefficients equal to the partial derivatives of equation* (2.6) *for the six unknowns*

$$b_{11} = \frac{x_a}{q}(-m_{33}\Delta Y + m_{32}\Delta Z) + \frac{f}{q}(-m_{13}\Delta Y + m_{12}\Delta Z)$$

$$b_{12} = \frac{x_a}{q}[\Delta X \cos\phi + \Delta Y(\sin\omega \sin\phi) + \Delta Z(-\cos\omega \sin\phi)]$$

$$+ \frac{f}{q}[\Delta X(-\sin\phi \cos\kappa) + \Delta Y(\sin\omega \cos\phi \cos\kappa) + \Delta Z(-\cos\omega \cos\phi \cos\kappa)]$$

$$b_{13} = \frac{f}{q}(s)$$

$$b_{14} = \frac{x_a}{q}(m_{31}) + \frac{f}{q}(m_{11})$$

$$b_{15} = \frac{x_a}{q}(m_{32}) + \frac{f}{q}(m_{12})$$

$$b_{16} = \frac{x_a}{q}(m_{33}) + \frac{f}{q}(m_{13})$$

b_{2j} – *coefficients equal to the partial derivatives of equation* (2.7) *for the six unknowns*

$$b_{21} = \frac{y_a}{q}(-m_{33}\Delta Y + m_{32}\Delta Z) + \frac{f}{q}(-m_{23}\Delta Y + m_{22}\Delta Z)$$

$$b_{22} = \frac{y_a}{q}[\Delta X \cos\phi + \Delta Y(\sin\omega \sin\phi) + \Delta Z(-\cos\omega \sin\phi)]$$

$$+ \frac{f}{q}[\Delta X(\sin\phi \sin\kappa) + \Delta Y(-\sin\omega \cos\phi \sin\kappa) + \Delta Z(\cos\omega \cos\phi \sin\kappa)]$$

$$b_{23} = \frac{f}{q}(-r)$$

$$b_{24} = \frac{y_a}{q}(m_{31}) + \frac{f}{q}(m_{21})$$

$$b_{25} = \frac{y_a}{q}(m_{32}) + \frac{f}{q}(m_{22})$$

$$b_{26} = \frac{y_a}{q}(m_{33}) + \frac{f}{q}(m_{23})$$

J and K — the residual errors in x and y respectively

$$J = x_a + \frac{f}{q}(r)$$

$$K = y_a + \frac{f}{q}(s)$$

$d\omega, d\phi, d\kappa$ — the small corrections to be applied to ω, ϕ and κ

dX_L, dY_L, dZ_L — the small corrections to be applied to X_L, Y_L and Z_L

dX_A, dY_A, dZ_A — the small corrections to be applied to X_A, Y_A and Z_A

For single photo space resection, there are six unknown elements in equations (2.8) and (2.9) because $v_{x_a}, v_{y_a}, dX_A, dY_A$ and dZ_A are considered as zero values. Therefore the equations can be simplified in the following forms which are used in numerical computation of single photo space resection:

$$v_{x_a} = b_{11}d\omega + b_{12}d\phi + b_{13}d\kappa - b_{14}dX_L - b_{15}dY_L - b_{16}dZ_L + J \qquad (2.10)$$

$$v_{y_a} = b_{21}d\omega + b_{22}d\phi + b_{23}d\kappa - b_{24}dX_L - b_{25}dY_L - b_{26}dZ_L + K \qquad (2.11)$$

The numerical values for ω, ϕ, κ, X_L, Y_L and Z_L are obtained by approximate computation. First, the initial values for the six unknowns need to be given to compute the coefficients in equations (2.10) and (2.11). Then, solving the linear equation system obtains the six unknown corrections, $d\omega$, $d\phi$, $d\kappa$, dX_L, dY_L and dZ_L. The computed corrections are added to the initial approximations to get revised approximations. The solution is then repeated to find new corrections. The procedure is iterated until the magnitudes of the corrections become insignificant. The procedure begins with reasonable approximations and stops when the approximations are extremely close to the true values under a certain restriction. Although the initial approximations need not be extremely close the true values, they should be as close as practical because some solutions of the iterative approximation method may be locally convergent. Moreover, this treatment can make convergence faster in iteration. By making certain assumptions, such as vertical photography, a satisfactory approximation can be easily obtained from control points (Moffitt and Mikhail, 1980).

The system of equations (2.10) and (2.11) may by expressed in matrix form as:

$$_mV_1 = {}_mA_{nn}X_1 - {}_mL_1$$

In the matrix, m is the number of equations; n is the number of unknowns; V is the matrix of residual errors for the solutions; A is the matrix of b's; X is the matrix of the unknown corrections to the initial approximations; and L is the matrix of constant terms J and K. When the number of equations exceeds the number of unknowns, the most probable values of the unknowns are computed based on a least-squares solution. At this time, the accuracy of the solution is evaluated by the residual matrix V and and standard deviation (S_o). The computational form of standard deviation is:

$$S_o = \sqrt{\frac{(V^T V)}{m - n}}$$

After the true values of the six unknowns are obtained, equations (2.4) and (2.5) are used to compute the photo coordinates, x_a and y_a, which are corresponding to point "A" with X_A, Y_A and Z_A

coordinates in the planimetric coordinate system. That is, it is feasible to compute x, y and z values in the digital photo for the point with known X, Y and Z coordinates in the planimetric map system. Z is the elevation of the ground point and can be obtained from DEM; z is the greyvalue of the point on the digital photo and can be obtained by resampling using x_a and y_a. Through the procedures of space resection, photo point computation and resampling, a single digital photo can be geometrically registered into the DEM ground coordinate system.

In conclusion, single digital photo correction using the collinearity condition includes four major steps (DeMars 1988); (1) identifying appropriate and accurate control point coordinates from the photo and the planimetric coordinate system, (2) developing a computer program to calculate the six elements of exterior orientation, ω, ϕ, κ, X_L, Y_L, and Z_L using space resection, (3) obtaining an appropriate and accurate DEM in the study area, and (4) developing a computer routine which transforms a point on the DEM to one on the digital photo using the collinearity condition equations, resamples the computed photo point for greyvalue and registers the greyvalue into the DEM grid.

2.4 Accuracy Assessment

Based on the procedures of single digital photo correction, accuracy is determined by the accuracy of control points and the DEM. Control points affect the accuracies of the six exterior orientation elements in space resection. The more accurate the control points, the closer the values of the six elements will be to the true values. However, as the true values of the six elements are generally unknown, the only way to control conversion accuracy is to control the accuracy of control points. Photo control point accuracy depends on the measurement instruments and methods. Errors in photo control points are varied and random in terms of different measurement instruments, methods and people. These errors are hard to estimate and generally small. They are usually considered

to be tolerable. Thus, error in control points generally refers only to error in ground control point coordinates. The accuracy of ground control data is quite variable by collection procedures. They may be obtained directly by field survey, by some form of photogrammetric aerotriangulation, or from large scale accurate topo-sheets. The best method depends on the accuracy required, cost, the nature and accessibility of the terrain, and the availability and location of existing control. In previous studies, ground control were obtained through different methods, such as stereoscopical photo measurement and surveying. But no detailed information of accuracy and error of ground control has been given in those studies (Veress and Youcai 1987, Hood et al. 1989, and Gagnon et al. 1990). In digital rectification, because the whole digital photo's correction is performed from DEM representation of the ground to photo x, y and z, DEM accuracy greatly influences the accuracy of the correction. DEMs exist for most GIS applications. This makes the integration of digital photos with GIS practical and accessible in spatial data analysis. However, the DEM accuracy may vary greatly, depending on DEM production methods. Rectifications based on inaccurate DEMs may not meet the accuracy requirement for the spatial analyses. Most of the articles related to the photo rectification only document the residual matrix and standard deviation in an iterative solution of the six orientation elements and vector errors of test points. There have been no articles related to error influence analysis of ground control and the DEM in single photo correction using space resection. Obviously, it is important to study the accuracy of digital photo rectification using space resection in terms of error in ground control and error in the DEM for the trend towards fully automatic aerial photo processing and integration with GIS.

Chapter 3

METHODOLOGY

3.1 Hypotheses and Assumptions

Based on the objectives of the thesis, there are three hypotheses for the study. They are:

1. Geometric error in the uncorrected digital aerial photo exists under most circumstances and may be quite large,

2. the use of collinearity condition equations for single digital-photo correction will significantly reduce the geometric error, and

3. the degree of geometric error in the corrected digital aerial photo is significantly influenced by errors in ground control data and DEM data.

In this study, all the hypothesis tests use 0.05 α significance level. Computed data and results maintain several decimal places only for test computation. The accuracy of control, test and DEM data could only be given to the nearest meters

Certain assumptions are applied to the study. The assumptions are:

1. Geometric accuracies of the USGS 1:24,000 topographic maps used in this study satisfy the United States National Map Accuracy Standard, and

2. errors in the digital aerial photo coordinates caused by film, lens distortion, atmospheric refraction, radiometric distortion, principal point displacement, measuring instrument and other sources are small in comparison with the distortion caused by image tilt and relief displacement.

3.2 Study Areas and Data Sources

This study will focus on data from two USGS 1:24,000 quad-maps. The first area is located near Prentiss, North Carolina. The second area is Blacksburg, Virginia. Both areas are situated in the southern Appalachian mountains, with relatively similar terrain. Prentiss is more hilly and less populated. There are fewer cultural features in the Prentiss area and most of the area is forest. Roads and buildings are concentrated in the eastern a half of the photo. In contrast with the Prentiss area, Blacksburg is flatter and more populated. There are many roads including a major road which crosses the area in a south to north direction. There are many cultural features and buildings in this area, especially in the Blacksburg downtown area. Therefore, there are many clearly defined points in the Blacksburg area, but fewer in the Prentiss area. For both study areas,

a digital photo, the focal length of the camera which took the photo, the average scale of the photo, control and test data, and a DEM were also collected.

The digital aerial photo data were obtained by scanning a positive transparency on an Optronics microdensitometer (an instrument which converts image density at any location to digital form). The Prentiss photo was scanned using 50 micron meter resolution and the Blacksburg photo was scanned using 100 micron meter resolution. The scanned photos were stored in three bands, green, red and infrared. The aerial photographs for both areas were taken as part of the NHAP (National High Altitude Photography program). They were purchased from the USDA-ASCS (US Department of Agriculture, American Soil Conservative Service). The average scales of the two photos are 1:58,000 with camera focal lengths of 0.21 meter. Both are infrared color (false color), "vertical" photographs taken with an optical axis tilt angle of less than 3°. The aerial photograph of Blacksburg was taken on April 12, 1983 and that of Prentiss on April 26, 1984. Although some ground features have been changed since the times the photos were taken, most of roads and buildings still remain unchanged.

In space resection, control points both from photo and ground are needed to compute the six photo orientation elements in the ground space. Control points from the photo can be obtained from the paper photo or the digital photo. Ground control points may be obtained by different procedures depending on expected use of the corrected photo and accuracy requirements. Field surveying can produce the best ground control data, but it is often limited by conditions, such as cost, time, and availability of instruments. Based on the current uses of digital photos in GIS applications, the spatial data extracted from the corrected photo are most likely to be used with data digitized from large-scale topographical maps, such as USGS quad-maps. The spatial data extracted from the digital photo in the Prentiss area, such as the landuse/landcover data, is to be used with thematic spatial data digitized from the USGS 1:24,000 topo-sheet. According to the United States National Map Accuracy Standards (Thompson, 1979), not more than 10 percent of the well-defined points on the USGS 1:24,000 topographic map or smaller scale map shall be in error by more than 1/50 inch for horizontal accuracy. Thus, the possible 90th percentile of horizontal error of a well-defined

point on the map shall not be greater than 12.192 meters on the ground. Well-defined points are those that are easily visible or recoverable on the ground, such as markers and intersections of roads. For vertical accuracy, not more than 10 percent of the elevations tested shall be in error more than one-half the contour interval. The contour interval for the Prentiss map is 40 feet and it is 20 feet for the Blacksburg map. Therefore, the possible 90th percentile of elevation error shall be less than 6.096 meters on the Prentiss map and 3.048 meters on the Blacksburg map. Based on the standards and the accuracy they imply, it is reasonable to obtain ground control points from the USGS 1:24,000 topographic maps for this study purpose because the control and test points used in photo rectification are always well-defined on the ground. In this study, ground control points and test data are obtained from the USGS 1:24,000 (7.5-minute) topographic maps of the two study areas and their accuracies are assumed to be within the map accuracy standards. The USGS 7.5-minute topographic map for Prentiss was photorevised in 1978 and that for Blacksburg was photorevised in 1983.

Photo rectification is actually a coordinate transformation from one coordinate space to the other. The coordinates of one space contain errors and the other are correct or a standard. In the transformation, errors may be removed or decreased to insignificant levels. In photo rectification, the photo is always considered as the space with errors and the ground is the error-free space. Using the collinearity condition to correct the digital aerial photo, the DEM of the photo area is used to represent the ground space. Knowing the coordinates of one space and six orientation elements, corresponding coordinates of the other space can be computed. The photo and DEM are in grid-based raster data format since the collinearity equations provide a point-by-point correction procedure. The only way to express the area as points is to rasterize into finite point components, thereby losing some accuracy. Generally, the ground resolution of the digital aerial photo grid may be less than 5 meters. But, at present, it is impossible to obtain a DEM with less than 5-meter ground cell resolution and accurate elevation data for most analysis areas. Therefore, the grid sizes of the digital photo and DEM are generally different. The DEMs used in both study areas are USGS 7.5-minute DEM data with UTM coordinates. The DEM data has 30-meter grid resolution

and 7-meter absolute elevation resolution. Both DEMs were established using NHAP photos by GPM (a highly automated photogrammetric system designed to produce orthophotos, digital terrain data, and contours). The DEM of Prentiss area has the elevation range from 626 to 1531 meters and that of Blacksburg area from 467 to 882 meters.

3.3 Methodology

3.3.1 Obtaining Control and Test Data

Control points and test points are selected from the USGS 7.5-minute maps based on the digital photos. Because control points must be visible and easily identifiable on the photo, they are road intersections or intersections of roads with rivers. It is impossible to obtain control points in mountain top areas which have higher relief displacements because there are no easily identifiable points. Selected control points can not be as well distributed in elevation as desired. Although this study mainly considers geometric error analysis, one river and one closed contour line are also selected as test features from each map for error impact analysis to simulate errors in possible GIS measurements of length and area on the corrected photo. To get the ground control and test features, the first step is to digitize the eight tic points on the map (4 map corner points and 4 tic marks inside the map) and all the ground control and test features. When digitizing the river, only the intersections of the river with contour lines are digitized. All digitized data are in the same digitizer table coordinate system. In a PC ARC/INFO system, the UTM coordinates of the eight tic points are obtained. The digitized coordinates and the UTM coordinates of the eight tic points were used to establish an affine transformation function to convert the digitized coordinates to UTM coordinates. The affine transformation is actually multiple linear regression models with UTM X and Y

as dependent variables and digitizer table X and Y as independent variables. The linear regression models are expressed in the following forms:

$$UTM\_X = \beta_{0X} + \beta_{1X}DIGI\_X + \beta_{2X}DIGI\_Y + e_X$$

$$UTM\_Y = \beta_{0Y} + \beta_{1Y}DIGI\_X + \beta_{2Y}DIGI\_Y + e_Y$$

Where:

β_{0X}, β_{1X} *and* β_{2X} – *unknown constants for dependent variable* UTM_X

β_{0Y}, β_{1Y} *and* β_{2Y} – *unknown constants for dependent variable* UTM_Y

e_X *and* e_Y – *random residual errors*

The elevations, Z values, of the ground control and test data were obtained directly from the map and then transformed from feet to meters.

The accuracy of the photo correction is tested using the test points. Line and polygon test features are only used in error impact analysis. Therefore, only the photo coordinates of control points and test points with the fiducial center as the origin are needed. First, rows and columns of photo control and test points are obtained from the digital photo using ERDAS software (Earth Resources Data Analysis Systems). The display module of ERDAS is used to display the photo and show the rows and columns of the points. Photo coordinates are obtained by affine transformation between rows and columns of the digital photo and x and y photo coordinates. The affine transformation was established in the photo correction program developed using C language based on five photo points with known x and y photo coordinates and rows and columns in the digital photo. The five photo points for the affine transformation between rows and columns and x and y coordinates are chosen in the digital photo and paper photo. They are easily identifiable and may be the fiducial points or road intersections. The photo coordinates of the five points are obtained by digitizing them and the four fiducial points on the film photo. Then, the four fiducial points and

fiducial center establishes an affine transformation from digitizer table coordinates to photo coordinates with the fiducial center as the origin and lines connected by opposite fiducial points as x and y axes. The photo coordinates of the five photo points are computed by the affine transformation equations. After obtaining the photo coordinates and rows and columns of the five photo points, the affine transformation from the row and column of the digital photo to the photo coordinates is established. Using the transformation, photo coordinates of the photo control points are computed according to the rows and columns of those points.

3.3.2 Testing Errors in Uncorrected Photos

Under the assumption that there is no image tilt when the photo is taken and the terrain is perfectly flat, there are no errors in the photo in this study. The photo coordinates and the ground coordinates have a perfect affine transformation relationship. That is, the sum of residuals will be zero and the sum of squared residuals will be very small in the x and y directions for photo control data when using control data to establish the affine transformation. In transforming ground coordinates of test points to photo coordinates, residuals will be also small. The sum of the residuals will be zero and the sum of squared residuals will approximate zero in x and y directions. The errors in the uncorrected photo can be tested using an affine transformation established by control points in both photo and ground spaces.

The affine transformation for error test in the uncorrected photo is established by control points using SAS software. The function transforms ground coordinates of test points into computed photo coordinates. Then residuals of computed coordinates of test points can be calculated using true photo coordinates of test points in both x and y directions. Residual distances of computed points from true points can also be calculated. Therefore, geometric error in the uncorrected photo can be tested based on residual distances. Because a certain level of error is allowed in the map or photo, to test that the error in the photo is equal to zero is pointless in practice. Although digital

maps or photos may have error levels different from their paper maps or photos, the error magnitudes are hard to estimate for all digital features. In the digitizing process, some features may lose accuracy and other may gain accuracy. But it is difficult to assess the change of the point position error due to the randomness of digitizing error. In this study, it is assumed that the map accuracy standards discussed above also apply to digital maps and photos. As a result, the error scaled to the ground in the digital photo is tested according to the possible maximum error on the map. The test hypotheses for point error in the uncorrected photo are:

$$H_0: \textit{point error in the uncorrected photo} \leq 12.192 \textit{ meters}$$

$$H_1: \textit{point error in the uncorrected photo} > 12.192 \textit{ meters}$$

3.3.3 Single Digital Photo Resection and Correction

The correction of the digital photo uses the single-photo resection method which has been discussed in detail in chapter 2. A C-language program has been developed on a PC computer for correction from the DEM to digital photo (Figure 3.1). The digital photo and DEM are stored in IDRISI (a Grid-Based Geographic Analysis System) data format. The corrected photo is also stored in this format. In the routine of space resection, control points are used to compute image orientation. The six approximate values of the orientation elements are computed based on the control data by assuming that the photo is a vertical photo (Moffitt and Mikhail 1980). The approximate values of the initial six orientation elements, ω^0, ϕ^0, κ^0, X_L, Y_L *and* Z_L, are given by the the following equations:

$$\omega^0 = 0$$

$$\phi^0 = 0$$

$$\kappa^0 = arctan\left(\frac{Y_{A1} - Y_{A2}}{X_{A1} - X_{A2}}\right) - arctan\left(\frac{y_{a1} - y_{a2}}{x_{a1} - x_{a2}}\right)$$

$$X_L^0 = \frac{1}{n}\sum_{i=1}^{n} X_i$$

$$Y_L^0 = \frac{1}{n}\sum_{i=1}^{n} Y_i$$

$$Z_L^0 = \frac{f}{s} + \frac{1}{n}\sum_{i=1}^{n} Z_i$$

Where:

$(a1, A1)$ *and* $(a2, A2)$ $-$ *two control points on the photo and ground*

n $-$ *the number of control points*

f $-$ *the focal length*

s $-$ *the average scale of the photo*

The linear algebraic equations with unknown six corrections (see equations (2.10) and (2.11)) are solved using the singular value decomposition method (Press et al., 1989). The iterations of computing the six corrections and updating the initial values are interrupted when the computed corrections, $d\omega, d\phi, d\kappa$, dX_L, dY_L *and* dZ_L, are less than 0.00001. In the computation, the angular elements, ω, ϕ and κ are in radian and the position elements, X_L, Y_L and Z_L are in meter.

For the best result, the terrain should be sampled at the same spatial resolution as the image data (Kawata et al. 1988). However, for many purposes this is impractical owing to the cost of acquiring the terrain data. According to Trotter (1991), it is feasible to use the DEM and image data with

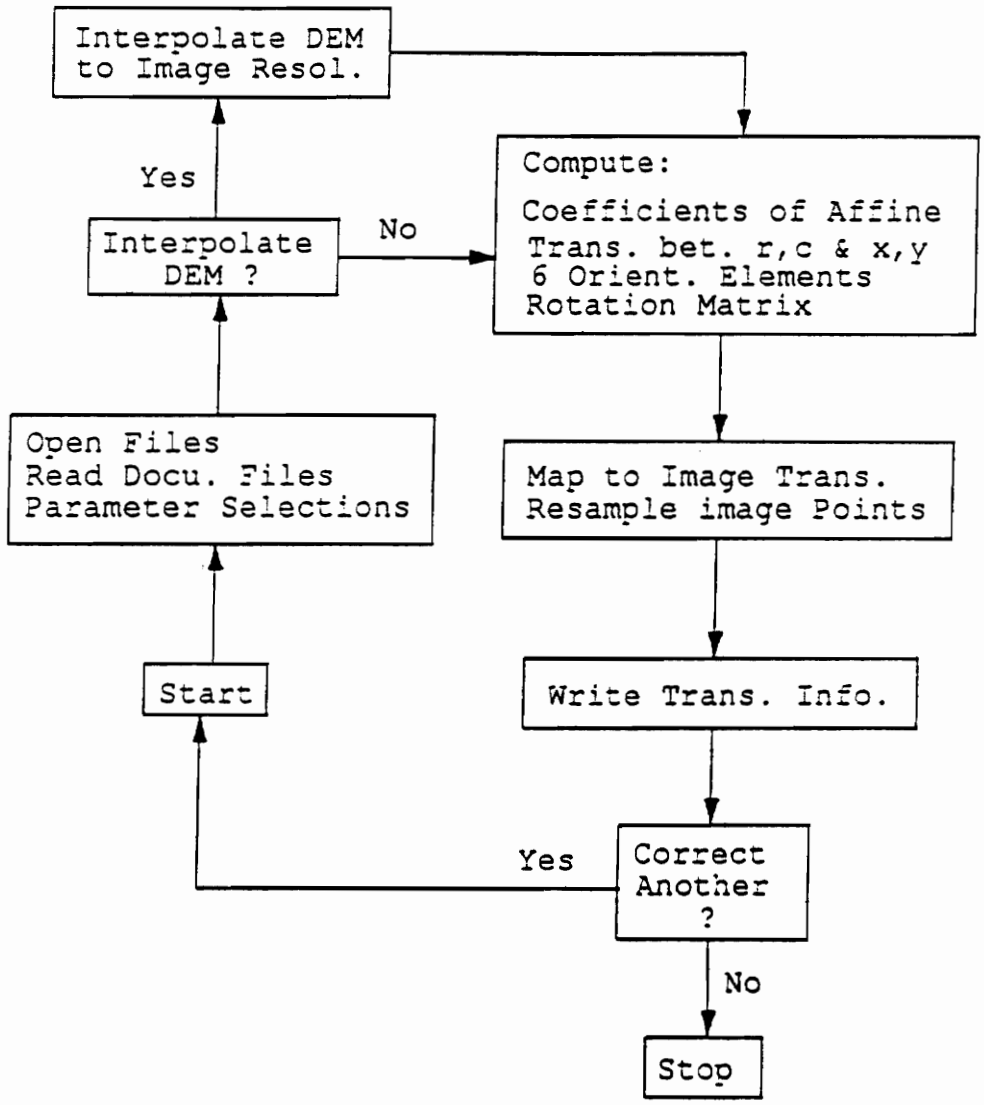

Figure 3.1. Flow Chart for Single Digital-Photo Resection and Correction

different resolutions. For the purpose of reducing the error caused by the different resolutions, the DEM needs to be interpolated to have the same or approximate resolution as the digital photo has when the resolution difference is large. Therefore, the errors caused by the ground coordinates, X, Y and Z, mainly come from the errors in Z values. DEM refinement can reduce the errors caused by both the registration from the DEM to photo and resampling of image greyvalues. In photo correction, the percentage of the resolution difference between the digital photo and DEM, which is the difference over the photo resolution, is computed. If the percent is greater than 50, the DEM is interpolated to the same resolution as that of the digital photo. For the reason of keeping the original elevation range, original DEM cell values are copied if interpolated points overlay on original DEM points. If interpolated points are on original cell margins, two marginal points are used to interpolate, otherwise; the nearest four points are used. The interpolation employs an inverse-distance weighting method. The resampling method is a nearest neighbor resampling in order to remain the original characteristics of the digital photo. The scanned digital photo of Prentiss has 50 micron meter photo resolution and around 3 meters ground resolution. The scanned digital photo of Blacksburg has 100 micron meter photo resolution and around 6 meters ground resolution. The DEM resolution is 30 meters. Therefore, before the photo is corrected, the DEM needs to be interpolated.

3.3.4 Testing Errors in Corrected Photos

Geometric errors also exist in the corrected photo. The errors may be caused by the qualities of control data and the DEM and the other error sources besides image tilt and relief displacement, discussed in chapter 2. Geometric error in the corrected photo must be tested to see whether the correction function has significantly reduced the error and whether geometric error in the corrected photo is significantly large. In this study, test points are used to assess geometric error in the corrected photo. As in testing error in the uncorrected photo, ground coordinates of test points are transformed into computed photo coordinates using the collinearity equations (eq. 2.4 and 2.5).

Then x and y residuals and residual distances of computed photo coordinates from true photo coordinates are calculated. The sum of residuals and the sum of squared residuals in x and y directions are also obtained. Based on the residual distances, the reduced and remaining errors can be tested. The test hypotheses for the remaining point position error are:

$$H_0: \textit{point error in the corrected photo} \leq 12.192 \textit{ meters}$$

$$H_1: \textit{point error in the corrected photo} > 12.192 \textit{ meters}$$

The test hypotheses for reduced error of point position are:

$$H_0: \textit{reduced point error in the corrected photo} = 0$$

$$H_1: \textit{reduced point error in the corrected photo} \neq 0$$

3.3.5 The Impact of Ground Control and the DEM on the Correction

As discussed in chapter 2, the accuracy of digital photo rectification is controlled by accuracies of control and DEM data. Photo control data are always assumed to be error-free, as accuracy can be highly controlled by the measuring instrument and procedure. As a result, accuracy of the rectification is mainly controlled by the accuracies of ground control and DEM data. Testing the impact of ground control and DEM data on the rectification has significant meaning for the digital photo correction used in GIS applications. The purpose of the impact study is to determine the relationship between error in the corrected photo and the error in the ground control and DEM data. Although accuracy of the rectification is influenced by ground control and DEM data simultaneously, it is reasonable and convenient to analyze the impact of these influence factors separately. When establishing the relationship between accuracy of the rectification and one influence factor, the other factor is held constant. In each study area, test points, a test line and a test polygon are used to obtain changes in point positions, line length and polygon area when randomly adding

errors to ground control coordinates or to elevations of test features. For point, line, and polygon test features, average distance offset of computed test points from computed "true" positions without added errors; average percentage of line length change and average percentage of polygon area change are used to build the relationships. The level of random errors added to ground control coordinates or elevation data is not fixed, to better model error in ground control and DEM data. Actually, the error added is a random error in the range [-ERROR, + ERROR], where ERROR is the absolute maximum error. ERROR can be any positive integer. For each given ERROR, distance offset of test points, percentage of line length change, and percentage of polygon area change are computed by averaging 30 iterations of randomly added errors. Average distance offset is computed by averaging average distance offsets of test points. Over a range of ERROR values, relationships of average distance offset, average percentage of line length change, and average percentage of polygon area change by ERROR value can be established using simple linear regression models.

In this study, error data are obtained by using a C-language program (Figure 3.2) on a PC computer and the regression models are created using SAS software. ERROR values studied range from 5 to 300 meters with 60 error ranges. The purpose of selecting 60 error ranges is to obtain more data for regression analysis. In practice, absolute errors in ground control and DEM data are seldom greater than 100 meters. They are often within $\pm$ 50 meters. Therefore, the impact of ERROR within 50 meters in ground control and the DEM is most important.

In studying the impact of the ground control points, point, line and polygon test data are considered accurate. For a given value of ERROR, generated random errors are added to ground control X, Y and Z separately. Then using erroneous ground control points, the photo orientation elements are computed. The linearized and simplified collinearity equations are used to compute the orientation elements. Utilizing the collinearity equations transforms ground coordinates of test point, line, and polygon data into photo coordinates. Line length and polygon area in photo coordinates are calculated. Computed point positions, line length, and polygon changes reflect the impact of added error in ground control coordinates.

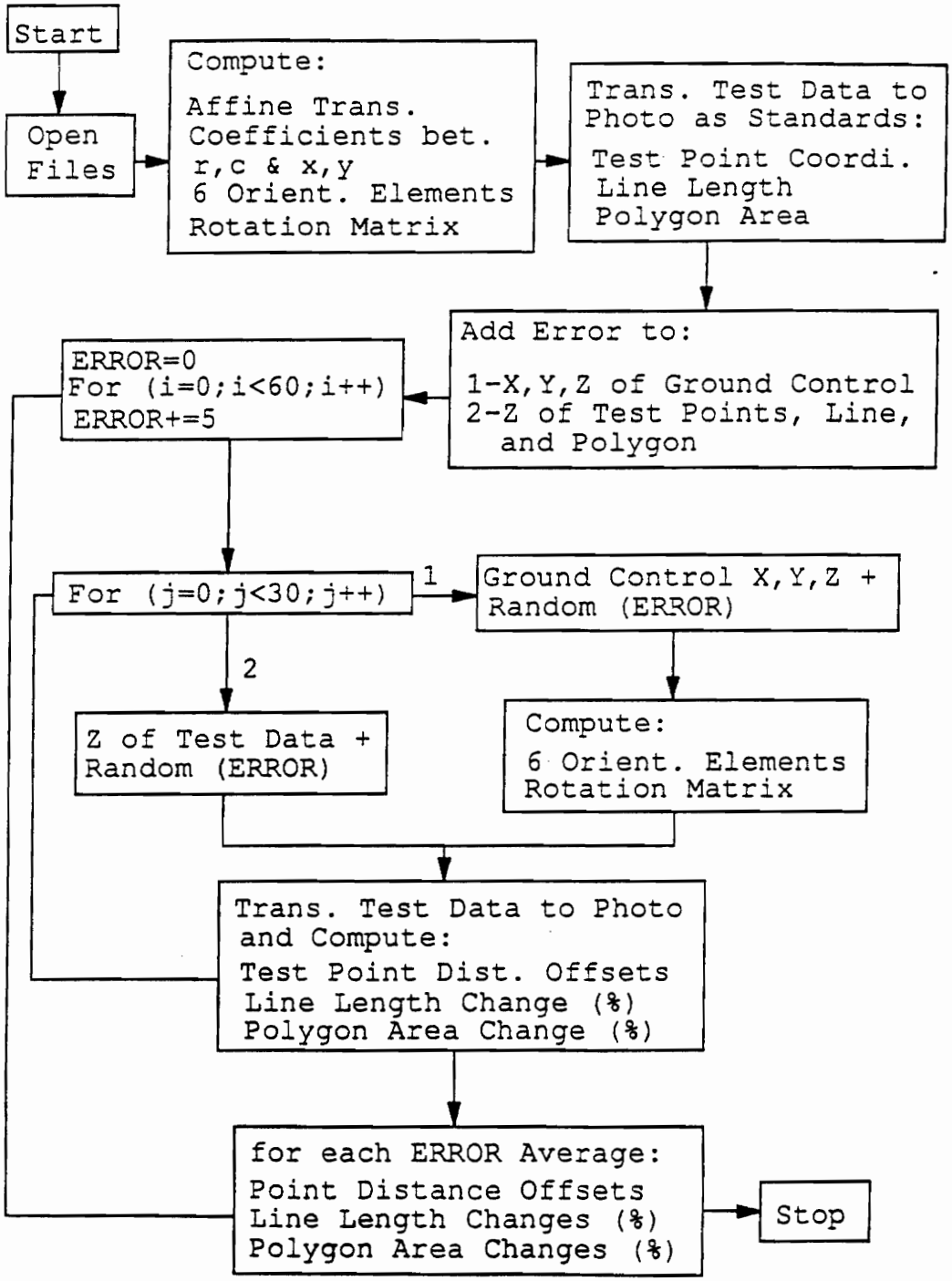

Figure 3.2. Flow Chart for the Impact of Ground Control and DEM on the Correction

Relationships of point position, line length, and polygon area changes with ERROR are tested using the simple linear regression model and the test hypotheses can be expressed in the following form:

$$H_0: \beta_1 = 0$$

$$H_1: \beta_1 > 0$$

Where:

β_1 – *the slope of the regression model.*

The hypotheses for testing the relationship between point offset in the corrected photo and the given error range (ERROR) in ground control coordinates are:

H_0: *point distance offset in the corrected photo is not correlated to ERROR in ground control*

H_1: *point distance offset in the corrected photo is positively correlated to ERROR in ground control*

The hypotheses for testing the relationship between line length change in the corrected photo and ERROR in ground control coordinates are:

H_0: *line length change is not correlated to ERROR in ground control*

H_1: *line length change is positively correlated to ERROR in ground control*

The hypotheses for testing the relationship between the polygon area change in the corrected photo and ERROR in ground control coordinates are:

H_0: *polygon area change is not correlated to ERROR in ground control*

H_1: *polygon area change is positively correlated to ERROR in ground control*

In analyzing the impact of the DEM on the rectification, control data are considered to be accurate. So, the computed six orientation elements are considered to be error-free and the collinearity equations without added errors are used as the transformation function. For each given error range (ERROR), ground coordinates of test point, line and polygon data with added random errors in their elevations are transformed into their photo coordinates in thirty iterations. Point position, line length, and polygon area changes reflect the impact of added error in their elevations. The hypotheses for testing the relationship between point error in the corrected photo and the given error range (ERROR) in elevation (or DEM) of point ground data are:

H_0: *point distance offset in the corrected photo is not correlated to ERROR in point elevation*

H_1: *point distance offset in the corrected photo is positively correlated to ERROR in point elevation*

The hypotheses for testing the relationship between line length change in the corrected photo and ERROR in line ground elevation data are:

H_0: *line length change is not correlated to ERROR in line elevations*

H_1: *line length change is positively correlated to ERROR in line elevations*

The hypotheses for testing the relationship between polygon area change in the corrected photo and ERROR in elevations of polygon ground coordinates are:

H_0: *polygon area change is not correlated to ERROR in polygon elevations*

H_1: *polygon area change is positively correlated to ERROR in polygon elevations*

Chapter 4

RESULTS

4.1 Control and Test Data

The X and Y UTM coordinates of the ground control and ground test data were obtained by affine transformations between the UTM and digitizer table coordinates of the eight tic points on the USGS 1:24,000 topographic map. Elevations were interpreted from the map. In using affine transformations, the digitizer table X and Y coordinates of the ground control and test features from the map were transformed into the UTM X and Y coordinates (Tables A.1 - A.5 in Appendix A). Because the accuracy of the affine transformation is determined by the accuracy of the eight tic points on the map and the distortion of the paper map, the affine transformation model needs to be evaluated. In Tables 4.1 and 4.2, it is evident that the affine transformation of eight tic points from digitizer table coordinates to UTM for Prentiss map is highly significant for the two dependent variables, UTM_X and UTM_Y. The sum of squared residuals for UTM_X is 9.53 m^2 and that for UTM_Y is 11.47 m^2. The F test value for model UTM_X is 37907677.96 and that for model UTM_Y is 46568091.86, considerately greater than the critical value, 5.79 (Ott, 1988), at the 0.05

significance level. The R-square and adjusted R-square are 1.000 for the transformation. Moreover, the largest absolute residual for model UTM_X is 2.357 meters and that for model UTM_Y is 2.158 meters. The affine transformation is almost a perfect fit. The affine transformation equations of UTM_X and UTM_Y for Prentiss are:

$$UTM\_X = 269351 + 0.609309DIGI\_X + 0.010730DIGI\_Y$$

$$UTM\_Y = 3875565 - 0.010904DIGI\_X + 0.609982DIGI\_Y$$

In Tables 4.3 and 4.4, the affine transformation of eight tic points from digitizer table coordinates to UTM for Blacksburg map is also highly significant. The sum of squared residuals for UTM_X is 17.64 m^2 and that for UTM_Y is 20.11 m^2. The F test value for model UTM_X is 19384103.24 and that for UTM_Y is 26560262.50, also far greater than the critical value, 5.79 at 0.05 α significance level. The R-square and adjusted R-square are also 1.000. The largest absolute residual for UTM_X is 2.428 meters and that for UTM_Y is 2.140 meters. The affine transformation for Blacksburg map is also near perfect. The affine transformation equations for Blacksburg are:

$$UTM\_X = 543245 + 0.609798DIGI\_X - 0.022707DIGI\_Y$$

$$UTM\_Y = 4107628 + 0.022472DIGI\_X + 0.609484DIGI\_Y$$

The affine transformations of both study areas are accurate for data transformation and the accuracy of obtained ground control and test data is mainly controlled by the position accuracy of those data on the map. By assuming an accurate USGS 1:24,000 topographical map and small random errors in digitizing those points, the maximum position error in obtained ground control and test data may still be considered to be within 12.192 meters.

The photo coordinates of the control points and test points were obtained through two-step coordinate affine transformations. The first is the transformation from digitizer table coordinates to

Table 4.1. Affine Transformation of Eight Tic Points from Digitizer Table to UTM Coordinates, Prentiss, N.C.

Model	Source	DF	Model Test Sum of Square	Mean Square	F Test Prob>F R Square Adj_R
	Regression	2	144567622.46	72283811.23	37907677.96
	Residual	5	9.53	1.91	0.0001
UTM_X	Total	7	144567631.99		1.0000
					1.0000
	Regression	2	213718143.44	106859071.72	46568091.86
	Residual	5	11.47	2.29	0.0001
UTM_Y	Total	7	213718154.92		1.0000
					1.0000

Table 4.2. Residuals of the Affine Transformation of Eight Tic Points from Digitizer Table to UTM coordinates, Prentiss, N.C.

Tic #	DIGI X	DIGI Y	UTM (m) X	UTM (m) Y	UTM Residual (m) X	UTM Residual (m) Y
1	4252	23032	272188	3889567	-0.506	0.412
2	22952	22909	283581	3889288	-0.407	0.308
3	10432	15409	275871	3884851	-0.697	1.008
4	16666	15370	279671	3884758	0.845	-0.190
5	10377	7835	275757	3880229	0.086	-1.640
6	16613	7795	279559	3880136	2.357	-2.158
7	4081	296	271840	3875701	-0.155	0.792
8	22812	173	283250	3875423	-1.523	1.466

Table 4.3. Affine Transformation of Eight Tic Points from Digitizer Table to UTM Coordinates, Blacksburg, Va.

Model	Source	DF	Model Test Sum of Square	Mean Square	F Test Prob>F R Square Adj_R
	Regression	2	136785538.31	68392769.16	19384103.24
	Residual	5	17.64	3.53	0.0001
UTM_X	Total	7	136785555.95		1.0000 1.0000
	Regression	2	213663208.02	106831604.01	26560262.50
	Residual	5	20.11	4.02	0.0001
UTM_Y	Total	7	213663228.13		1.0000 1.0000

Table 4.4. Residuals of the Affine Transformation of Eight Tic Points from Digitizer Table to UTM coordinates, Blacksburg, Va.

Tic #	DIGI X	DIGI Y	UTM (m) X	UTM (m) Y	UTM Residual (m) X	UTM Residual (m) Y
1	2709	24337	544343	4122519	-0.953	-1.973
2	20863	23769	555429	4122585	1.783	2.139
3	8521	16568	548064	4117917	0.222	0.484
4	14577	16383	551762	4117939	0.421	-0.899
5	8285	8990	548091	4113295	-1.526	2.140
6	14346	8809	551790	4113317	-2.253	-1.802
7	1977	1607	544416	4108652	2.428	1.120
8	20170	1048	555520	4108718	-0.124	-1.209

photo coordinates to obtain photo coordinates of five points which are most accurate and easily identified on the photo. This transformation was processed in a C program. Then, based on the five photo points with known rows and columns in the digital photo and known photo coordinates, the affine transformation from digital photo rows and columns to the fiducial axis coordinates was established. The transformation from rows and columns to photo x and y coordinates was manipulated within the photo correction program (Tables A.1 and A.3 in Appendix A). Because photo coordinate computation was only the coordinate transformation, there were no errors involved in the transformation. Only the errors caused by digitizing the points and scanning the paper photo existed. Those errors are small and random and it is difficult to control them. In photo correction, those errors are always considered to be negligible. The obtained photo control and test point coordinates are considered to be accurate.

There are 27 control points and 20 test points for the photo of Prentiss, and 30 control points and 29 test points for the photo of Blacksburg (Tables A.1 - A.4 in Appendix A). There are more control and test points for Blacksburg due to the many well-defined points in this area. The control and test points for Prentiss (Figures A.1 - A.2) are not well distributed around the photo fiducial center; they are mainly distributed on the right side of the fiducial center due to the presence of few well-defined points on the left side. The distributions of the control and test points (Figures A.3 - A.4) for Blacksburg are relatively well distributed around the photo fiducial center. All the control and test points in both areas are located in low-elevation areas and not well distributed in elevation due a lack of well-defined points in high-elevation areas for both area photos. Because photo correction is based on the principal of the collinearity condition geometrically, the control point distribution will not in principle influence the photo rectification. But, because there always exist errors in the control data, well distributed control data will reduce the influence of random errors on the correction. Well-distributed control points are preferable in photo correction because of the nature of existing random errors in control data. For the test points, their rather poor elevational distribution will greatly influence test results due to different error levels existing for different point locations.

From Table A.5 in Appendix A, the river selected on the Prentiss map has elevation range from 698 to 1280 meters and the length of the line is 4015 meters. The elevation range of the river selected on the Blacksburg map is from 469 to 609 meters and the line length is 3843 meters. The area of the closed contour line selected on the Prentiss map is 1031321 m^2 with elevation 975 meters. The closed contour line selected on the Blacksburg map has an area of 509688 m^2 and elevation of 731 meters.

4.2 Errors in Uncorrected Photos

The geometric error in the uncorrected photo was tested by the test points using the affine transformation of the control points from UTM coordinates to the photo coordinates. In Table 4.5, the affine transformation for the photo of Prentiss with adjusted R-square 0.9999 for dependent variable x_a and adjusted R-square 1.0000 for dependent variable y_a is highly significant. The affine transformation equations are:

$$x_a = -205020 + 0.964280X_A - 0.016116Y_A$$

$$y_a = -3760915 + 0.011059X_A + 0.968328Y_A$$

The root mean square error for the computed photo control x coordinates is 10.412 meters and that for the computed photo control y coordinates is 12.461 meters (Table 4.6). The average residual distance of the computed photo control points is 14.668 meters. The means of x and y residuals of the photo control points are zero. The mean of x residuals for the computed photo test points using the transformation is 2.141 meters and the mean of y residuals for the computed photo test points is -1.988 meters. Because the means of x and y residuals are not approximately zero, there were some systematic errors in the digital photo (Maling,1989). Systematic error is hard to interpret since there are various sources which may cause systematic error in the digital photo. The root

mean square error for computed x coordinates of the photo test points is 8.353 meters and that for computed y coordinates of the photo test points is 13.978 meters. Estimated error in the uncorrected photo of Prentiss is 14.599 meters.

From Table 4.7, the affine transformation of Blacksburg with adjusted R-square 1.0000 for both dependent variable x_a and y_a is highly significant. The affine transformation equations are:

$$x_a = -494401 + 0.970713X_A - 0.009602Y_A$$

$$y_a = -4004635 + 0.012021X_A + 0.970972Y_A$$

The root mean square error for the computed photo control x coordinates is 10.816 meters and that for the computed photo control y coordinates is 10.233 meters (Table 4.8). The average residual distance of the computed photo control points is 12.707 meters. The means of x and y residuals of the photo control points are zero. The mean of x residuals for the computed photo test points using the transformation is 1.322 meters and the mean of y residuals for the computed photo test points is 0.765 meters. Because the means of x and y residuals are not approximately zero, there were some systematic errors in the digital photo. The root mean square error for the computed photo x coordinates of the test points is 8.888 meters and that for the computed photo y coordinates of the test points is 9.774 meters. Estimated error in the uncorrected photo of Blacksburg is 11.252 meters. The estimated error for the Blacksburg photo is smaller than that for the Prentiss photo because the terrain in the Blacksburg area is relatively smooth. The error in the uncorrected photo of Prentiss is greater than that in the uncorrected photo of Blacksburg (Figures A.5 - A.6 in Appendix A).

The residual distances of the computed photo test points in each study area were evaluated for normal fit using the SAS UNIVARIATE procedure. The procedure produces a test statistic for the null hypothesis that the input data values are a random sample from a normal distribution. If the sample size is less than fifty-one, the Shapiro-Wilk statistic, W, is computed. W must be greater than zero and less or equal to one, with small values of W leading to rejection of the null hypoth-

Table 4.5. Affine Transformation of Control Points from UTM to Scaled Photo Coordinates, Prentiss, N.C.

Model	Source	DF	Model Test Sum of Square	Mean Square	F Test Prob>F R Square Adj_R
x_a	Regression	2	52480051.92	26240025.96	223392.17 0.0001 0.9999 0.9999
	Residual	24	2819.08	117.46	
	Total	26	52482871.00		
y_a	Regression	2	197578774.31	98789387.12	587252.62 0.0001 1.0000 1.0000
	Residual	24	4037.35	168.22	
	Total	26	197582811.66		

Table 4.6. Affine Transformation Residuals of Control and Test Points from UTM to Scaled Photo Coordinates, Prentiss, N.C.

Control Points				Test Points			
P#	Residual (m)			P#	Residual (m)		
27	x_a	y_a	Dist.	20	x_a	y_a	Dist.
1	14.161	1.569	14.248	2	8.671	-9.661	12.982
3	6.476	-26.299	27.084	15	-4.649	0.072	4.649
6	3.407	-18.331	18.645	17	7.403	-14.299	16.102
7	-1.485	-7.049	7.204	21	8.033	5.772	9.892
8	-4.626	-12.197	13.045	23	12.349	-24.337	27.291
9	-21.599	0.002	21.599	27	4.873	-11.981	12.934
13	18.479	12.123	22.101	29	14.860	-11.987	19.092
14	7.661	7.758	10.904	30	-10.655	-0.896	10.692
16	-3.688	8.445	9.216	33	13.556	-13.361	19.033
18	-18.053	-2.118	18.177	38	-10.224	-9.993	14.296
20	3.634	9.610	10.275	40	3.137	-19.565	19.815
22	-6.397	15.301	16.585	41	9.152	-6.711	11.349
25	1.761	18.070	18.156	44	0.762	-1.715	1.877
28	-5.233	14.027	14.971	48	-7.193	16.868	18.338
31	-9.369	7.458	11.975	51	-2.155	18.324	18.450
32	-14.100	10.874	17.806	52	-1.396	25.359	25.398
34	9.053	13.538	16.286	57	0.362	11.042	11.048
37	-0.369	4.120	4.136	59	2.851	18.536	18.754
39	10.492	8.971	13.805	60	-11.393	-5.328	12.578
42	2.155	6.016	6.390	62	4.477	-5.892	7.400
43	4.223	-1.639	4.530				
45	2.025	-14.025	14.171	RMSE	8.353	13.978	
46	1.415	-4.957	5.155	Mean	2.141	-1.988	14.599
49	2.174	-25.271	25.364				
50	17.016	-0.648	17.028	W:Normal 0.975		Prob<W	0.838
55	-21.100	-13.196	24.886	Std Dev			6.390
56	1.883	-12.157	12.302	T Critical			1.729
				T Test Statistic			1.684
RMSE	10.412	12.461					
Mean	0.000	0.000	14.668				

Table 4.7. Affine Transformation of Control Points from UTM to Scaled Photo Coordinates, Blacksburg, Va.

Model	Source	DF	Model Test Sum of Square	Mean Square	F Test Prob>F R Square Adj_R
	Regression	2	217042263.14	108521131.57	863587.55
	Residual	27	3392.91	125.66	0.0001
x_a	Total	29	217045656.04		1.0000 1.0000
	Regression	2	320977809.28	160488904.64	1426731.33
	Residual	27	3037.15	112.49	0.0001
y_a	Total	29	320980846.43		1.0000 1.0000

Table 4.8. Affine Transformation Residuals of Control and Test Points from UTM to Scaled Photo Coordinates, Blacksburg, Va.

Control Points				Test Points			
P#	Residual (m)			P#	Residual (m)		
30	x_a	y_a	Dist.	29	x_a	y_a	Dist.
2	-13.784	-5.516	14.847	3	5.359	0.365	5.371
4	-11.011	-5.513	12.314	5	13.333	-5.640	14.477
7	-14.342	13.103	19.426	6	-3.735	0.928	3.848
9	-17.447	-10.774	20.505	8	19.099	-6.512	20.179
10	1.154	8.136	8.217	11	7.976	-10.127	12.891
13	1.764	19.462	19.541	12	2.959	-14.531	14.829
14	12.383	5.310	13.474	16	-17.429	-21.747	27.870
15	-6.083	-0.638	6.117	18	-12.060	-5.436	13.229
17	8.883	9.883	13.289	20	-3.117	-1.383	3.410
19	14.298	4.638	15.032	21	-9.165	-8.273	12.347
23	13.214	-8.241	15.573	22	-0.476	2.133	2.186
28	20.854	-7.181	22.055	24	-2.878	6.381	7.000
29	-8.694	-8.766	12.346	25	3.002	1.389	3.308
30	7.032	-1.186	7.131	26	9.103	-5.843	10.817
32	2.126	0.407	2.165	27	-11.449	-3.823	12.070
34	2.937	1.615	3.351	39	9.415	13.851	16.748
36	-0.702	-1.812	1.944	40	14.732	6.237	15.998
37	9.505	4.401	10.475	41	12.383	7.253	14.351
38	4.233	-2.314	4.824	42	2.669	1.554	3.089
43	-2.817	-4.889	5.643	46	1.368	-1.520	2.045
44	3.430	-17.225	17.563	48	-7.663	23.221	24.453
47	-8.651	-5.997	10.527	50	2.962	15.385	15.668
49	-13.553	-0.663	13.569	51	1.331	16.024	16.079
53	-0.210	-10.940	10.942	52	6.901	5.406	8.767
57	-25.004	14.679	28.995	55	-3.799	5.795	6.930
58	1.903	2.195	2.906	56	7.730	6.670	10.210
60	-7.482	-14.513	16.328	59	2.067	3.312	3.904
63	5.225	-2.187	5.665	61	-10.677	3.887	11.362
64	14.250	-5.817	15.392	62	-1.601	-12.766	12.866
68	6.585	30.347	31.053				
RMSE	10.816	10.233		RMSE	8.888	9.774	
Mean	0.000	0.000	12.707	Mean	1.322	0.765	11.252
				W:Normal	0.940	Prob<W	0.117
				Std Dev			6.588
				T Critical			1.701
				T Test Statistic			-0.768

esis. From Tables 4.6 and 4.8, the two data sets of the residual distances of both areas are normally distributed since the W values are large and the probabilities less than W are greater than 0.05 and the null hypothesis for normal fit test was accepted. Therefore, a t-test was used in testing the null hypothesis stated in section 3.3.2 for testing error in the uncorrected photo. The average residual distance of Prentiss photo is greater than 12.192 meters and that of Blacksburg photo is less than 12.192 meters. For Prentiss, the null hypothesis was accepted and for Blacksburg the null hypothesis was obviously accepted with a negative test statistic. Based on the test results, position error in the uncorrected photo was less than or equal to 12.192 meters.

Because both study areas are located in mountain areas with great relief, it is suspected that estimated errors in uncorrected photos are actually significantly greater than 12.192 meters. Three points, well distributed both around the fiducial center and in elevation, were selected from each photo to estimate average relief displacement of an image point over the plane with mean elevation of study area. According to elevation range of the DEM, mean elevation for the Prentiss area is 1079 meters and that for the Blacksburg area is 675 meters. Flying height over the plane was obtained by subtracting photo orientation element Z_L (Table 4.10) by mean elevation of study area. According to Wolf (1974), the equation used to calculate relief displacement on a tilted photograph is:

$$d = \frac{rh}{HS}$$

d = *relief displacement on the plane with mean elevation of study area*

r = *radial distance on the photo from the fiducial center to the displaced image*

h = *elevation of the displaced image over the plane*

H = *height of the perspective center over the plane*

S = *photo average scale*

Computed average relief displacement is 91 meters for the Prentiss area and 17 meters for the Blacksburg area (Table 4.9). Relief displacement for the Prentiss photo is greater than that for Blacksburg because the Prentiss area has greater relief in comparison with the Blacksburg area.

Estimated relief displacements for both areas are greater than estimated errors in the uncorrected photos, which represent errors mainly caused by image tilt and relief displacement. Because the control and test points selected are road intersections and intersections between roads and rivers, which are generally located in low-elevation and flat areas, all control and test points have relatively similar elevations. As a result, the affine transformation fitted control points well, root mean square errors of test points were small, and estimated errors in the uncorrected photos were underestimated. If there were some control and test points in high elevation areas and control and test points were well distributed over the photos, estimated errors should be larger and errors in the uncorrected photos should be significantly greater than 12.192 meters. Appropriately distributed control and test points will generate more accurate estimations of errors in uncorrected photos. Otherwise, errors will be underestimated.

4.3 Space Resection and Errors in Corrected Photos

Space resection computes six exterior orientation elements of the perspective center in the ground coordinate system. The six elements were computed iteratively by giving initial approximate values and control point coordinates (Table 4.10). The computations of space resection for both area photos converged well with standard deviations of residuals 0.000122 meter for Prentiss and 0.000130 meter for Blacksburg. Based on the six orientation elements, the collinearity equations were established for both study areas. These equations were used to transform points from the ground to photo coordinates. Photo coordinates were further transformed into rows and columns

Table 4.9. Relief Displacement Estimation

	Prentiss			Blacksburg		
H (m)	12163			12487		
S	1:58,000			1:58,000		
P#	h (m)	r (m)	d (m)	h (m)	r (m)	d (m)
1	441	0.0890	187	81	0.0500	19
2	218	0.0813	85	65	0.0915	28
3	6	0.0452	1	5	0.1078	3
Mean			91			17

in the digital photo using the affine transformation established by the five photo points with known rows and columns and photo coordinates. Through resampling, the computed photo points were registered into the DEM grid and the digital photo was geometrically corrected.

The transformation equations from point "A" in the UTM coordinate system to the corresponding point "a" in the photo coordinate system for Prentiss are:

$$\begin{bmatrix} m_{11} & m_{12} & m_{13} \\ m_{21} & m_{22} & m_{23} \\ m_{31} & m_{32} & m_{33} \end{bmatrix} = \begin{bmatrix} 0.999897 & -0.008899 & -0.011288 \\ 0.009136 & 0.999735 & 0.021136 \\ 0.011097 & -0.021237 & 0.999713 \end{bmatrix}$$

$$x_a = -f\left[\frac{m_{11}(X_A - 277646.184453) + m_{12}(Y_A - 3880469.013122) + m_{13}(Z_A - 13242.432280)}{m_{31}(X_A - 277646.184453) + m_{32}(Y_A - 3880469.013122) + m_{33}(Z_A - 13242.432280)} \right]$$

$$y_a = -f\left[\frac{m_{21}(X_A - 277646.184453) + m_{22}(Y_A - 3880469.013122) + m_{23}(Z_A - 13242.432280)}{m_{31}(X_A - 277646.184453) + m_{32}(Y_A - 3880469.013122) + m_{33}(Z_A - 13242.432280)} \right]$$

From table 4.11, the root mean square error for the computed x coordinates of the photo control points is 7.716 meters and that for the computed y coordinates of the photo control points is 5.756 meters. The average residual distance of the computed photo control points is 8.154 meters. The means of x and y residuals of photo control points are near to zero. The mean of x residuals for the computed photo test points using the transformation is 1.998 meters and the mean of y residuals for the computed photo test points is 0.961 meters. Because the means of x and y residuals are not approximately zero, there were some systematic errors in the corrected digital photo. The systematic errors may be caused by many sources, such as paper photo scanning, paper map distortion or digitizing. The root mean square error for the computed x coordinates of the photo test points is 9.091 meters and that for the computed y coordinates of the photo test points is 9.622 meters. Estimated error in the corrected photo of Prentiss is 11.396 meters.

The transformation equations from point "A" in the UTM coordinate system to the corresponding point "a" in the photo coordinate system for Blacksburg are:

Table 4.10. Space Resection

	Prentiss		Blacksburg	
	Initial	Computed	Initial	Computed
ω	0.000000	0.021240	0.000000	-0.006750
ϕ	0.000000	0.011097	0.000000	0.000256
κ	-0.010709	-0.009137	-0.010923	-0.010911
X_L	281650.132	277646.184	550100.596	550053.996
Y_L	3881420.266	3880469.013	4117690.501	4117637.264
Z_L	12836.923	13242.432	12806.120	13162.694
Std Dev		0.000122		0.000130

Where: ω, ϕ and κ are in radians and X_L, Y_L and Z_L are in meters.

Table 4.11. Space Resection Residuals of Control and Test Points from UTM to Scaled Photo Coordinates, Prentiss, N.C.

Control Points				Test Points			
P#	Residual (m)			P#	Residual (m)		
27	x_a	y_a	Dist.	20	x_a	y_a	Dist.
1	-1.945	-1.743	2.611	2	7.839	10.338	12.974
3	-4.542	-1.899	4.923	15	-10.954	9.379	14.420
6	-4.039	-0.622	4.087	17	5.423	-2.699	6.058
7	5.741	2.988	6.472	21	1.740	20.033	20.108
8	4.134	0.473	4.161	23	2.582	-9.577	9.919
9	17.971	-0.123	17.972	27	-6.315	3.460	7.201
13	-7.529	-2.119	7.822	29	11.410	0.946	11.449
14	-7.612	1.835	7.830	30	-14.585	10.040	17.707
16	-1.910	-1.076	2.192	33	18.808	-5.377	19.562
18	10.743	11.777	15.941	38	-6.987	-3.385	7.764
20	-8.107	1.829	8.311	40	8.235	-17.842	19.651
22	-4.667	-1.321	4.851	41	14.502	-5.522	15.518
25	-9.159	-9.490	13.189	44	3.403	-0.581	3.452
28	2.722	0.844	2.849	48	-4.584	0.860	4.664
31	7.473	2.838	7.994	51	4.485	1.400	4.699
32	11.312	-0.173	11.313	52	11.543	3.076	11.946
34	-2.502	-5.903	6.411	57	0.442	18.672	18.677
37	3.470	0.929	3.592	59	0.982	2.100	2.318
39	-11.415	-4.110	12.132	60	-9.790	-13.792	16.913
42	2.112	-4.507	4.977	62	1.786	-2.313	2.922
43	-2.631	3.279	4.204				
45	1.256	13.797	13.854	RMSE	9.091	9.622	
46	1.540	2.940	3.319	Mean	1.998	0.961	11.396
49	-1.615	8.171	8.329				
50	-9.815	-15.091	18.002	W:Normal	0.918	Prob<W	0.096
55	15.363	0.523	15.372	Std Dev			6.207
56	-6.265	-4.030	7.449	T Critical			1.729
				T Test Statistic			-0.573
RMSE	7.716	5.756					
Mean	0.003	0.005	8.154				

$$\begin{bmatrix} m_{11} & m_{12} & m_{13} \\ m_{21} & m_{22} & m_{23} \\ m_{31} & m_{32} & m_{33} \end{bmatrix} = \begin{bmatrix} 0.999940 & -0.010912 & -0.000182 \\ 0.010910 & 0.999918 & -0.006753 \\ 0.000256 & 0.006750 & 0.999977 \end{bmatrix}$$

$$x_a = -f\left[\frac{m_{11}(X_A - 550053.995984) + m_{12}(Y_A - 4117637.264110) + m_{13}(Z_A - 13162.694282)}{m_{31}(X_A - 550053.995984) + m_{32}(Y_A - 4117637.264110) + m_{33}(Z_A - 13162.694282)} \right]$$

$$y_a = -f\left[\frac{m_{21}(X_A - 550053.995984) + m_{22}(Y_A - 4117637.264110) + m_{23}(Z_A - 13162.694282)}{m_{31}(X_A - 550053.995984) + m_{32}(Y_A - 4117637.264110) + m_{33}(Z_A - 13162.694282)} \right]$$

From table 4.12, the root mean square error for the computed x coordinates of the photo control points is 8.063 meters and that for the computed y coordinates of the photo control points is 6.391 meters. The average residual distance of the computed photo control points is 9.195 meters. The means of x and y residuals of photo control points are near to zero. The mean of x residuals for the computed photo test points using the transformation is 0.415 meters and the mean of y residuals for the computed photo test points is -0.942 meters. Because the means of x and y residuals are not approximately zero, there were some systematic errors in the corrected digital photo. The root mean square error for the computed x coordinates of the photo test points is 5.309 meters and that for the computed y coordinates of the photo test points is 5.607 meters. Estimated error in the corrected photo of Blacksburg is 7.071 meters.

In comparison with the affine transformation, the transformation using the collinearity equations has decreased residuals (errors) of computed photo control and test points (Figures A.7 - A.8 in Appendix A) and root mean square errors. For Prentiss photo, the average residual distance of the computed photo test points has been decreased by 3.202 meters and the average residual distance has been reduced by 4.181 meters for Blacksburg photo (Table 4.13). For both areas, the computed average residual distances are less than 12.192 meters. However, errors still exist in the corrected photos. Those errors may be caused by errors in control and test points and the other error sources (except image tilt and relief displacement). Therefore, errors removed and existing in the corrected photo must be evaluated using residual distances of computed photo test points. From Tables 4.11

Table 4.12. Space Resection Residuals of Control and Test Points from UTM to Scaled Photo Coordinates, Blacksburg, Va.

Control Points				Test Points			
P#	Residual (m)			P#	Residual (m)		
30	x_a	y_a	Dist.	29	x_a	y_a	Dist.
2	10.009	-0.510	10.022	3	-0.006	-5.099	5.099
4	3.085	0.448	3.117	5	2.399	-4.383	4.997
7	2.868	-9.806	10.217	6	-8.535	-0.825	8.575
9	9.041	8.302	12.275	8	8.788	-3.038	9.298
10	-8.126	-3.573	8.877	11	3.895	-0.235	3.902
13	1.013	-2.435	2.637	12	0.587	-5.649	5.680
14	-5.306	2.897	6.045	16	3.355	-5.947	6.828
15	4.193	-6.547	7.774	18	-0.735	-6.169	6.213
17	9.962	-0.042	9.962	20	1.843	-1.514	2.386
19	2.055	-6.596	6.908	21	-7.721	-1.956	7.965
23	-15.075	3.014	15.374	22	-4.912	-3.412	5.980
28	-17.569	-1.626	17.644	24	-6.527	-1.056	6.612
29	13.066	-3.672	13.572	25	0.151	-6.089	6.091
30	6.819	-7.481	10.122	26	4.317	-12.350	13.083
32	-9.339	-1.531	9.463	27	-7.162	-10.796	12.955
34	-8.626	-4.050	9.530	39	3.834	9.729	10.457
36	-4.296	2.222	4.837	40	8.841	1.997	9.063
37	-6.975	-3.909	7.996	41	5.821	3.689	6.892
38	-6.840	-0.755	6.882	42	-4.060	-0.937	4.167
43	-1.795	-1.683	2.461	46	-1.682	-7.202	7.396
44	-4.702	13.354	14.158	48	-4.532	10.190	11.153
47	5.218	-0.406	5.233	50	3.649	4.249	5.602
49	4.274	-4.885	6.491	51	0.634	8.004	8.029
53	1.294	1.417	1.918	52	5.206	3.457	6.249
57	12.232	-0.398	12.239	55	-2.878	-0.328	2.897
58	-1.512	7.283	7.439	56	9.562	-0.544	9.577
60	8.436	14.116	16.445	59	3.066	1.384	3.365
63	-1.454	7.238	7.382	61	-8.771	4.575	9.893
64	-9.364	11.560	14.877	62	3.599	2.933	4.643
68	7.456	-11.796	13.955				
RMSE	8.063	6.391		RMSE	5.309	5.607	
Mean	0.001	0.005	9.195	Mean	0.415	-0.942	7.071
				W:Normal	0.967	Prob<W	0.531
				Std Dev			2.802
				T Critical			1.701
				T Test Statistic			-9.843

Table 4.13. Errors Removed Using the Collinearity Condition Equations

Prentiss				Blacksburg			
Test Residual Dist.				Test Residual Dist.			
P# 20	Affine Tran.	Collin. Equa.	Diff. Score (m)	P# 29	Affine Tran.	Collin. Equa.	Diff. Score (m)
2	12.982	12.974	0.007	3	5.371	5.099	0.272
15	4.649	14.420	-9.771	5	14.477	4.997	9.480
17	16.102	6.058	10.044	6	3.848	8.575	-4.726
21	9.892	20.108	-10.215	8	20.179	9.298	10.880
23	27.291	9.919	17.372	11	12.891	3.902	8.989
27	12.934	7.201	5.733	12	14.829	5.680	9.149
29	19.092	11.449	7.642	16	27.870	6.828	21.041
30	10.692	17.707	-7.014	18	13.229	6.213	7.016
33	19.033	19.562	-0.528	20	3.410	2.386	1.024
38	14.296	7.764	6.532	21	12.347	7.965	4.382
40	19.815	19.651	0.164	22	2.186	5.980	-3.794
41	11.349	15.518	-4.169	24	7.000	6.612	0.388
44	1.877	3.452	-1.575	25	3.308	6.091	-2.783
48	18.338	4.664	13.673	26	10.817	13.083	-2.266
51	18.450	4.699	13.751	27	12.070	12.955	-0.885
52	25.398	11.946	13.451	39	16.748	10.457	6.291
57	11.048	18.677	-7.629	40	15.998	9.063	6.934
59	18.754	2.318	16.436	41	14.351	6.892	7.459
60	12.578	16.913	-4.335	42	3.089	4.167	-1.078
62	7.400	2.922	4.477	46	2.045	7.396	-5.350
				48	24.453	11.153	13.300
Mean			3.202	50	15.668	5.602	10.066
Std Dev			8.958	51	16.079	8.029	8.050
T Critical			2.093	52	8.767	6.249	2.517
T Test Statistic			1.598	55	6.930	2.897	4.033
				56	10.210	9.577	0.633
				59	3.904	3.365	0.539
				61	11.362	9.893	1.469
				62	12.866	4.643	8.223
				Mean			4.181
				Std Dev			6.088
				T Critical			2.048
				T Test Statistic			3.698

and 4.12, the two data sets of residual distances were also normally distributed since the probabilities less than W are greater than 0.05 and the null hypothesis for normal fit test was accepted. A t-test was used to test the null hypothesis stated in section 3.3.4. The alternative hypothesis for testing error in the corrected photo was significantly rejected with a negative test statistic for both areas. Geometric errors in the corrected photos were less than or equal to 12.192 meters. It can be concluded that the corrected digital photos satisfy the USGS 1:24,000 topographical map accuracy standard because the correction using the collinearity equations is not influenced by the distribution of control and test points in principle.

For testing error removed in correction, difference scores of residual distances of photo test points using affine transformation and the collinearity equations were assessed via a t-test. For Prentiss, the test statistic failed to reject the null hypothesis, but for Blacksburg, the null hypothesis was rejected. Based solely on test results, error removed for the Prentiss photo is not significantly greater than zero and error removed for the Blacksburg photo is significantly greater than zero. Because estimated error in the uncorrected photo was underestimated, estimated removed error was also underestimated. Estimated removed errors should be larger than those computed for both areas. In fact, error removed in the photo of the Prentiss area should be clearly significant and even larger than that for the photo of the Blacksburg area due to more irregular and higher terrain. The distribution of the test and control points in the Prentiss area contributed to the non-significant result. Better distributed control and test points and larger sample size will lead to rejection of the null hypothesis. For the Blacksburg area, because the control and test points were relatively better distributed and the sample size was larger, the test result was significant.

In a GIS application, there also exist errors in those spatial data layers digitized from the USGS 1:24,000 topographical maps. The range of the average position error is generally supposed to be around the map accuracy, 12.192 meters. Based on test results of errors in corrected digital photos, average point errors in the corrected digital photos are less than or equal to 12.192 meters. The spatial data layers extracted from the corrected digital photos can correctly overlay with other spatial data layers and produce correct results of spatial data analyses. It is feasible to correct the digital

photo by space resection using the control points obtained from the USGS 1:24,000 topographical map when the photo is going to be used in a GIS application which includes spatial data layers digitized from topographical maps.

4.4 Degree of Error Caused by Errors in Ground Control and DEM data

Point distance offset, line length change, and polygon area change increase with an increase of the absolute maximum error (ERROR) in control points and test data elevations (Tables A.6 and A.7 in Appendix A). As expected, errors in point, line, and polygon in corrected digital photo are positively related to errors in ground control data for space resection and DEM data for photo registration.

For the digital photo of Prentiss, point distance offset (D1) caused by error in ground control points and point distance offset (D2) caused by error in test point elevations are significantly and positively related to the magnitude of errors (ERROR) in ground control points and in test point elevations (Figure 4.1 and Table 4.14). Both model tests for dependent variables D1 and D2 and independent variable ERROR (regressor) are highly significant with P values 0.0001 and near 1.0 adjusted R-square values. The t-test statistic for slope in model D1 is 72.512 and in model D2 is 146.581. For the digital photo of Blacksburg, point distance offsets D1 and D2 are also significantly and positively related to ERROR (Figure 4.2 and Table 4.15). Both model tests for dependent variables D1 and D2 and regressor ERROR are highly significant with P values 0.0001 and adjusted R-square values near 1.0. The t-test statistic for slope in model D1 is 62.294 and in model D2 is 170.091. All estimated slopes of the models in both areas are positive. The H_1 hypotheses stated in section 3.3.6 for testing the relationships of point error in the corrected photo with error in

ground control points and error in the corresponding point ground elevation are significant. Point error in the corrected digital photo is positively related to error in ground control points and error in the corresponding ground point elevation.

From Figures 4.1 and 4.2 and Tables 4.14 and 4.15, it can be seen that point distance offset caused by error in the X, Y, and Z coordinates of the ground control points is greater than point distance offset caused by the same error range in the elevation of the corresponding ground point. The slopes of the linear regression models of point distance offsets caused by errors in ground control points for both areas are greater than those caused by errors in the corresponding point elevation. When the absolute maximum error (ERROR) in the ground control points is 50 meters, point distance offset is around 10 meters (Tables A.6 and A.7 in Appendix A). Point distance offset is only around 10 meters when ERROR in the corresponding ground point elevation is 60 meters. Because the accuracy of ground control points is assumed to be within 12.192 meters and the absolute accuracy of the DEM is 7 meters, the impact of ERROR with 15 meters in ground control points and the impact of ERROR with 10 meters in test feature elevations must be evaluated. When ERROR in ground control points is 15 meters, point distance offset is within 4 meters in both areas. Point distance offset is less than 2 meters as ERROR in point ground elevation is 10 meters. Therefore, in both area photo corrections, the accuracy of ground control points has a greater impact than the accuracy of the DEM on point accuracy of the corrected digital photo. Because the accuracy of ground control and test data obtained from 1:24,000 USGS topographical maps is considered to be within the map accuracy standard and the USGS DEM for digital photo registration has 7-meters absolute accuracy, it is confirmed that the obtained ground control data and the DEM are appropriate and accurate for digital photo resection and correction for most GIS applications.

For the digital photo of Prentiss, line length change percentage (L1) caused by error in ground control points and line length change percentage (L2) caused by error in line ground elevations are significantly and positively related to errors (ERROR) in control points and in line ground elevations (Figure 4.3 and Table 4.16). Both model tests for dependent variables L1 and L2 and

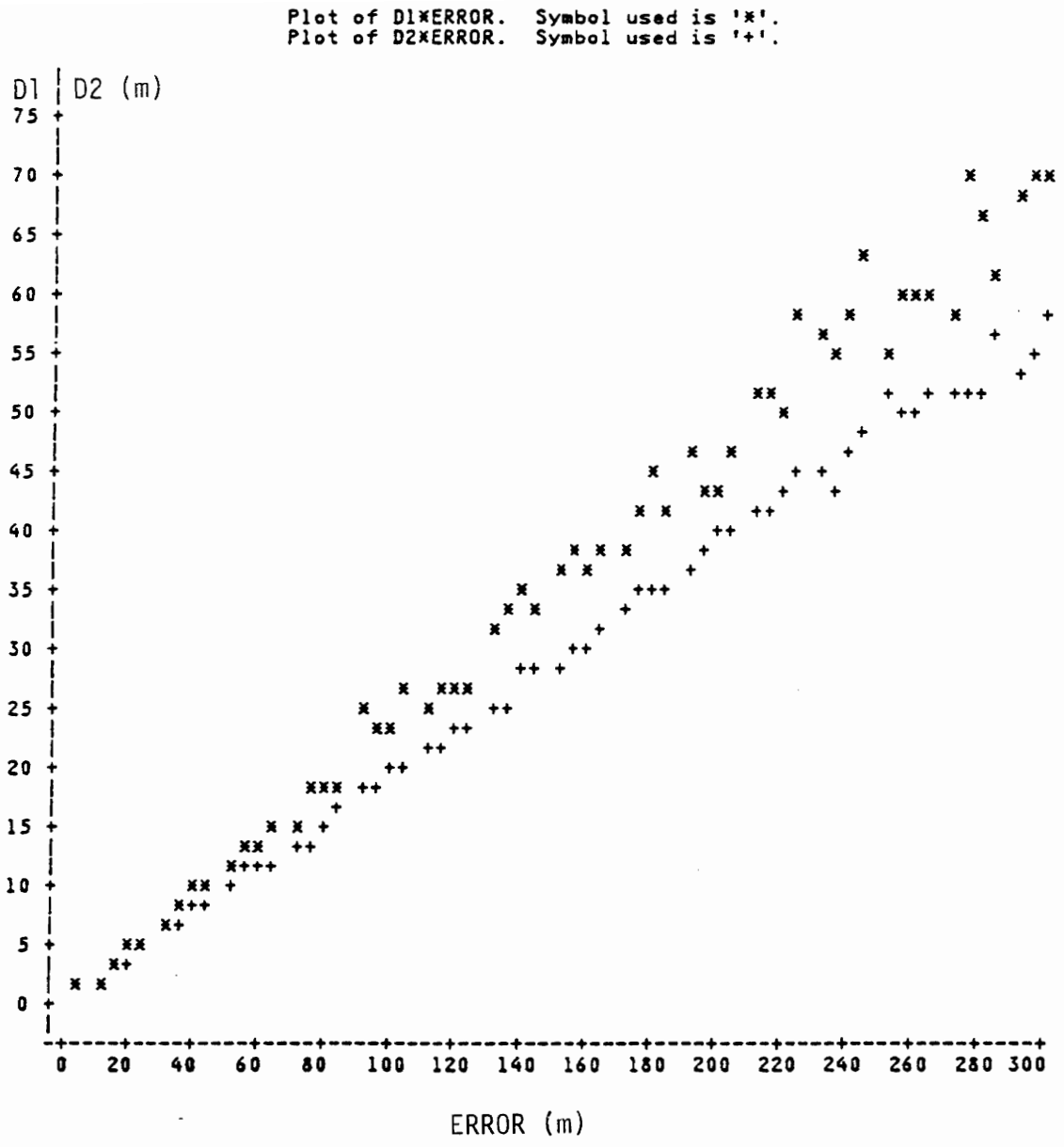

Figure 4.1. **Plotting Point Distance Offsets versus Errors in Ground Control Points and Point Elevation, Prentiss, N.C.:** D1 is point distance offset caused by error in ground control; D2 is point distance offset caused by error in point elevation; and ERROR is absolute maximum error.

Table 4.14. Linear Regression Analyses of Point Distance Offsets, Prentiss, N.C.

Model Test

Model	Source	DF	Sum of Square	Mean Square	F Test Prob>F R Square Adj_R
	Regression	1	24771.27198	24771.27198	5257.9250
	Residual	58	273.25108	4.71123	0.0001
D1	Total	59	25044.52305		0.9891
					0.9889
	Regression	1	16594.15167	16594.15167	21485.8590
	Residual	58	44.79508	0.77233	0.0001
D2	Total	59	16638.94675		0.9973
					0.9973

Parameter Estimates

Model	Vari.	DF	Parameter Estimate	Standard Error	T for H0: Parameter=0	Prob>|T|
	Intercept	1	0.222350	0.56750932	0.392	0.6966
D1	ERROR	1	0.234654	0.00323609	72.512	0.0001
	Intercept	1	0.150254	0.22977735	0.654	0.5158
D2	ERROR	1	0.192058	0.00131025	146.581	0.0001

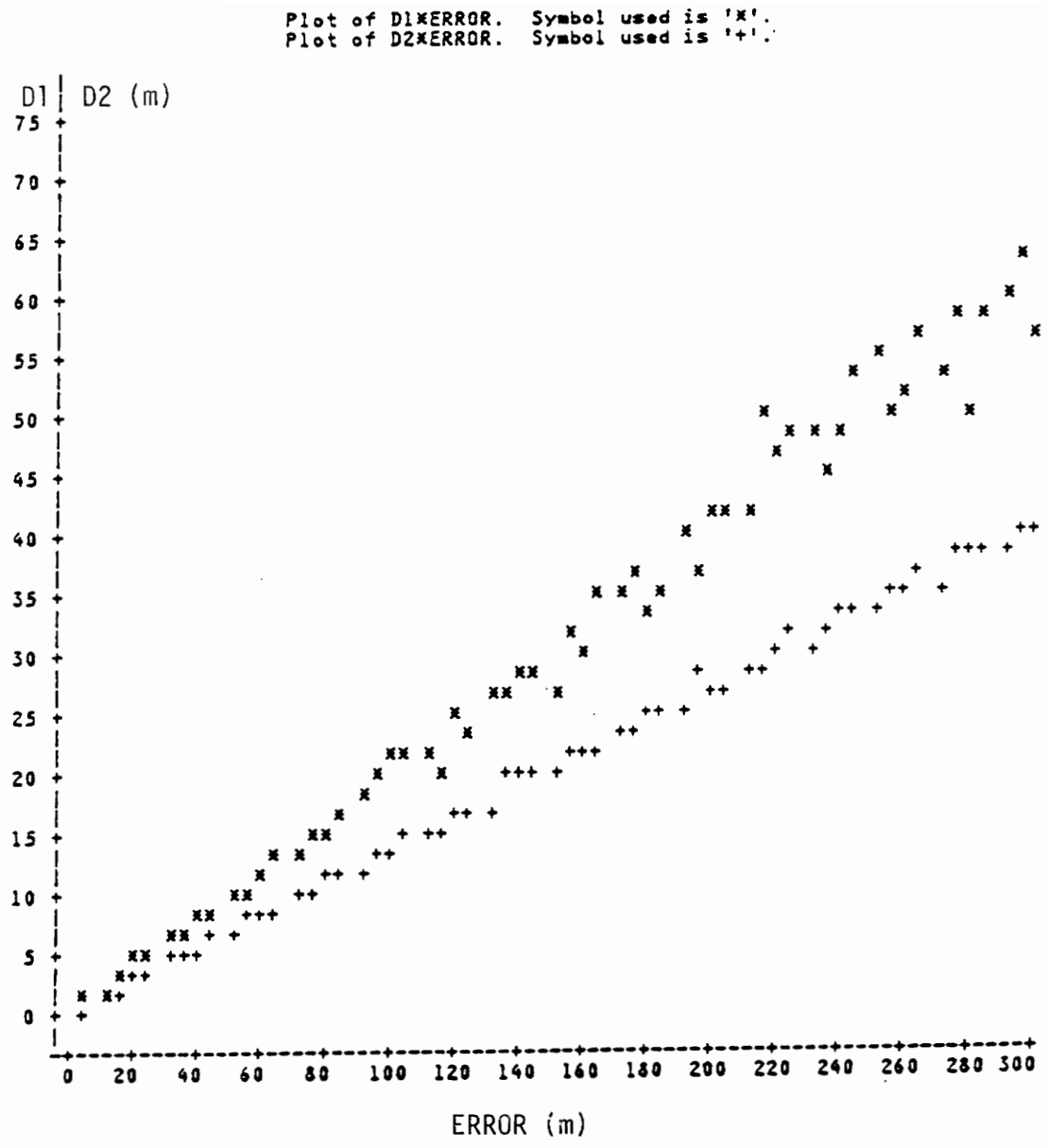

Figure 4.2. **Plotting Point Distance Offsets versus Errors in Ground Control Points and Point Elevation, Blacksburg, Va.:** D1 is point distance offset caused by error in ground control; D2 is point distance offset caused by error in point elevation; and ERROR is absolute maximum error.

Table 4.15. Linear Regression Analyses of Point Distance Offsets, Blacksburg, Va.

Model Test

Model	Source	DF	Sum of Square	Mean Square	F Test Prob>F R Square Adj_R
	Regression	1	18885.53644	18885.53644	3880.5930
	Residual	58	282.26640	4.86666	0.0001
D1	Total	59	19167.80285		0.9853
					0.9850
	Regression	1	8127.24296	8127.24296	28931.0140
	Residual	58	16.29324	0.28092	0.0001
D2	Total	59	8143.53620		0.9980
					0.9980

Parameter Estimates

Model	Vari.	DF	Parameter Estimate	Standard Error	T for H0: Parameter=0	Prob>|T|
	Intercept	1	-0.403076	0.57679522	-0.699	0.4875
D1	ERROR	1	0.204889	0.00328904	62.294	0.0001
	Intercept	1	0.180818	0.13857850	1.305	0.1971
D2	ERROR	1	0.134408	0.00079021	170.091	0.0001

regressor ERROR are highly significant with P values 0.0001 and adjusted R-square values near 0.94. The t-test statistic for slope in model L1 is 27.434 and in model L2 is 29.262. For the digital photo of Blacksburg, line length change percentages L1 and L2 are also significantly and positively related to ERROR in ground control points and in line ground elevations (Figure 4.4 and Table 4.17). Both model tests for dependent variables L1 and L2 and regressor ERROR are greatly significant with P values 0.0001 and near 0.93 adjusted R-square values. The t-test statistic for slope in model L1 is 27.232 and in model L2 is 27.920. All estimated slopes in both areas are positive. The H_1 hypotheses stated in section 3.3.6 for testing the relationships of line length change in the corrected photo with error in ground control points and with error in line ground elevations are significant. Line length change in the corrected digital photo is positively related to error in ground control points and error in line ground elevations.

From the linear regression models of line length change percentages for both areas (Figures 4.3 and 4.4 and Tables 4.16 and 4.17), line length change percentage caused by error in X, Y and Z coordinates of ground control points is less than that caused by the same range of error in elevations for error ranges greater than 80 meters (the impact on point position and polygon area is opposite to the impact on line length). The slopes of the linear regression models of line length change percentages versus ERROR in ground control points are less than those caused by ERROR in line ground elevations. In photo correction using the collinearity condition equations, the accuracy of the DEM has a greater impact on photo line length. When the corrected photo is going to be used for line feature extraction (roads or rivers), a more accurate DEM is preferable. From Figures 4.3 and 4.4, line length changes caused by errors in ground elevations are parabolically related to those errors. Within $\pm$ 80 meters, error in ground control points and test feature ground elevations have almost the same impact on line length. When ERROR in ground control points is 15 meters, line length change percentage is less than 0.12% (Tables A.6 and A.7 in Appendix A). Line length change percentage is less than 0.11% as error in line ground elevations is within $\pm$ 10 meters. Line length error is small with photo correction using ground control from the USGS 1:24,000 topographic map and USGS DEM data.

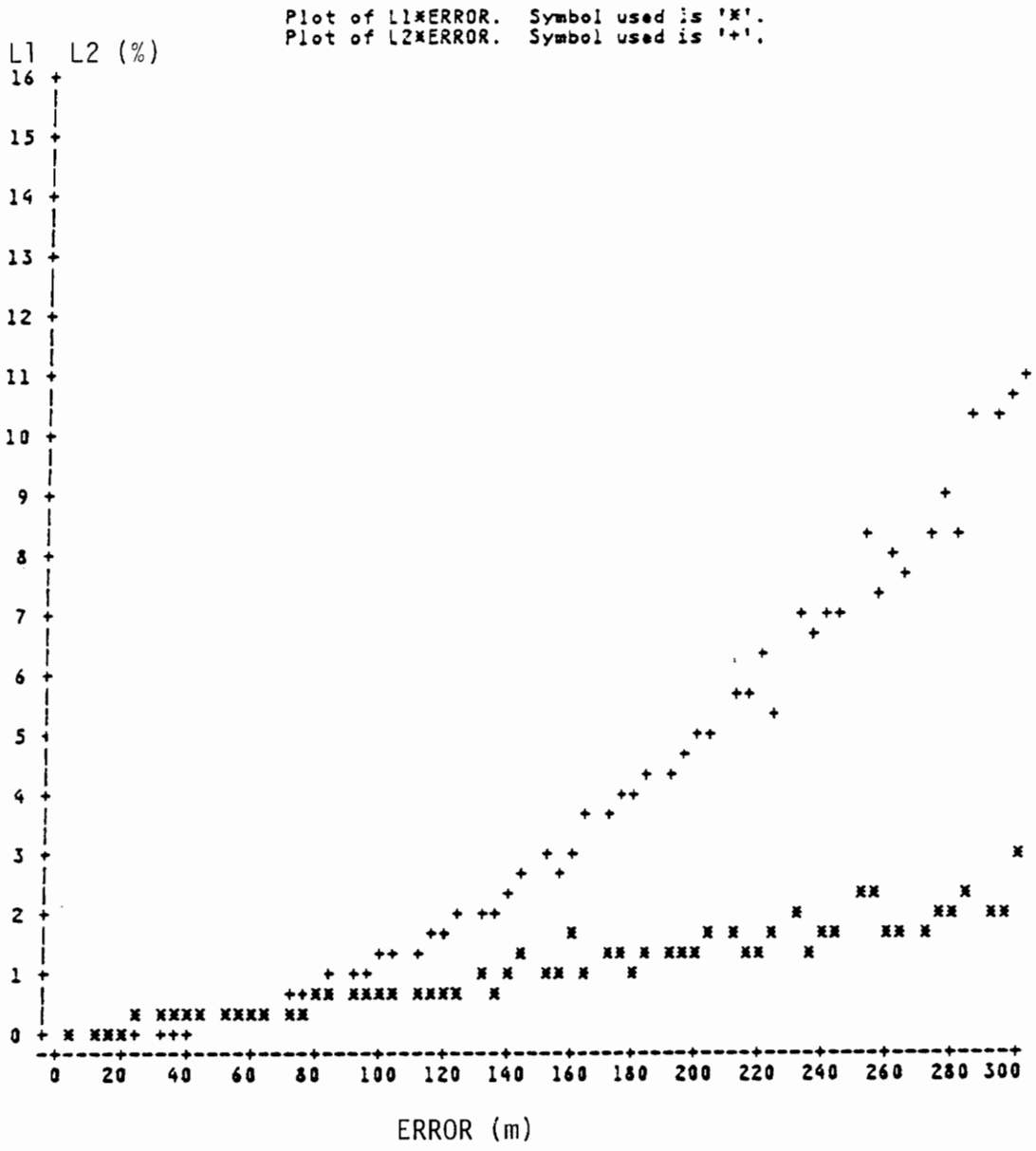

Figure 4.3. **Plotting Line Length Change Percentages versus Errors in Ground Control Points and Line Elevations, Prentiss, N.C.:** L1 is line length change caused by error in ground control; L2 is line length change caused by error in line elevations; and ERROR is absolute maximum error.

Table 4.16. Linear Regression Analyses of Line Length Change Percentages, Prentiss, N.C.

Model Test

Model	Source	DF	Sum of Square	Mean Square	F Test Prob>F R Square Adj_R
	Regression	1	25.06617	25.06617	752.6260
	Residual	58	1.93169	0.03330	0.0001
L1	Total	59	26.99786		0.9285
					0.9272
	Regression	1	605.43651	605.43651	856.2460
	Residual	58	41.01077	0.70708	0.0001
L2	Total	59	646.44729		0.9366
					0.9355

Parameter Estimates

Model	Vari.	DF	Parameter Estimate	Standard Error	T for H0: Parameter=0	Prob>|T|
	Intercept	1	-0.039033	0.04771559	-0.818	0.4167
L1	ERROR	1	0.007464	0.00027209	27.434	0.0001
	Intercept	1	-1.887096	0.21985737	-8.583	0.0001
L2	ERROR	1	0.036685	0.00125369	29.262	0.0001

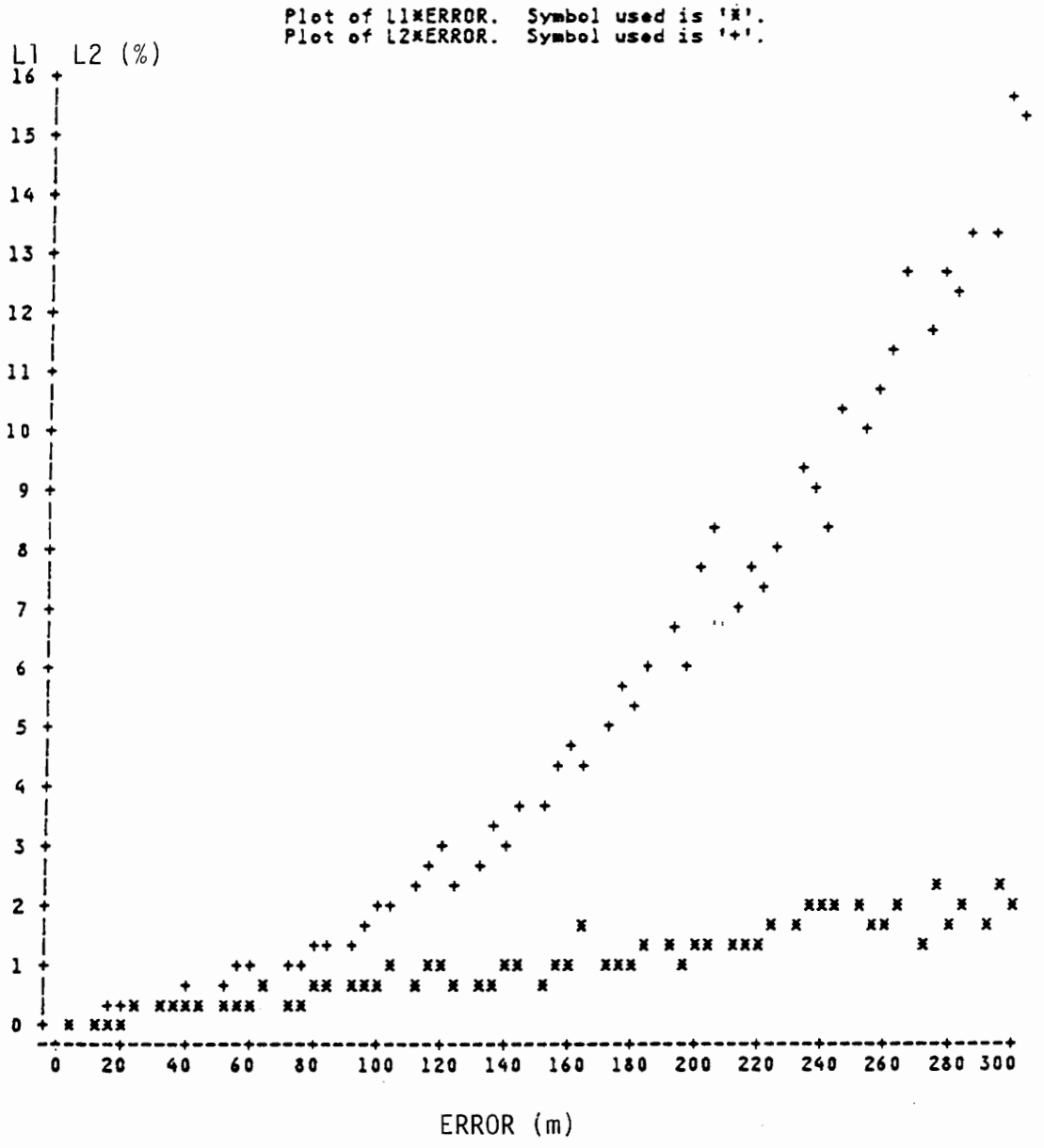

Figure 4.4. **Plotting Line Length Change Percentages versus Errors in Ground Control Points and Line Elevations, Blacksburg, Va.:** L1 is line length change caused by error in ground control; L2 is line length change caused by error in line elevations; and ERROR is absolute maximum error.

Table 4.17. Linear Regression Analyses of Line Length Change Percentages, Blacksburg, Va.

Model Test

Model	Source	DF	Sum of Square	Mean Square	F Test Prob>F R Square Adj_R
	Regression	1	23.36909	23.36909	741.5820
	Residual	58	1.82772	0.03151	0.0001
L1	Total	59	25.19681		0.9275
					0.9262
	Regression	1	1118.99871	1118.99871	779.5110
	Residual	58	83.25980	1.43551	0.0001
L2	Total	59	1202.25851		0.9307
					0.9296

Parameter Estimates

Model	Vari.	DF	Parameter Estimate	Standard Error	T for H0: Parameter=0	Prob>|T|
	Intercept	1	-0.042552	0.04641381	-0.917	0.3630
L1	ERROR	1	0.007207	0.00026466	27.232	0.0001
	Intercept	1	-2.377965	0.31326345	-7.591	0.0001
L2	ERROR	1	0.049873	0.00178631	27.920	0.0001

For the digital photo of Prentiss, polygon area change percentage (A1) caused by error in ground control points and polygon area change percentage (A2) caused by error in polygon ground elevations are significantly and positively related to ERROR in ground control points and in polygon ground elevations (Figure 4.5 and Table 4.18). Both model tests for dependent variables A1 and A2 and regressor ERROR are highly significant with P values 0.0001 and adjusted R-square values near 0.95. The t-test statistic for slope in model A1 is 29.054 and in model A2 is 33.266. For the digital photo of Blacksburg, polygon area change percentages A1 and A2 are also significantly and positively related to ERROR in ground control points and in polygon ground elevations (Figure 4.6 and Table 4.19). Both model tests for dependent variables A1 and A2 and regressor ERROR are highly significant with P values 0.0001 and adjusted R-square values near 0.95. The t-test statistic for slope in model A1 is 27.298 and in model A2 is 32.648. All estimated slopes of test models in both areas are positive. The H_1 hypotheses stated in section 3.3.6 for testing the relationship between polygon area change in the corrected photo with error in ground control points and with error in polygon ground elevations are significant. Polygon area change in the corrected digital photo is positively related to error in ground control points and error in polygon ground elevations.

From the linear regression models of polygon area change (Tables 4.18 and 4.19), the slopes of the linear regression models caused by error in ground control points are greater than those caused by error in ground elevations. In photo correction using collinearity equations, the accuracy of ground control points has a greater impact on polygon areas. When the corrected photo is to be used for area feature extraction, such as land use polygon, more accurate ground control points are preferable. For the Prentiss photo, the impact of ground control point error on polygon area is much greater than the same range of error in ground elevations (Figure 4.5). For the Blacksburg photo, the difference is not so obvious (Figure 4.6). When ERROR in ground control points is 15 meters, polygon area error is less than 0.3%. Polygon area error is less than 0.065% when error in polygon ground elevations is within $\pm$ 10 meters. Therefore, the impact on polygon area is small with photo correction using ground control points obtained from 1:24,000 USGS topographical maps and USGS DEMs.

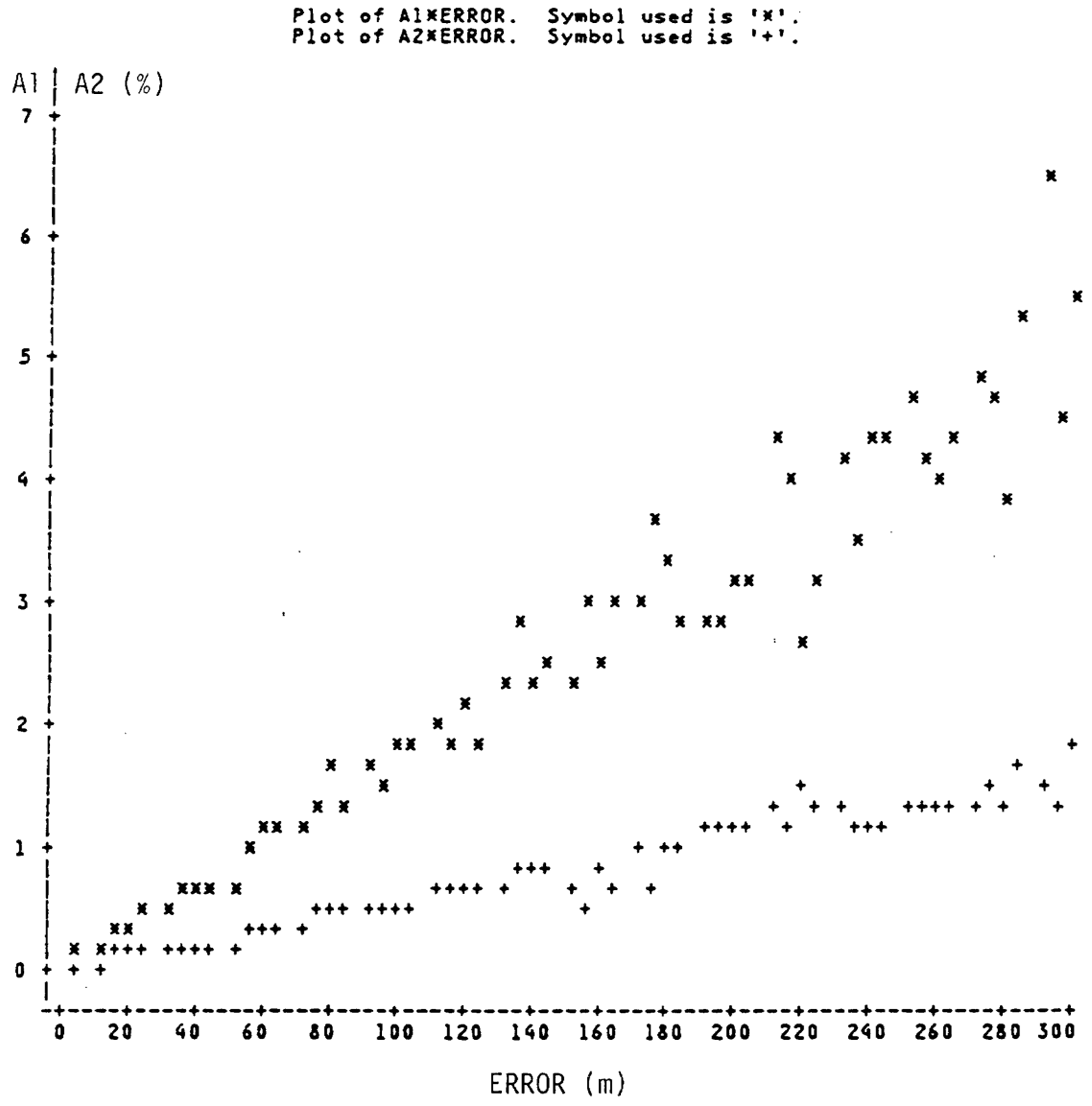

Figure 4.5. Plotting Polygon Area Change Percentages versus Errors in Ground Control Points and Polygon Elevations, Prentiss, N.C.: A1 is polygon area change caused by error in ground control; A2 is polygon area change caused by error in polygon elevations; and ERROR is absolute maximum error.

Table 4.18. Linear Regression Analyses of Polygon Area Change Percentages, Prentiss, N.C.

Model Test

Model	Source	DF	Sum of Square	Mean Square	F Test Prob>F R Square Adj_R
	Regression	1	129.94251	129.94251	844.1370
	Residual	58	8.92825	0.15394	0.0001
A1	Total	59	138.87076		0.9357
					0.9346
	Regression	1	12.95100	12.95100	1106.6010
	Residual	58	0.67880	0.01170	0.0001
A2	Total	59	13.62979		0.9502
					0.9493

Parameter Estimates

Model	Vari.	DF	Parameter Estimate	Standard Error	T for H0: Parameter=0	Prob>|T|
	Intercept	1	0.024553	0.10258294	0.239	0.8117
A1	ERROR	1	0.016995	0.00058496	29.054	0.0001
	Intercept	1	0.014356	0.02828538	0.508	0.6137
A2	ERROR	1	0.005365	0.00016129	33.266	0.0001

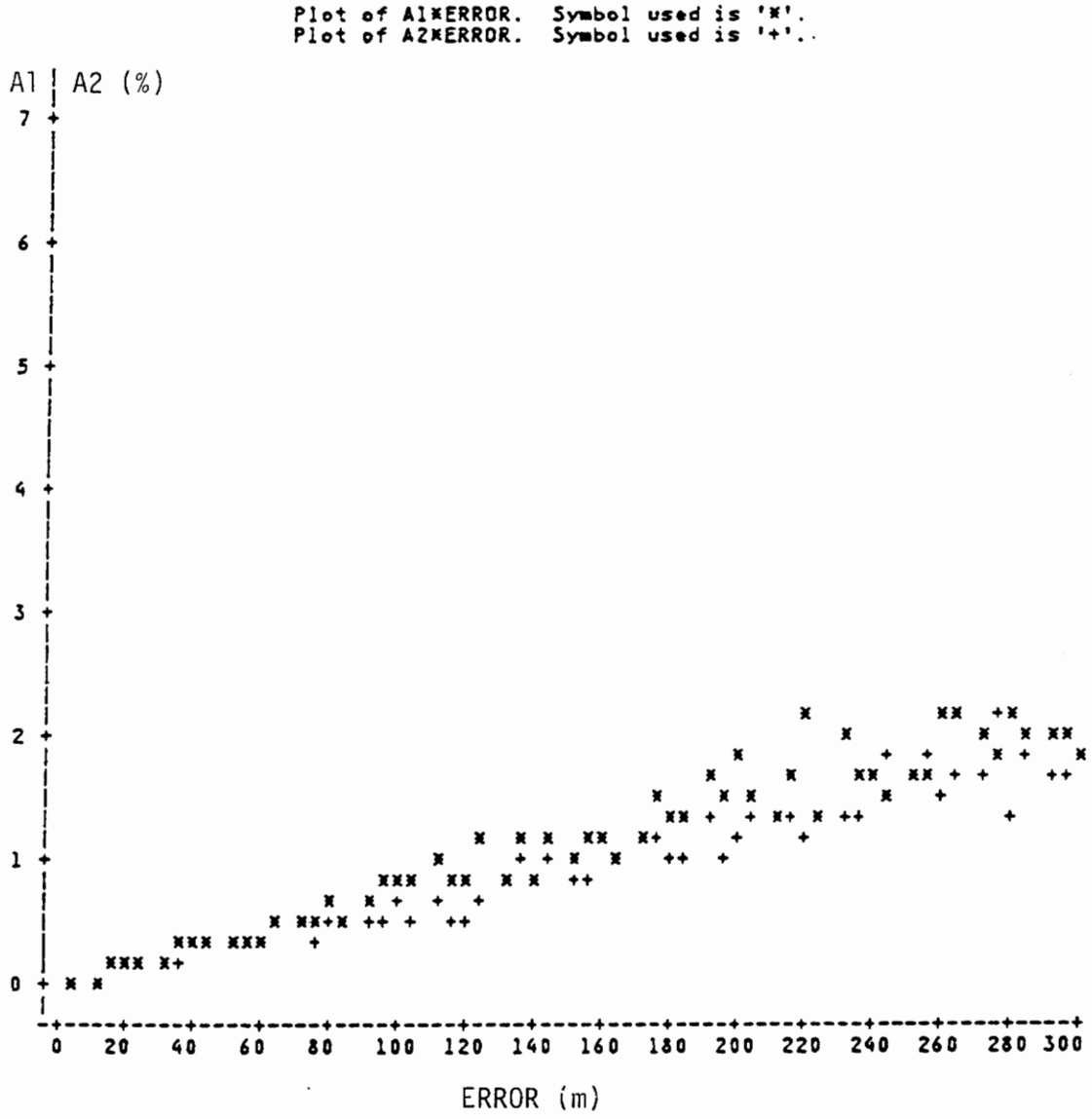

Figure 4.6. Plotting Polygon Area Change Percentages versus Errors in Ground Control Points and Polygon Elevations, Blacksburg, Va.: A1 is polygon area change caused by error in ground control; A2 is polygon area change caused by error in polygon elevations; and ERROR is absolute maximum error.

Table 4.19. Linear Regression Analyses of Polygon Area Change Percentages, Blacksburg, Va.

Model Test

Model	Source	DF	Sum of Square	Mean Square	F Test Prob>F R Square Adj_R
	Regression	1	22.26540	22.26540	745.1660
	Residual	58	1.73303	0.02988	0.0001
A1	Total	59	23.99843		0.9278
					0.9265
	Regression	1	17.40100	17.40100	1065.9050
	Residual	58	0.94686	0.01633	0.0001
A2	Total	59	18.34785		0.9484
					0.9475

Parameter Estimates

Model	Vari.	DF	Parameter Estimate	Standard Error	T for H0: Parameter=0	Prob>|T|
	Intercept	1	0.039619	0.04519545	0.877	0.3843
A1	ERROR	1	0.007035	0.00025772	27.298	0.0001
	Intercept	1	-0.014637	0.03340672	-0.438	0.6629
A2	ERROR	1	0.006219	0.00019049	32.648	0.0001

Chapter 5

CONCLUSIONS AND RECOMMENDATIONS

5.1 Conclusions

A computer program for a single digital-photo correction using the collinearity condition equations was developed to register data for use in a geographic information system. By knowing control points, average photo scale, and camera focal length, the mathematical correction model incorporates the digital elevation model (DEM) of photo area to correct geometric error caused by image tilt and relief displacement and to register the digital photo to the DEM ground coordinate system. The corrected single digital photo can then be digitized on computer screens or automatically interpreted to obtain thematic layers used in a GIS with spatial data layers from diverse data sources. Assessment of geometric error in photos before and after tilt and terrain correcting and a ground control and DEM data sensitivity analysis led to the following conclusions:

1. In single digital-photo correction using the collinearity condition equations for a GIS application, it is reasonable to obtain the ground control and test points from the corresponding

USGS 1:24,000 topographical map when control and test points are easily identifiable and well-defined on the map.

2. Geometric errors in the uncorrected digital photos were not significantly greater than 12.192 meters due to a lack of control and test points in high-elevation areas. Estimated errors in the uncorrected digital photos were underestimated.

3. Estimated error in the corrected digital photo of the Prentiss area is 11.397 meters and that is 7.071 meters in the corrected photo of the Blacksburg area. Geometric errors in the corrected photos were clearly not significantly different from the 90th percentile horizontal error of National Map Accuracy Standards compliant 1:24,000 scale maps. Photos corrected using the collinearity equations, developed using ground control data from the USGS 1:24,000 topographic map, photo control data from the digital photo and ground points from the USGS 7.5-minute DEM, will be compliant with National Map Accuracy Standards for 1:24,000 or smaller scale maps.

4. Estimated removed errors were also underestimated for both areas. Test results for errors removed in both areas were also influenced by the control and test point distribution and sample size. For the Blacksburg area, error removed was significant. However, error removed was not significant for the Prentiss photo due to the relatively poor distribution of control and test points and smaller sample size.

5. Errors in point position, line length and polygon area were positively related to the range of error both in ground control points and in the DEM data of point, line, and polygon features. For both study areas, point distance offset caused by error in X, Y and Z coordinates of ground control points was greater than point distance offset caused by the same range of error in point elevation. When error in ground control points was within $\pm$ 15 meters, point distance offset for both areas was less than 4 meters. Point distance offset was less than 2 meters when error in point ground elevation was within $\pm$ 10 meters. Line length change was parabolically and

positively related to error in line ground elevations for both areas. Line length change caused by error in X, Y and Z coordinates of ground control points was less than that caused by the same range of error in line ground elevations when ERROR was greater than 80 meters. When error in ground control points was within ± 15 meters, line length change was less than 0.12% for both photos. Line length change was less than 0.11% when error in line elevations was within ± 10 meters. Polygon area change caused by error in X, Y and Z coordinates of ground control points was greater than that caused by the same range of error in polygon ground elevations for both area photos. When error in ground control points was within ± 15 meters, polygon area change was less than 0.3%. Polygon area change was less than 0.065% when error in polygon elevations was within ± 10 meters. In conclusion, the accuracy of ground control points has greater impact on point position and polygon area and the accuracy of DEM data has greater impact on line length.

Based on the accuracy analyses of the uncorrected and corrected digital photos and the impact of errors in ground control points and DEM data on the accuracy of the corrected digital photos, it is both practical and accurate to use ground control points obtained from a USGS 1:24,000 topographical map and USGS DEM data for single digital photo correction by the collinearity condition equations for most GIS applications.

5.2 Recommendations for Further Study

It is recommended that further study and analysis be conducted. For the complete mathematical model for single digital photo correction, accurate ground data are needed to verify the accuracy of the correction model and the spatial data extracted from the photo. By using the USGS 1:24,000 topographical map to obtain ground control and test data for this study, the accuracy of ground control and test data is not as well-defined as it would be if field data were used. More accurate

ground points, lines, and polygons can be used to test the accuracy of photo exterior orientation and errors in point position, line length and polygon area. Test lines and polygons from the photo can be overlaid on lines and polygons obtained from maps. Recently, Global Positioning System (GPS) technology has been used to effectively obtain ground coordinates of field verification data with increased accuracy. GPS has great potential for obtaining field verification data whose locations can be positively identified on the image.

It is also recommended that more study areas and more lines and polygons be used in testing the impact of the errors in the ground control points and DEM data. Because both study areas are situated in the southern Appalachian mountains, they have relatively similar terrains. Study areas with different terrains are advisable to determine whether the relationships tested have the same patterns in error impact analyses. In this study, only one test line and one test polygon were used in each study area for error impact analysis. More lines and polygons can be used in test to obtain more stable relationship results.

Although the photo control and test points were considered accurate in this study, errors always exist in those points and they are significantly related to photo scale. It is recommended that different study areas with diverse photo scales be used in testing the impact of digital photo scale on rectification and testing the impact of error in photo control points on point position, line length and polygon area.

In applications requiring more accurate GIS overlay, or in close-range photogrammetry, errors caused by other sources, such as film distortion, lens distortion, atmospheric refraction, and principal point displacement, should also be corrected by incorporating additional parameters in the correction function and using continuous functions

5.3 Recommendations for Applications of the Study

Recently, the integration of geographic data from geographic information systems with remotely sensed data for analysis in environmental studies is becoming popular. Many GIS applications employ digital aerial photographs to provide current spatial data. This study makes routine correction of geometric error caused by image tilt and relief displacement in single digital photo prior to thematic data extraction feasible. The correction routine is generalized to study areas with relief displacement.

By having at least three control points in both the ground and photo, the camera focal length, and the DEM of photo area, a digital aerial photo can be corrected geometrically using the developed routine. Although the distribution of control points does not influence the accuracy of the correction in principle, it is still recommended that control points be well distributed around the fiducial center for the purpose of reducing random error in control points. The control for the accuracies of control points and the DEM depends on accuracy requirement for spatial data on the corrected digital photo. Most GIS applications in the United States have spatial data digitized from USGS 1;24,000 or smaller scale topographic maps. Based on error assessment in the corrected photo and impact analysis of errors in ground control and the DEM, it is appropriate and accurate to obtain ground control from USGS 1:24,000 topographic maps and to use USGS 7.5-minute DEMs for corrections of digital photos used in those GIS applications.

BIBLIOGRAPHY

Brouwer, Hans de, Valenzuela Carlos R, Valencia, Luz M and Sijmons, Koert, 1990, Rapid assessment of urban growth using GIS - RS techniques. *ITC Journal* , 1990-3, pp. 233 - 235.

Burrough, P. A., 1986, *Principles of Geographic Information Systems for Land Resources Assessment* . Oxford, New York: Clarendon Press, pp. 1 - 193.

Carson, W. W., 1985, An accuracy test of a new stereoscopic instrument. *Kartog. Plan.*, 2 (85): 227 - 233.

Carson, W. W., 1987, An analytical plotter based upon a personal computer. *In: Proc. Int. Conf. and workshop on analytical instrumentation* , International Society for Photogrammetry and Remote Sensing, 2 - 6 November 1987, Phoenix, AZ. American Society for Photogrammetry and Remote Sensing, Falls Church, VA, pp. 251 - 259.

DeMars, Clarence J. Jr., 1988, Advantages of single-photo resection in mapping detail from panoramic optical bar photographs. *Remote Sensing For Resource Inventory, Planning, And Monitoring* . The Second Forest Service Remote Sensing Application Conference, April 11 - 15, Slidell, Louisiana & NSTL, Mississippi.

Ehlers, Manfred, Edwards, Geoffrey, and Bedard, Yuan, 1989, Integration of remote sensing with geographic information systems: a necessary evolution. *Photogrammetric Engineering & Remote Sensing*, Vol. 55, pp. 1619 - 1627.

Ekelund, L., 1952, Photogrammetric triangulation with separately oriented stereo models. *Photogrammetria*, VIII (4): 276 - 284.

Gagnon, P. A., Agnard, J. P., Nolette, C., and Boulianne, M., 1990, A microcomputer-based general photogrammetric system. *Photogrammetric Engineering and Remote Sensing*, Vol. 56, May, pp. 623 - 625.

Ghosh, Sanjib K., 1988, *Analytical Photogrammetry*. 2nd ed., New York: Pergamon Press, pp. 1 - 308.

Gruen, Armin W., 1989, Digital photogrammetric processing systems: Current status and prospects. *Photogrammetric Engineering and Remote Sensing* , Vol. 55, pp. 581 - 586.

Hallert, B., 1957, Das Prinzip der numerischen Korrektionen und die Radialtriangulation. *Bildmess. Luftbildwes.*, 1: 1 - 5.

Harris, W. D., Tewinkle, G. C. and Whitten, C. A., 1963, Analytic aerotriangulation. *Technical Bulletin N0. 21, Corrected* , U.S. Department of Commerce, Coast and Geodetic Survey.

Helava, U. V., 1987, Digital comparator correlator system. *Proceedings "Intercommission Conference on Fast Processing of Photogrammetric Data"*, American Society for Photogrammetry and Remote Sensing, Interlaken, 2 - 4 June, pp. 404 - 418.

Hood, J., Ladner L., and Champion, R., 1989, Image processing techniques for digital orthophotoquad production. *Photogrammetric Engineering and Remote Sensing*, Vol. 55, pp. 1323 - 1329.

Hudson, William D., 1991, Photo interpretation of Montane Forests in the Dominican Republic. *Photogrammetric Engineering & Remote Sensing*, Vol. 57, pp. 79 - 84.

Kawata, Y., Ueno, S., and Kusaka, T., 1988, Radiometric correction for atmospheric and topographic effects on Landsat MSS images. *International Journal of Remote Sensing*, 9, 729 - 748.

Kleinn, K. E., 1987, PC power in analytical photogrammetry. *In: Proc. Int. Conf. Workshop on Analytical Instrumentation Society for Photogrammetry and Remote Sensing* , 2 - 6 November, 1987, Phoenix, AZ. American Society for Photogrammetry and Remote Sensing, Falls Church, VA, pp. 260 - 267.

Koency, G., 1980, How the analytical plotter works and differs from an analog plotter. *In: Proc. Analytical Plotter Symp. and Workshop* , 20 - 25 April, American Society for Photogrammetry and Remote Sensing, Falls Church, VA, pp. 31 - 75.

Koency, G., 1979, Methods and possibilities for digital differential rectification. *Photogrammetric Engineering and Remote Sensing*, 45, 727 - 734.

Lunetta, Ross S., Congalton, Russell G., Fenstermaker, Lynn K., Jensen, John R., McGwire, Kenneth C., and Tinney, Larry R., 1991, Remote Sensing and Geographic Information System Data Integration: Error Sources and Research Issues. *Photogrammetric Engineering & Remote Sensing*, Vol. 57, No. 6, pp. 677 - 687.

Maling, D. H., 1989, *Measurements from Maps*. 1st ed., New York: Pergamon Press, pp. 1 - 577.

Marble, D. F., and Peuquet, D. J., 1983, Geographic information systems and remote sensing. *Manual of Remote Sensing*, 2nd ed., Falls Church: American Society of Photogrammetry, pp. 923 - 958.

Moffitt, Francis H. and Mikhail, Edward M., 1980, *Photogrammetry*. 3rd ed., New York: Harper & Row, pp. 1 - 648.

Naithani, Krishna K, 1990, Can satellite images replace aerial photographs ? A photogrammetrist's view. *ITC Journal*, 1990 - 1, pp. 29 - 31.

Ott, Lyman, 1988, *An Introduction to Statistical Methods and Data Analysis*. 3rd ed., Boston: PWS-Kent Pub. Com., pp. 1 - 835.

Piwowar, Joseph M., LeDrew, Ellsworth F. and Dudycha, Douglas J., 1990, Integration of spatial data in vector and raster forms in a geographic information system environment. *INT.J. Geographic Information systems*, Vol. 4, No. 4, 429 - 444.

Piwowar, Joseph M., LeDrew, and Ellsworth F., 1990, Integrating spatial data: A user's perspective. *Photogrammetric Engineering & Remote Sensing*, Vol. 56, pp. 1497 - 1502.

Press, William H., Flannery, Brian P., Teukolsky, Saul A. and Vetterling, William T., 1989, *Numerical Recipes: the art of scientific computing* . New York, N.Y.: Cambridge University Press, pp. 1 - 702.

Reutebuch, S. E., 1987, PC- based analytical stereoplotter for use in Forest Service field offices. *1987 ASPRS-ACSM Fall Convension* , American Society for Photogrammetry and Remote Sensing, Falls Church, VA, pp. 223 - 236.

Robinson, G. J., and Jackson, M. J., 1985, Expert systems in map design. *Proceedings, Autocarto 7* , Washington D. C., pp. 430 - 439.

Thompson, Morris M., 1979, *Maps for America - Cartographic Products of the U.S. Geological Survey & Others.* Reston, Va.: The Survey, pp. 1 - 265.

Torlegard, Kennert, 1988, Transference of methods from analytical to digital photogrammetry. *Photogrammetria*, Vol. 42, pp. 197 - 208.

Trotter, Craig M., 1991, Remotely-sensed data as an information source for geographical information systems in natural resource management: a review. *INT. J. Geographical Information Systems*, Vol. 5, No. 2, 225 - 239.

Veress, J. and Youcai, S., 1987, A method for improving the efficiency of the sequential estimation procedure in photogrammetry. *Photogrammetric Engineering and Remote Sensing*, Vol. 53, No. 6, June 1987, pp. 613 - 616.

Warnei, William S., 1990, A PC-based analytical stereoplotter for wetland inventories: An efficient and economical photogrammetric instrument for field offices. *Forest Ecology and Management*, 33/34, 571 - 581.

Wolf, Paul R., 1974, *Elements of Photogrammetry*. New York: McGraw-Hill, pp. 1 - 562.

Appendix A

ADDITIONAL DATA TABLES AND FIGURES

Table A.1. Control Points, Prentiss, N.C.

P# 5	Row	Col.	Photo_x (m)	Photo_y (m)
1	1039	375	-0.030778	0.076701
2	2869	373	0.060763	0.076100
3	3378	1434	0.085902	0.022926
4	3148	2533	0.073857	-0.031953
5	2557	2761	0.044213	-0.043097

P# 27	Row	Col.	UTM_X (m)	UTM_Y (m)	UTM_Z (m)
1	1132	55	275990	3886324	743
3	2704	15	280732	3886383	656
6	3607	248	283435	3885626	637
7	3183	472	282147	3884968	661
8	2869	373	281213	3885288	654
9	2884	763	281246	3884107	649
13	3486	1104	282991	3883040	660
14	3378	1434	282653	3882063	637
16	3213	1277	282179	3882542	632
18	2885	1259	281209	3882625	644
20	2740	1146	280758	3882959	662
22	2624	1455	280396	3882035	652
25	2608	1068	280369	3883192	655
28	2858	1840	281071	3880871	676
31	3318	1925	282453	3880598	634
32	3302	1676	282428	3881340	633
34	3586	2019	283233	3880295	633
37	3345	2316	282496	3879430	644
39	3116	2382	281790	3879240	658
42	3364	2469	282539	3878969	644
43	3369	2502	282550	3878878	637
45	3148	2533	281885	3878810	667
46	3386	2635	282594	3878482	637
49	3272	3095	282216	3877133	644
50	3395	2992	282578	3877409	646
55	2956	2952	281300	3877566	669
56	2557	2761	280089	3878160	760

Table A.2. Test Points, Prentiss, N.C.

P# 20	Row	Col.	UTM_X (m)	UTM_Y (m)	UTM_Z (m)
2	1039	375	275709	3885363	766
15	3279	1522	282351	3881814	626
17	2996	1264	281531	3882587	656
21	2666	1322	280535	3882453	665
23	2449	1310	279887	3882470	666
27	2691	1826	280569	3880925	660
29	3043	1843	281637	3880854	653
30	3242	1912	282205	3880648	635
33	3555	2001	283165	3880351	632
38	3167	2254	281954	3879619	664
40	3282	2442	282300	3879040	655
41	3336	2468	282467	3878973	650
44	3437	2512	282759	3878840	632
48	3309	3046	282326	3877269	645
51	3443	3058	282733	3877227	638
52	3522	3127	282967	3877023	643
57	3426	1288	282817	3882517	635
59	3325	325	282587	3885412	640
60	3273	435	282407	3885061	650
62	2895	851	281255	3883837	654

Table A.3. Control Points, Blacksburg, Va.

P# 5	Row	Col.	Photo_x (m)	Photo_y (m)
1	1149	12	0.000000	0.112965
2	2258	1154	0.112673	0.000000
3	10	1122	-0.112724	0.000000
4	1442	368	0.029865	0.077683
5	1548	2152	0.043003	-0.100942

P# 30	Row	Col.	UTM_X (m)	UTM_Y (m)	UTM_Z (m)
2	565	535	546640	4121157	580
4	817	383	548143	4122070	586
7	829	552	548222	4121039	624
9	987	458	549170	4121629	601
10	1144	535	550093	4121150	637
13	1442	368	551873	4122142	662
14	1580	525	552693	4121218	660
15	1841	367	554272	4122173	602
17	1694	645	553382	4120496	693
19	1752	832	553729	4119383	678
23	1374	844	551466	4119320	634
28	1562	1029	552589	4118213	648
29	1591	1251	552798	4116886	653
30	1806	982	554063	4118491	667
32	526	807	546396	4119522	610
34	641	950	547088	4118666	614
36	285	1075	544962	4117917	618
37	404	1236	545668	4116948	605
38	703	1139	547462	4117539	612
43	1085	943	549753	4118720	609
44	937	1267	548868	4116791	605
47	1374	1426	551502	4115832	612
49	1701	1525	553468	4115238	600
53	1409	1809	551712	4113545	647
57	1739	2144	553722	4111516	602
58	1244	2114	550729	4111703	620
60	1063	1807	549647	4113556	627
63	902	1975	548673	4112536	628
64	771	1842	547876	4113335	619
68	513	2064	546343	4111965	612

Table A.4. Test Points, Blacksburg, Va.

P# 29	Row	Col.	UTM_X (m)	UTM_Y (m)	UTM_Z (m)
3	603	481	546857	4121476	582
5	707	507	547489	4121315	610
6	355	641	545366	4120516	593
8	937	511	548873	4121293	624
11	1258	471	550784	4121533	650
12	1331	453	551215	4121637	647
16	1697	564	553389	4120969	699
18	1653	795	553137	4119602	672
20	1558	713	552575	4120096	654
21	1456	518	551953	4121256	649
22	1290	756	550973	4119839	618
24	1312	929	551107	4118808	620
25	1379	910	551514	4118917	623
26	1191	867	550393	4119165	615
27	1547	961	552507	4118609	654
39	848	1063	548343	4118008	626
40	994	939	549220	4118744	627
41	950	855	548952	4119248	621
42	1032	802	549432	4119560	629
46	1299	1414	551045	4115896	611
48	1502	1376	552251	4116151	655
50	1364	1568	551440	4114992	647
51	1353	1604	551373	4114777	634
52	1334	1755	551269	4113862	621
55	1420	1988	551778	4112468	645
56	1548	2152	552561	4111488	652
59	1130	1893	550045	4113031	636
61	1020	1920	549373	4112869	633
62	971	2058	549092	4112024	608

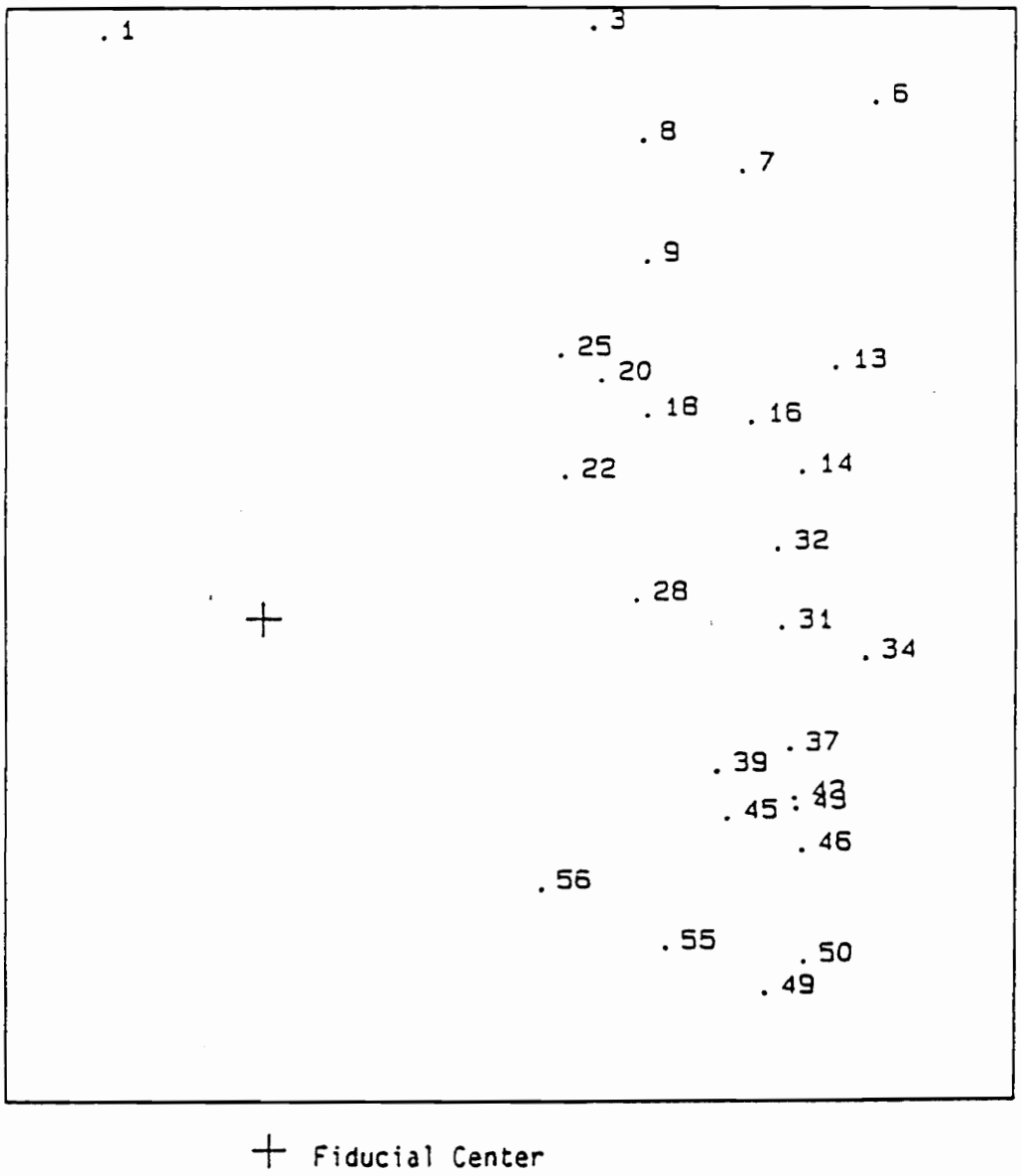

Figure A.1. Control Point Distribution, Prentiss, N.C.: Figure frame does not cover whole photo area.

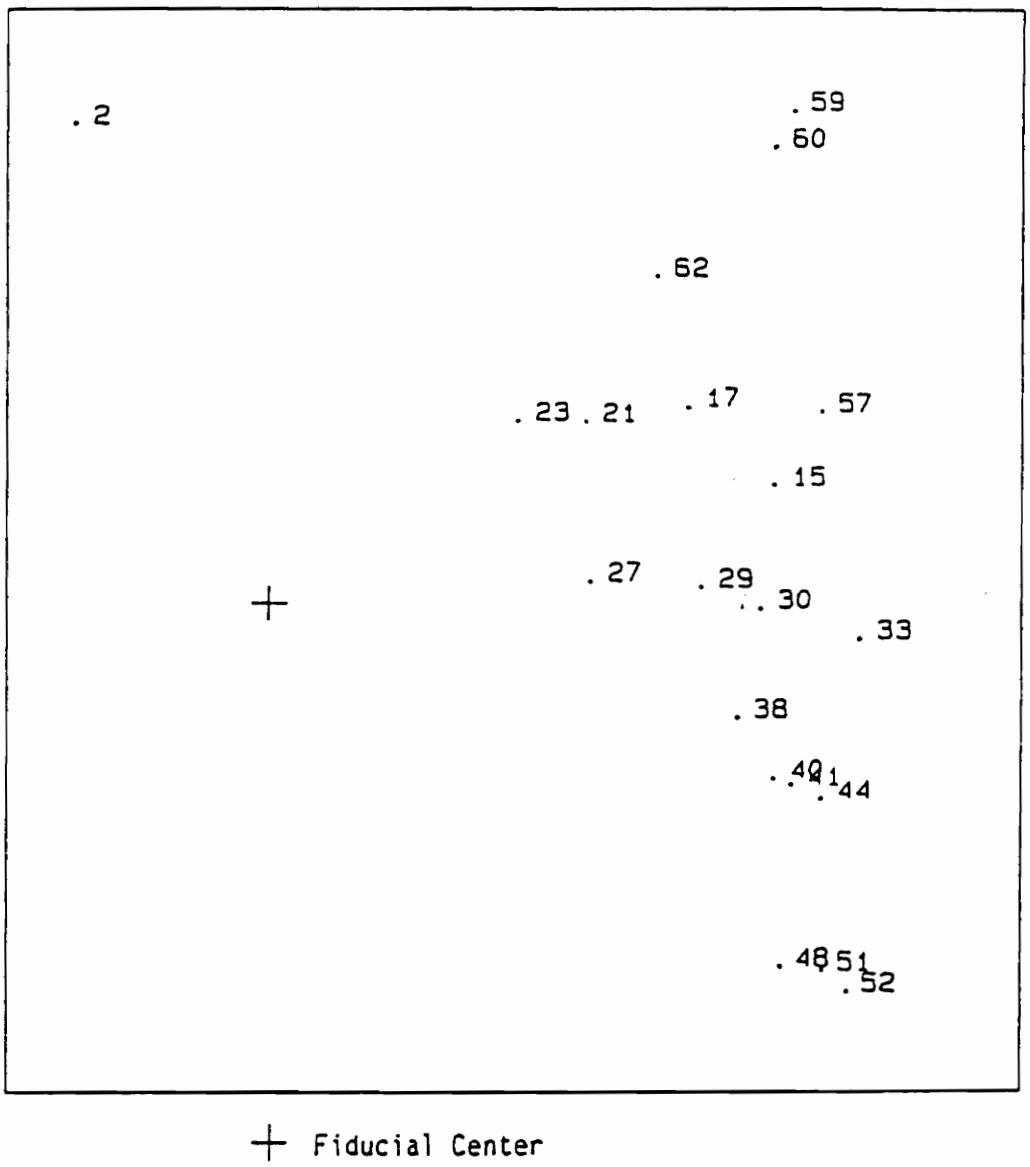

Figure A.2. Test Point Distribution, Prentiss, N.C.

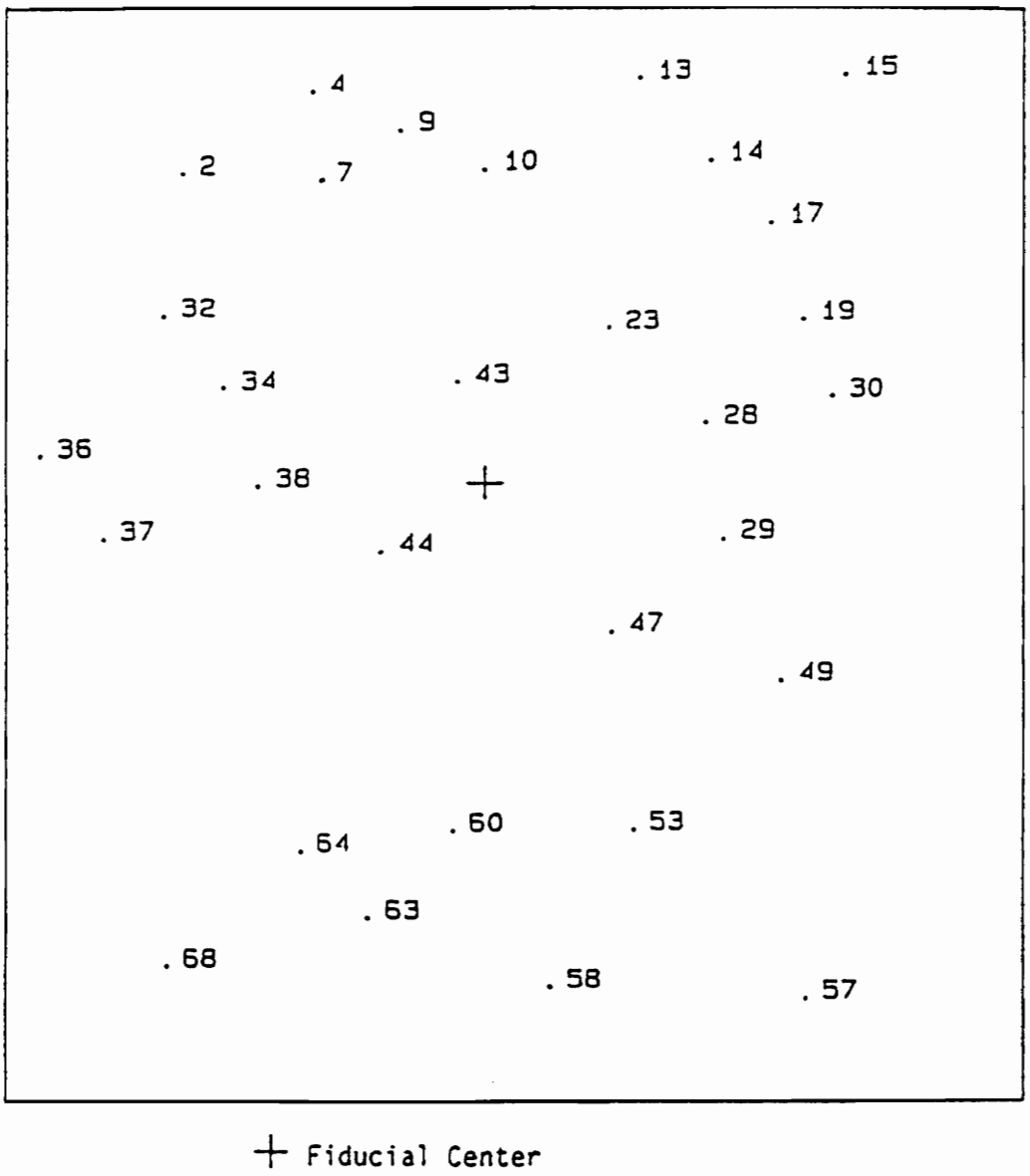

Figure A.3. Control Point Distribution, Blacksburg, Va.

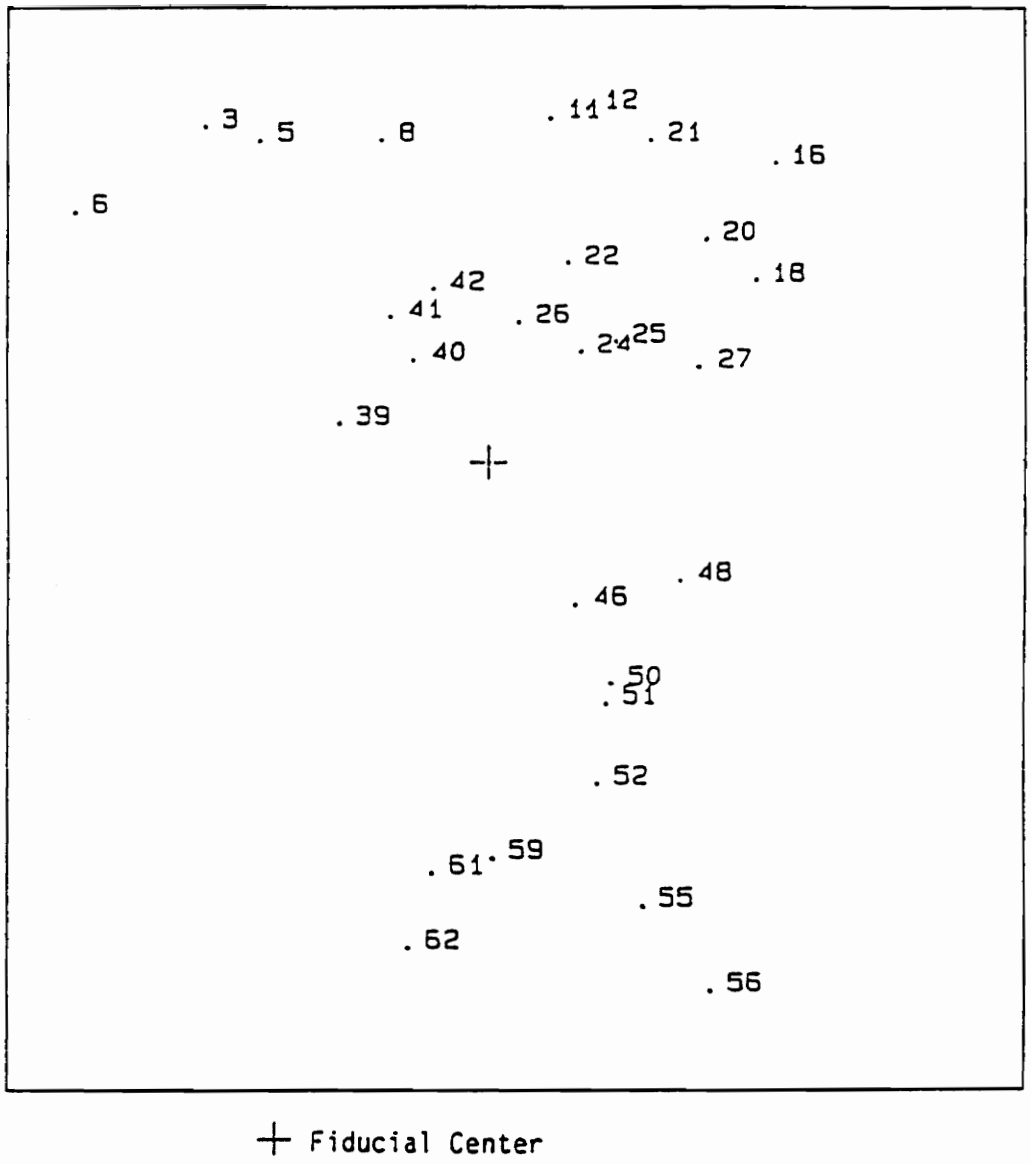

Figure A.4. Test Point Distribution, Blacksburg, Va.

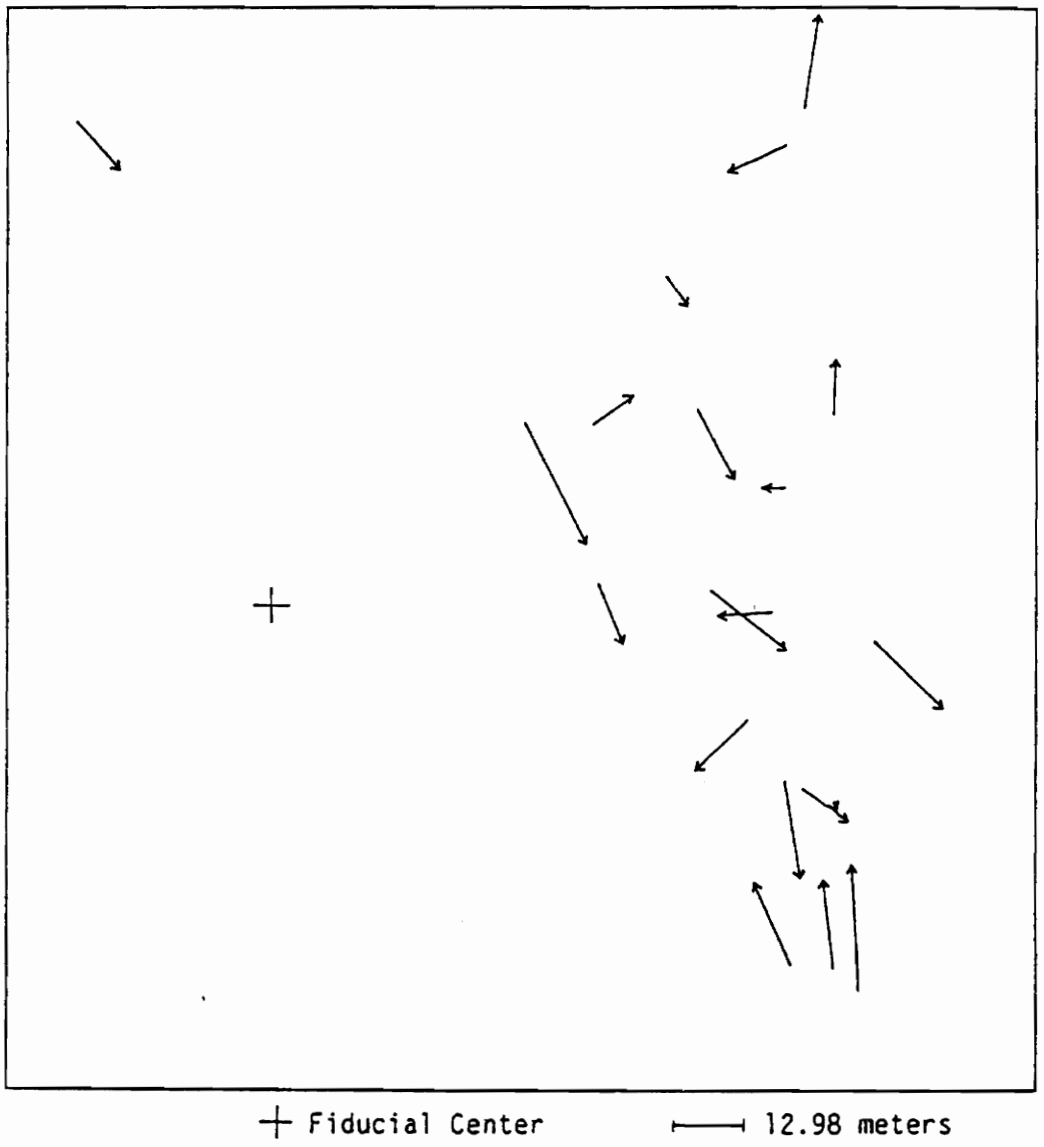

Figure A.5. Vector Errors of Computed Test Points by Affine Transformation, Prentiss, N.C.

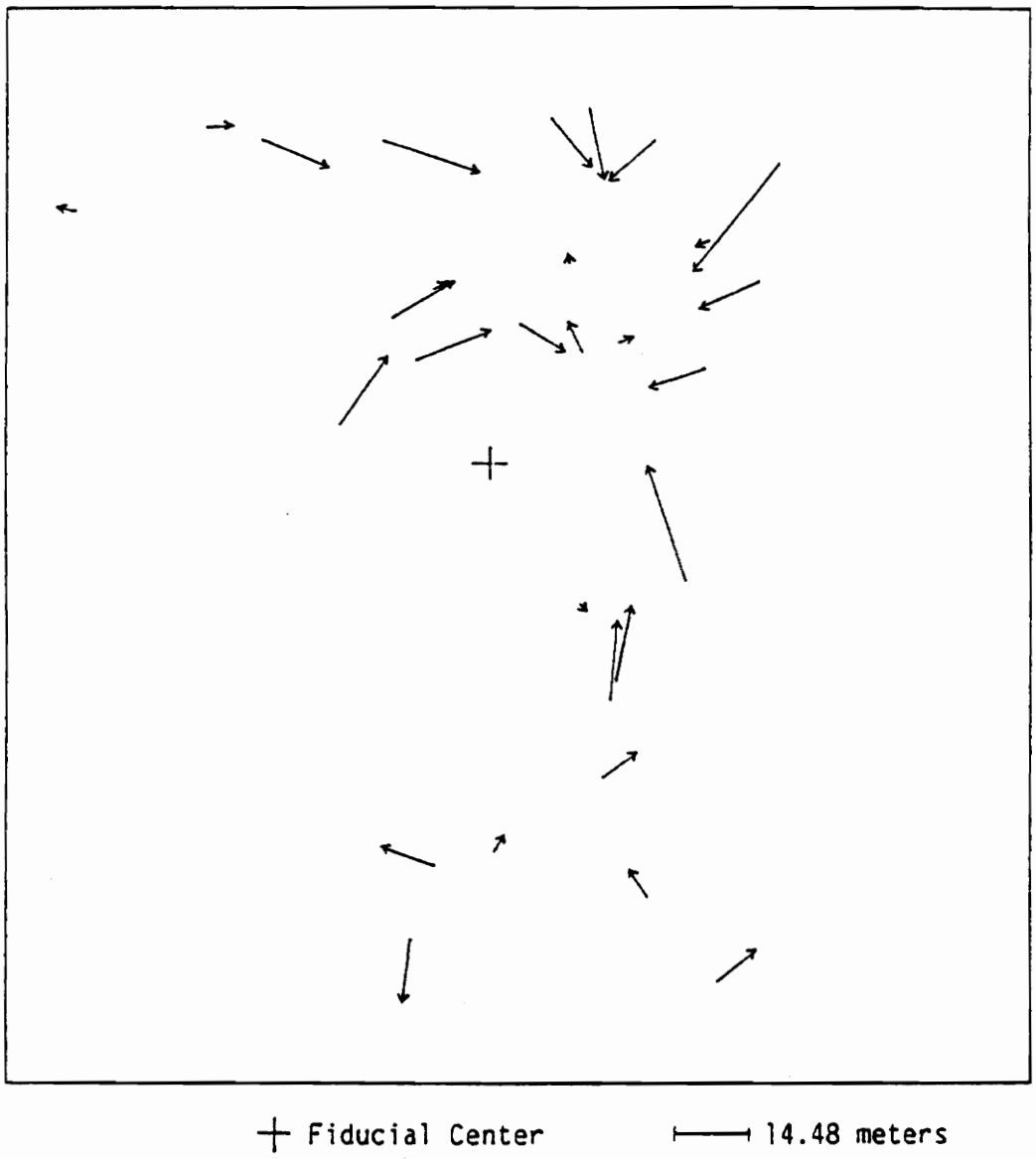

Figure A.6. Vector Errors of Computed Test Points by Affine Transformation, Blacksburg, Va.

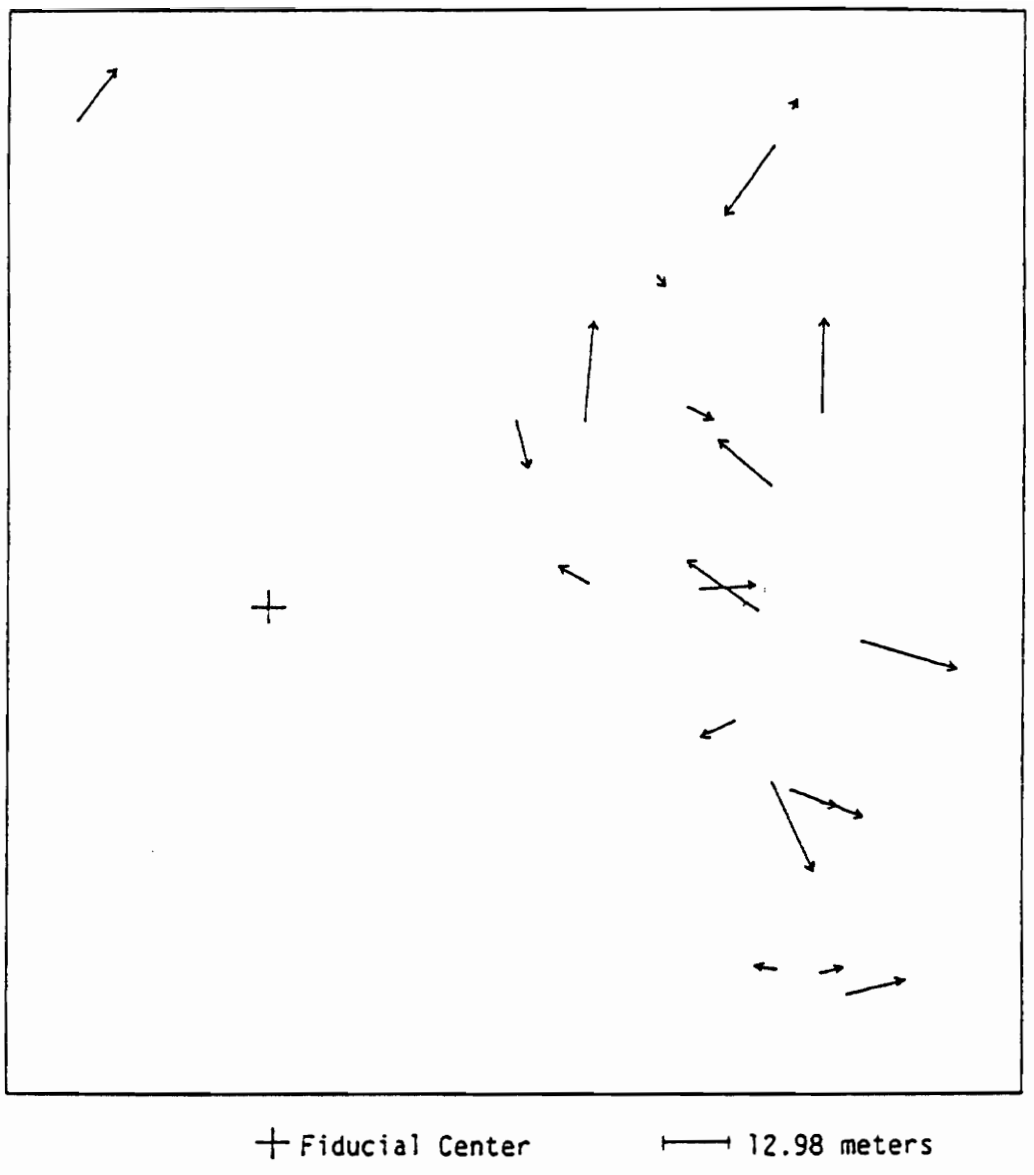

Figure A.7. Vector Errors of Computed Test Points by the Collinearity Equations, Prentiss, N.C.

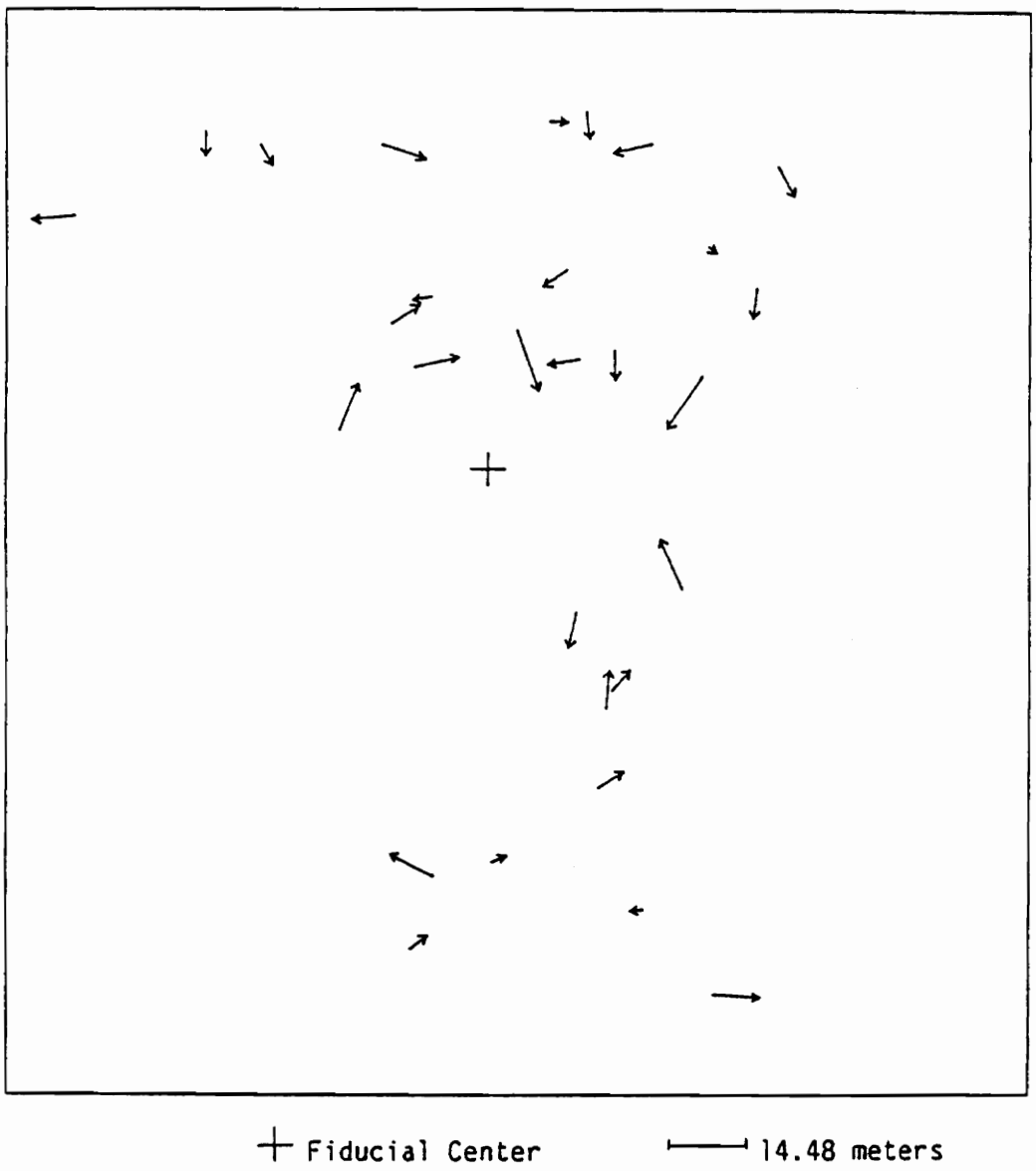

Figure A.8. Vector Errors of Computed Test Points by the Collinearity Equations, Blacksburg, Va.

Table A.5. Test Line and Polygon

		Prentiss	Blacksburg
Line	Elevation Range (m)	698 - 1280	469 - 609
	Scaled Map Length (m)	4015	3843
	Scaled Photo Length (m) by Collin. Equs.	4023	3665
Polygon	Elevation (m)	975	731
	Scaled Map Area (m^2)	1031321	509688
	Scaled Photo Area (m^2) by Collin. Equs.	989641	487630

Table A.6. Point, Line and Polygon Errors Caused by Errors in Ground Control Points and DEM Data, Prentiss, N.C.

	by Error in Control Data			by Error in Elevation Data		
ERROR (m)	D1 (m)	L1 (%)	A1 (%)	D2 (m)	L2 (%)	A2 (%)
5	1.2523	0.0449	0.1123	0.9536	0.0142	0.0314
10	2.3144	0.0613	0.2182	1.8191	0.0267	0.0578
15	3.8201	0.1158	0.2911	2.8857	0.0454	0.0870
20	4.8659	0.1458	0.3743	3.8507	0.0594	0.1294
25	5.7849	0.1818	0.4771	5.0792	0.0941	0.1466
30	6.9683	0.2155	0.5332	5.9042	0.1103	0.1179
35	8.8780	0.2635	0.6977	6.9598	0.1537	0.2282
40	9.6680	0.3130	0.6508	7.6726	0.1635	0.1905
45	9.6520	0.2432	0.6612	8.4282	0.2512	0.2164
50	12.0298	0.3104	0.6657	10.1103	0.2615	0.2352
55	12.6022	0.4687	0.9454	10.8346	0.4028	0.3230
60	14.0804	0.3349	1.2392	11.8697	0.4315	0.3837
65	15.2380	0.4956	1.1537	12.4455	0.4119	0.3537
70	15.4569	0.4763	1.1974	13.6887	0.5794	0.4074
75	18.7386	0.4572	1.3063	13.8595	0.6612	0.5131
80	18.2115	0.6716	1.6651	15.0353	0.7456	0.5560
85	19.0702	0.5932	1.3791	16.5574	0.8594	0.5015
90	25.3085	0.6677	1.6738	17.5281	0.9257	0.4510
95	23.2619	0.7123	1.5015	17.9999	1.0244	0.5669
100	23.3650	0.7981	1.7662	19.5940	1.1914	0.5599
105	26.4801	0.7738	1.7961	19.9092	1.3258	0.5483
110	24.7910	0.7300	1.9422	21.3727	1.4429	0.5960
115	26.5414	0.6006	1.7943	22.4260	1.5674	0.6684
120	26.5157	0.7076	2.1715	23.2465	1.6025	0.6007
125	27.0908	0.7161	1.8841	22.8795	1.8673	0.6820
130	31.0388	0.9891	2.2835	25.7280	1.9481	0.5849
135	33.6606	0.7947	2.8815	25.5819	2.0414	0.7677
140	35.5443	0.9843	2.3071	27.7056	2.3510	0.9072
145	33.4921	1.2182	2.4926	28.2936	2.5477	0.8609
150	35.9955	1.0254	2.3534	28.7927	2.9039	0.7438
155	38.7571	1.0560	3.0674	30.1199	2.5217	0.5544
160	36.4835	1.5275	2.5481	29.9271	3.1047	0.8868
165	38.9003	1.0903	3.0098	31.6140	3.5412	0.7020
170	39.0642	1.4599	2.9409	32.9937	3.6629	0.9532
175	41.5142	1.3896	3.7119	34.6653	4.0169	0.7281
180	44.8248	1.1523	3.4077	34.9906	4.1124	0.9541
185	41.9896	1.2199	2.8900	34.8970	4.4174	1.0352
190	46.8586	1.3083	2.8952	36.0151	4.3518	1.1624
195	43.6582	1.2211	2.7977	38.3644	4.5649	1.2457
200	42.9417	1.2836	3.2017	40.5991	5.1314	1.1318
205	46.3370	1.5439	3.1042	39.5289	5.0403	1.1938
210	51.5775	1.5095	4.2620	41.3741	5.5015	1.3472
215	51.4824	1.3738	4.0371	41.8722	5.5756	1.1153

Continue...

220	50.2734	1.4648	2.6976	43.1698	6.2642	1.4252
225	58.3843	1.5560	3.2249	45.0170	5.4571	1.4066
230	56.4525	2.0544	4.2128	44.1775	6.9845	1.4103
235	55.1503	1.4550	3.5332	43.6194	6.7546	1.2390
240	59.1554	1.6838	4.3586	46.8366	6.8828	1.2215
245	63.0894	1.7973	4.3764	47.5152	7.1510	1.1992
250	55.7118	2.1860	4.7012	50.9525	8.3103	1.2897
255	60.6004	2.2184	4.1283	49.6895	7.2132	1.3790
260	60.7164	1.6587	4.0737	50.0873	8.0778	1.3064
265	60.3124	1.6946	4.3125	51.5046	7.7896	1.3473
270	59.0619	1.7619	4.7760	51.6269	8.4306	1.3967
275	69.7415	2.0153	4.6748	51.8268	8.9972	1.5148
280	66.2457	1.9631	3.8102	51.6042	8.3933	1.3188
285	60.8926	2.1840	5.3023	56.3648	10.1833	1.7143
290	68.9376	2.0869	6.4260	53.8309	10.2548	1.5370
295	70.3485	1.9536	4.5691	54.8873	10.5792	1.4118
300	69.2460	2.9777	5.5136	57.6592	11.1644	1.8111

Where: ERROR is the absolute maximum error.
D1, L1 and A1 are the average point distance offset, line length change percentage and polygon area change percentage caused by ERROR in the control data.
D2, L2 and A2 are the average point distance offset, line length change percentage and polygon area change percentage caused by ERROR in elevations of point, line and polygon ground data.

Table A.7. Point, Line and Polygon Errors Caused by Errors in Ground Control Points and DEM Data, Blacksburg, Va.

	by Error in Control Data			by Error in Elevation Data		
ERROR (m)	D1 (m)	L1 (%)	A1 (%)	D2 (m)	L2 (%)	A2 (%)
5	1.0428	0.0421	0.0415	0.6916	0.0656	0.0256
10	1.8148	0.0646	0.0744	1.3536	0.1023	0.0630
15	3.1633	0.1000	0.1361	2.0532	0.1699	0.1070
20	4.2357	0.1619	0.1378	2.6990	0.1940	0.1121
25	5.2313	0.1808	0.1554	3.4252	0.2152	0.1525
30	6.6285	0.1851	0.2006	4.2144	0.3240	0.2186
35	7.1380	0.2264	0.2571	4.7103	0.3844	0.2451
40	8.9221	0.2458	0.3219	5.4048	0.5550	0.2777
45	9.0351	0.3413	0.3119	6.1411	0.4408	0.2985
50	9.5956	0.3135	0.3859	6.9617	0.5869	0.3065
55	10.7067	0.4560	0.2989	7.6970	0.9227	0.3457
60	11.9026	0.3475	0.3595	8.2141	0.9960	0.3818
65	12.9308	0.5340	0.4536	8.6861	0.7962	0.4445
70	14.0466	0.4599	0.5306	9.8890	1.0313	0.5012
75	14.5704	0.4885	0.5207	10.4025	0.9421	0.3257
80	15.6585	0.5780	0.7289	11.0542	1.2626	0.5318
85	17.2683	0.5033	0.5538	11.6509	1.2608	0.5568
90	17.6957	0.5021	0.7310	12.1526	1.4782	0.4498
95	19.8822	0.6637	0.7916	12.9608	1.5657	0.5545
100	20.8946	0.7681	0.7509	13.1111	2.0916	0.6179
105	21.8483	0.9040	0.8945	14.1711	2.0364	0.5746
110	21.6331	0.5177	0.9356	15.0769	2.4320	0.6239
115	19.9734	0.8998	0.7897	15.3634	2.7051	0.5300
120	24.3273	0.9011	0.9127	15.9570	2.9328	0.5740
125	22.5164	0.7535	1.0898	16.8245	2.4944	0.7262
130	26.2765	0.7959	0.8645	17.1619	2.7295	0.7898
135	25.9143	0.7753	1.1267	19.2158	3.3044	1.0003
140	27.5906	1.0439	0.7737	19.8773	2.8950	0.8390
145	28.8622	0.8855	1.1318	19.9562	3.6997	1.0200
150	25.9951	0.8169	1.0805	20.2582	3.6211	0.7927
155	32.2010	1.0224	1.0837	21.1989	4.3766	0.7714
160	29.8830	0.9477	1.1649	22.3468	4.7223	1.0939
165	35.4637	1.5004	1.0662	22.4585	4.4299	0.9258
170	34.8200	1.0852	1.1390	23.1261	4.9866	1.1267
175	36.7892	1.1065	1.5079	23.3990	5.7311	1.1639
180	33.7240	1.0057	1.3209	24.6396	5.3383	1.0323
185	35.4477	1.2160	1.2661	24.8345	6.0958	0.9759
190	40.4161	1.1849	1.6541	25.5095	6.6015	1.3018
195	36.5184	1.0746	1.4448	28.1136	5.8611	1.0054
200	41.1476	1.4852	1.9061	27.4118	7.5797	1.1369
205	42.1612	1.4748	1.4695	26.4820	8.1825	1.3008
210	41.5989	1.2534	1.3549	28.9556	6.8398	1.2873
215	49.8171	1.4270	1.6771	28.7965	7.5320	1.3940

Continue...

220	46.9732	1.3733	2.2181	29.3440	7.2414	1.2315
225	48.0065	1.5978	1.2839	30.9025	7.9210	1.3686
230	47.5778	1.8040	1.9260	30.5022	9.2532	1.2778
235	44.7669	2.0538	1.6054	32.4490	9.0832	1.3555
240	49.1062	1.8830	1.6732	33.0324	8.2320	1.6014
245	53.9445	2.1480	1.4678	33.6269	10.3807	1.7817
250	54.5977	1.9921	1.6056	33.6067	10.1330	1.6146
255	50.3101	1.6808	1.6371	34.9091	10.5934	1.8835
260	51.1435	1.7553	2.1258	34.9086	11.3712	1.5665
265	56.2620	1.9618	2.1314	35.9083	12.8214	1.6530
270	52.5294	1.4736	1.9194	34.6759	11.5228	1.6924
275	58.8587	2.3535	1.7992	37.9268	12.5222	2.1215
280	50.5193	1.6697	2.2177	37.9073	12.2720	1.3222
285	58.9886	2.1344	1.9555	38.1466	13.2337	1.8166
290	59.5468	1.7974	1.9540	37.9745	13.4125	1.6934
295	64.0202	2.3587	1.9578	39.4662	15.7970	1.7368
300	56.1101	2.1168	1.8735	40.7890	15.3600	1.8084

Where: ERROR is the absolute maximum error.
D1, L1 and A1 are the average point distance offset, line length change percentage and polygon area change percentage caused by ERROR in the control data.
D2, L2 and A2 are the average point distance offset, line length change percentage and polygon area change percentage caused by ERROR in elevations of point, line, and polygon ground data.

Appendix B

SOURCE CODE FOR SINGLE DIGITAL PHOTO CORRECTION USING THE COLLINEARITY EQUATIONS

```
/*****************************************************************************

                Programmed by:  Limei Ran
                Geography Graduate Student
                Virginia Polytechnic Institute
                December 1991 to Spring 1992

                Program For Master Thesis
                Used Turbo C on PC WIN/486
*****************************************************************************/
#include <alloc.h>
#include <stdio.h>
#include <ctype.h>
#include <io.h>
#include <math.h>
#include <string.h>
#include <conio.h>
#include <stdlib.h>
#include <stddef.h>
#define COLUMN1 80
#define MP   200
#define NP   10
#define NMAX 15
#define PROW 100
/*------------------------  Global Variables  ----------------------*/

FILE   *inimage,*indocum;          /*pointers - input image files*/
FILE   *outimage,*outdocum;        /*pointers - output image files*/
FILE   *DEMimage,*DEMdocum;        /*pointers - DEM file*/
FILE   *points;                    /*pointer - control file*/
FILE   *in_DEM,*in_DEM1;           /*interpolated DEM file pointers*/
FILE   *info1;                     /*pointer - all information file*/

char   datatype[3], filetype[3];   /*input file data types and file types*/
long   row[3],col[3];              /*input file row and column numbers*/
float  zmin[3],zmax[3];            /*input file value range*/
float  resolx[3],resoly[3];        /*input file resolutions*/
float  in_resolx[3],in_resoly[3];  /*interpolated DEM & output resolutions*/
long   scale;                      /*scale of image*/
long   in_row[2],in_col[2];        /*interpolated DEM & output rows, columns*/
float  out_zmin[2],out_zmax[2];    /*interpolated DEM & output cell ranges*/
double DEMx[3],DEMy[3];            /*3 UTM points in DEM ,UL, UL and LR*/
int    choice;                     /*DEM processing selection*/
double e[6];                       /*store six orientation elements*/
double tol[2];                     /*iterative tolerances in computing*/
double f;                          /*camera focus length*/
double rm[9];                      /*rotation matrix*/
double affine[4][3];               /*affine transformation coefficients*/

main()
{
char   fname6[40],fname66[40];     /*names - store interpolated DEM*/
float  *pointer[PROW];             /*pointers to store many rows*/
float  ratio;
char   yn;
```

```
void    open_image ();
void    open_DEM ();
void    open_other ();
void    selection ();
void    compute ();
void    DEM_interpolation (char *fname6, char *fname66, float *pointer[]);
void    map_to_image (float *pointer[]);
void    write_info ();
char    another ();

  do
   {
   flushall ();
   open_image ();
   selection ();
   open_DEM ();
   open_other ();

   compute ();

   if (resolx[2]!=in_resolx[1] || resoly[2]!=in_resoly[1])
    DEM_interpolation (fname6,fname66,pointer);

   map_to_image (pointer);

   write_info ();
   fcloseall ();

   yn = another ();
   }
  while (yn=='y' || yn=='Y');
  printf ("\n\n\t\t\tThe program has ended.\n\n");
}

/*****************************************************************************
   open_image (in IDRISI format)
   December 10, 1991
*****************************************************************************/
void open_image ()
{
char    fname1[40],fname11[40];     /*names - input image files*/
char    fname2[40],fname22[40];     /*names - output image files*/
int     control;                    /*variable - control Do loop*/
char    buffer[COLUMN1+1];          /*string - fgets statemnet*/
char    value_doc[21];              /*string - read documentation file*/
int     i;                          /*loop and control variables*/

   clrscr ();
   flushall ();
   gotoxy (5,6);
   printf ("Opening image files ...");

   do
    {
```

```
 clrscr ();
 gotoxy (5,10);
 printf ("INPUT THE SCALE OF IMAGE (DENOMINATOR OF SCALE) --> ");
 scanf ("%ld",&scale);
 }
while (scale < 1);
do
 {
 clrscr ();
 gotoxy (5,10);
 printf ("INPUT THE FOCUS LENGTH OF THE IMAGE CAMERA --> ");
 scanf ("%lf",&f);
 }
while (f < 0.0);

/*input the image to be processed*/
flushall ();
clrscr ();
do
 {
 gotoxy (2,8);
 control = 1;
 printf("ENTER THE NAME OF IMAGE TO BE CORRECTED (no extension) -> ");
 scanf("%s",fname1);
 strcpy(fname11,fname1);
 strcat(fname1,".img\0");
 strcat(fname11,".doc\0");
 if ((indocum = fopen(fname11,"r")) = = NULL)
  {
  clrscr ();
  gotoxy (2,6);
  printf("Error in opening the input documentation file.  Try again !");
  control = 0;
 }}
while (control = = 0);

datatype[3] = '\0';
filetype[3] = '\0';
for (i = 0;i < 10;i + + )
 {
 fgets(buffer,COLUMN1,indocum);
 strncpy (value_doc,buffer + 14,20*sizeof(char));
 value_doc[21] = '\0';
 if (i = = 1) datatype[1] = buffer[14];
 if (i = = 2) filetype[1] = buffer[14];
 if (i = = 3) row[1] = atol(value_doc);
 if (i = = 4) col[1] = atol(value_doc);
 if (i = = 7) resolx[1] = atof(value_doc);
 if (i = = 8) resoly[1] = atof(value_doc);
 }
rewind (indocum);


clrscr ();
flushall ();
```

```
    gotoxy (5,10);
    printf ("ENTER THE OUTPUT NAME OF THE CORRECTED IMAGE (no extension) -> ");
    scanf ("%s", fname2);
    strcpy(fname22, fname2);
    strcat(fname2, ".img\0");
    strcat(fname22, ".doc\0");

    if (filetype[1] = = 'a')
     {
     if ((inimage = fopen(fname1,"r")) = = NULL ||
        (outimage = fopen(fname2,"w")) = = NULL)
      {
      gotoxy (5,12);
      printf ("Error in opening the input or output image.");
      gotoxy (5,14);
      printf ("The program was terminated !");
      exit (0);
     }}
    else if (filetype[1] = = 'b')
     {
     if ((inimage = fopen(fname1,"rb")) = = NULL ||
        (outimage = fopen(fname2,"wb")) = = NULL)
      {
      gotoxy (5,12);
      printf ("Error in opening the input or output image.");
      gotoxy (5,14);
      printf ("The program was terminated !");
      exit (0);
     }}
    else
     {
     gotoxy (5,12);
     printf ("The input image is packed binary file !   Convert it");
     gotoxy (5,13);
     printf ("to be the ASCII or binary file type.");
     gotoxy (5,15);
     printf ("The program was terminated !");
     exit (0);
     }

    if ((outdocum = fopen(fname22,"w")) = = NULL)
     {
     clrscr ();
     gotoxy (5,12);
     printf ("Error in opening the documentation file of output image.");
     gotoxy (5,14);
     printf ("The program was terminated !");
     exit (0);
     }

    return;
}

/*****************************************************************************
   selection (select some procedures and input some parameters)
```

```
   December 12, 1991
*****************************************************************************/
void  selection ()
{
int     option;                  /*input variable*/
int     i;                      /*loop and control variables*/

    clrscr ();
    flushall ();
    gotoxy (5,6);
    printf ("Entering all selections and parameters ...");

    clrscr ();
    flushall ();
    gotoxy (10,12);
    printf ("INPUT THE ITERATIVE TOLERANCE OF ROTATION ANGLES --> ");
    scanf ("%lf",&tol[0]);
    gotoxy (10,14);
    printf ("INPUT THE ITERATIVE TOLERANCE OF PERSPECTIVE CENTER --> ");
    scanf ("%lf",&tol[1]);

    do
     {
     flushall ();
     clrscr ();
     gotoxy (10,10);
     printf ("Select the DEM area to be used.");
     gotoxy (10,12);
     printf ("1.  The whole DEM area");
     gotoxy (10,13);
     printf ("2   Portion of the DEM");
     gotoxy (10,14);
     printf ("3.  Exit program");
     gotoxy (10,16);
     printf ("Enter selection --> ");
     scanf ("%d",&option);
     }
    while (option < 1 || option > 3);
    if (option = = 3)
    exit (0);
    else
    choice = option;

    return;
}

/*****************************************************************************
    open_DEM  (in IRDISI format)
    December 15, 1991
*****************************************************************************/
void open_DEM ()
{
char    fname3[40],fname33[40];     /*names - DEM file*/
int     control;                  /*variable - control Do loop*/
int     i;                      /*loop and control variable*/
```

```
char    buffer[COLUMN1 + 1];          /*string - fgets statemnet*/
char    value_doc[21];                /*string - read documentation file*/
char    change;                       /*change selection variable*/
double  ratio;

   clrscr ();
   flushall ();
   gotoxy (10,6);
   printf ("Opening the DEM file ...");

   do
    {
    gotoxy (2,8);
    control = 1;
    printf("ENTER THE NAME OF THE DEM FILE TO BE USED (no extension) -> ");
    scanf ("%s",fname3);
    strcpy (fname33,fname3);
    strcat(fname3,".img\0");
    strcat(fname33,".doc\0");
    if ((DEMdocum = fopen(fname33,"r")) = = NULL)
     {
     clrscr ();
     gotoxy (2,6);
     printf ("Error in opening DEM image documentation file.  Try again !");
     control = 0;
    }}
   while (control = = 0);

   for (i = 0;i < 10;i + + )
    {
    fgets(buffer,COLUMN1,DEMdocum);
    strncpy (value_doc,buffer + 14,20*sizeof(char));
    value_doc[21] = '\0';
    if (i = = 1) datatype[2] = buffer[14];
    if (i = = 2) filetype[2] = buffer[14];
    if (i = = 3) row[2] = atol(value_doc);
    if (i = = 4) col[2] = atol(value_doc);
    if (i = = 5) zmin[2] = atof(value_doc);
    if (i = = 6) zmax[2] = atof(value_doc);
    if (i = = 7) resolx[2] = atof(value_doc);
    if (i = = 8) resoly[2] = atof(value_doc);
    }
   rewind (DEMdocum);

   clrscr ();
   do
    {
    control = 1;
    flushall ();
    for (i = 0;i < 3;i + + )
     {
     DEMx[i] = 0.0;
     DEMy[i] = 0.0;
     }
    gotoxy (2,8);
```

```
printf ("INPUT UPPER LEFT UTM X OF THE INPUT DEM -> ");
scanf ("%lf",&DEMx[0]);
gotoxy (2,10);
printf ("INPUT UPPER LEFT UTM Y OF THE INPUT DEM -> ");
scanf ("%lf",&DEMy[0]);
if (choice = = 2)
 {
 gotoxy (2,12);
 printf ("INPUT UPPER LEFT UTM X OF THE DESIRED DEM PORTION-> ");
 scanf ("%lf",&DEMx[1]);
 gotoxy (2,14);
 printf ("INPUT UPPER LEFT UTM Y OF THE DESIRED DEM PORTION-> ");
 scanf ("%lf",&DEMy[1]);
 gotoxy (2,16);
 printf ("INPUT LOWER RIGHT UTM X OF THE DESIRED DEM PORTION-> ");
 scanf ("%lf",&DEMx[2]);
 gotoxy (2,18);
 printf ("INPUT LOWER RIGHT UTM Y OF THE DESIRED DEM PORTION-> ");
 scanf ("%lf",&DEMy[2]);
 }
do
 {
 gotoxy (2.20);
 printf ("DO YOU WANT TO CHANGE THE INPUT X AND Y COORDINATES ? (y/n) -> ");
 scanf ("%c",&change);
 if (change = = 'Y' || change = = 'y')
  {
  control = 0;
  clrscr ();
 }}
 while (change! = 'Y'&&change! = 'y'&&change! = 'N'&&change! = 'n');
 }
while (control = = 0);
for (i = 0;i < 3;i + + )
 {
 DEMx[i] = (ceil(DEMx[i]/resolx[2]))*resolx[2];   /*round up*/
 DEMy[i] = (ceil(DEMy[i]/resoly[2]))*resoly[2];
 if (choice = = 1)
  {
  DEMx[1] = DEMx[0];
  DEMy[1] = DEMy[0];
  break;
 }}

clrscr ();
if (filetype[2] = = 'a')
 {
  if ((DEMimage = fopen(fname3,"r")) = = NULL)
  {
  gotoxy (5,12);
  printf ("Error in opening the DEM image file.");
  gotoxy (5,14);
  printf ("The program was terminated !");
  exit (0);
 }}
```

```
else if (filetype[2] = = 'b')
 {
 if ((DEMimage = fopen(fname3,"rb")) = = NULL)
  {
  gotoxy (5,12);
  printf ("Error in opening the DEM image file.");
  gotoxy (5,14);
  printf ("The program was terminated !");
  exit (0);
 }}
else
 {
 gotoxy (5,12);
 printf ("The DEM image file is packed binary file !   Convert it");
 gotoxy (5,13);
 printf ("to be the ASCII or binary file type.");
 gotoxy (5,15);
 printf ("The program was terminated !");
 exit (0);
 }

/*judge if DEM is needed to be interpolated in x & y directions*/
/*compute the row and column numbers of interpolated DEM or output image*/
ratio = (resolx[2]-resolx[1])/resolx[1];
if (ratio < 0.5)
 {
 in_resolx[1] = resolx[2];
 if (choice = = 1)
 in_col[1] = col[2];
 }
else
 {
 in_resolx[1] = resolx[1];
 if (choice = = 1)
 in_col[1] = ((col[2]-1)*resolx[2])/in_resolx[1] + 1;
 }
if (choice = = 2)
in_col[1] = (DEMx[2]-DEMx[1])/in_resolx[1] + 1;

ratio = (resoly[2]-resoly[1])/resoly[1];
if (ratio < 0.5)
 {
 in_resoly[1] = resoly[2];
 if (choice = = 1)
 in_row[1] = row[2];
 }
else
 {
 in_resoly[1] = resoly[1];
 if (choice = = 1)
 in_row[1] = ((row[2]-1)*resoly[2])/in_resoly[1] + 1;
 }
if (choice = = 2)
in_row[1] = (DEMy[1]-DEMy[2])/in_resoly[1] + 1;
```

```
    return;
}

/*****************************************************************************
    open_other (open other files needed in the program)
    December 20, 1992
*****************************************************************************/
void  open_other ()
{
char    fname5[40];              /*name - control points*/
char    fname7[40];              /*name - store all rectification info.*/
int     control;                 /*variable - control Do loop*/

    clrscr ();
    flushall ();
    gotoxy (10,8);
    printf ("Opening all other files ...");

    do
     {
     gotoxy (2,10);
     control = 1;
     printf("ENTER THE NAME OF THE CONTROL POINT FILE (with extension) -> ");
     scanf ("%s",fname5);
     if ((points = fopen(fname5,"r")) = = NULL)
      {
      clrscr ();
      gotoxy (2,8);
      printf ("Error in opening the control point file.  Try again !");
      control = 0;
     }}
    while (control = = 0);

    clrscr ();
    do
     {
     control = 1;
     gotoxy (3,15);
     printf("INPUT THE FILE NAME TO STORE ALL INFORMATION --> ");
     scanf ("%s",fname7);
     if((info1 = fopen(fname7,"w")) = = NULL)
      {
      clrscr ();
      gotoxy (3,13);
      printf ("Error in opening the information file. Try again !");
      control = 0;
     }}
    while (control = = 0);

    return;
}

/*****************************************************************************
    compute  (compute six orientation elements using space resection and
            coefficients of affine transformation between r,c and x,y)
```

```
   December 25, 1991
*****************************************************************************/
void compute ()
{
int     i,j,n,m,npoint,k,jj,ii,np;
double  DX,DY,DZ,So;
double  q.r,s,xq,yq,fq;
double  A[MP][NP],B[MP],XX[NP],RV1[MP];
double  x,y,X,Y,Z,P[MP][NP],prow,pcol;
int     control,iter;

void  SVD_compute (double A[][NP], double B[], double *XX, int m, int n);

   clrscr ();
   gotoxy (5,8);
   printf ("Computing affine transformations between rows, columns and");
   printf ("x, y of photo points and computing orientation elements ...");

   /*compute affine transformation coefficients*/
   n = 3;
   fscanf(points,"%d",&npoint);
   for (i = 1;i < = npoint;i + + )
   fscanf(points,"%d%lf%lf%lf%lf",&np,&P[i][1],&P[i][2],&P[i][3],&P[i][4]);
   m = npoint;
   for (i = 1;i < = npoint;i + + )
    {
    A[i][1] = 1.0;
    A[i][2] = P[i][1];
    A[i][3] = P[i][2];
    B[i] = P[i][3];
    }
   SVD_compute (A,B,XX,m,n);
   for (i = 0;i < n;i + + )
    affine[0][i] = XX[i + 1];
   for (i = 1;i < = npoint;i + + )
    B[i] = P[i][4];
   SVD_compute (A,B,XX,m,n);
   for (i = 0;i < n;i + + )
    affine[1][i] = XX[i + 1];

   for (i = 1;i < = npoint;i + + )
    {
    A[i][1] = 1.0;
    A[i][2] = P[i][3];
    A[i][3] = P[i][4];
    B[i] = P[i][1];
    }
   SVD_compute (A,B,XX,m,n);
   for (i = 0;i < n;i + + )
    affine[2][i] = XX[i + 1];
   for (i = 1;i < = npoint;i + + )
    B[i] = P[i][2];
   SVD_compute (A,B,XX,m,n);
   for (i = 0;i < n;i + + )
    affine[3][i] = XX[i + 1];
```

```
for (i=0;i<4;i++)
 {
 printf("\naffine transformation coefficients");
 printf("\n%lf  %lf  %lf",affine[i][0],affine[i][1],affine[i][2]);
 }



/*compute six orientation elements iteratively*/
iter=0;
n=6;
fscanf(points,"%d",&npoint);
for (i=1;i<=npoint;i++)
 {
 fscanf(points,"%d%lf%lf%lf%lf%lf",&np,&prow,&pcol,&P[i][3],
                                   &P[i][4],&P[i][5]);
 P[i][1]=affine[0][0]+prow*affine[0][1]+pcol*affine[0][2];
 P[i][2]=affine[1][0]+prow*affine[1][1]+pcol*affine[1][2];
 }

m=2*npoint;

/*compute initial values of six unknown elements*/
ii=1;
jj=npoint;
e[0]=0.0;
e[1]=0.0;
e[3]=0.0;
e[4]=0.0;
e[5]=0.0;
for (i=1;i<=npoint;i++)
 {
 if (P[i][1]<P[ii][1] && P[i][2]>P[ii][2])
 ii=i;
 if (P[i][1]>P[jj][1] && P[i][2]<P[jj][2])
 jj=i;
 e[3]+=P[i][3];
 e[4]+=P[i][4];
 e[5]+=P[i][5];
 }
e[2]=atan((P[ii][4]-P[jj][4])/(P[ii][3]-P[jj][3]))-
     atan((P[ii][2]-P[jj][2])/(P[ii][1]-P[jj][1]));
e[3]=e[3]/npoint;
e[4]=e[4]/npoint;
e[5]=scale*f+e[5]/npoint;

/*iterative procedure*/
do
 {
 iter++;

 /*compute rotation matrix*/
 rm[0]=cos(e[1])*cos(e[2]);
 rm[1]=sin(e[0])*sin(e[1])*cos(e[2]) + cos(e[0])*sin(e[2]);
 rm[2]=-cos(e[0])*sin(e[1])*cos(e[2]) + sin(e[0])*sin(e[2]);
```

```
rm[3] = -cos(e[1])*sin(e[2]);
rm[4] = -sin(e[0])*sin(e[1])*sin(e[2]) + cos(e[0])*cos(e[2]);
rm[5] = cos(e[0])*sin(e[1])*sin(e[2]) + sin(e[0])*cos(e[2]);
rm[6] = sin(e[1]);
rm[7] = -sin(e[0])*cos(e[1]);
rm[8] = cos(e[0])*cos(e[1]);

/*compute the A & B matrix for linear equations for AX = B*/
for (i = 1;i < = npoint;i + + )
 {
 j = 2*i-1;
 k = j + 1;
 x = P[i][1];
 y = P[i][2];
 DX = P[i][3]-e[3];
 DY = P[i][4]-e[4];
 DZ = P[i][5]-e[5];
 q = rm[6]*DX + rm[7]*DY + rm[8]*DZ;
 r = rm[0]*DX + rm[1]*DY + rm[2]*DZ;
 s = rm[3]*DX + rm[4]*DY + rm[5]*DZ;
 xq = x/q;
 yq = y/q;
 fq = f/q;
 A[j][1] = xq*(-rm[8]*DY + rm[7]*DZ) + fq*(-rm[2]*DY + rm[1]*DZ);
 A[j][2] = xq*(DX*cos(e[1]) + DY*sin(e[0])*sin(e[1])-DZ*cos(e[0])*sin(e[1])) +
        fq*(-DX*sin(e[1])*cos(e[2]) + DY*sin(e[0])*cos(e[1])*cos(e[2])-
        DZ*cos(e[0])*cos(e[1])*cos(e[2]));
 A[j][3] = fq*s;
 A[j][4] = -(xq*rm[6] + fq*rm[0]);
 A[j][5] = -(xq*rm[7] + fq*rm[1]);
 A[j][6] = -(xq*rm[8] + fq*rm[2]);
 A[k][1] = yq*(-rm[8]*DY + rm[7]*DZ) + fq*(-rm[5]*DY + rm[4]*DZ);
 A[k][2] = yq*(DX*cos(e[1]) + DY*sin(e[0])*sin(e[1])-DZ*cos(e[0])*sin(e[1])) +
        fq*(DX*sin(e[1])*sin(e[2])-DY*sin(e[0])*cos(e[1])*sin(e[2]) +
        DZ*cos(e[0])*cos(e[1])*sin(e[2]));
 A[k][3] = fq*(-r);
 A[k][4] = -(yq*rm[6] + fq*rm[3]);
 A[k][5] = -(yq*rm[7] + fq*rm[4]);
 A[k][6] = -(yq*rm[8] + fq*rm[5]);
 B[j] = -x-fq*r;
 B[k] = -y-fq*s;
 }
SVD_compute (A,B,XX,m,n);

fprintf(info1,"information of the transformation\n");
fprintf(info1,"iteration  %d\n",iter);
fprintf(info1,"six orientation elements\n");
fprintf(info1,"%lf  %lf  %lf  %lf  %lf  %lf\n",
                e[0],e[1],e[2],e[3],e[4],e[5]);
fprintf(info1,"corrections for the six elements\n");
fprintf(info1,"%lf  %lf  %lf  %lf  %lf  %lf\n",
          XX[1],XX[2],XX[3],XX[4],XX[5],XX[6]);
fprintf(info1,"the residual matrix of the coefficients\n");
So = 0.0;
for (i = 1;i < = m;i + + )
```

```
    {
    RV1[i]=0;
    for (k=1;k<=n;k++)
    RV1[i]+=A[i][k]*XX[k];
    RV1[i]-=B[i];
    fprintf(info1,"%lf\n",RV1[i]);
    So+=RV1[i]*RV1[i];
    }
   if (m!=n)
   So=sqrt((double)So/(m-n));
   fprintf(info1,"standard deviation of residuals    %lf\n",So);

   /*add the corrections to the initial approximations of unknowns*/
   for (i=1;i<=n;i++)
    e[i-1] += XX[i];

   printf("\ncorrections");
   printf("\n%lf,%lf,%lf,%lf,%lf,%lf",XX[1],XX[2],XX[3],XX[4],XX[5],XX[6]);
   printf("\nsix orientation elements");
   printf("\n%lf,%lf,%lf,%lf,%lf,%lf",e[0],e[1],e[2],e[3],e[4],e[5]);

   control=0;
   for (i=1;i<=3;i++)
    {
    if (fabs(XX[i])>tol[0] || fabs(XX[i+3])>tol[1])
    control++;
   }}
  while (control != 0);

  rm[0]=cos(e[1])*cos(e[2]);
  rm[1]=sin(e[0])*sin(e[1])*cos(e[2]) + cos(e[0])*sin(e[2]);
  rm[2]=-cos(e[0])*sin(e[1])*cos(e[2]) + sin(e[0])*sin(e[2]);
  rm[3]=-cos(e[1])*sin(e[2]);
  rm[4]=-sin(e[0])*sin(e[1])*sin(e[2]) + cos(e[0])*cos(e[2]);
  rm[5]=cos(e[0])*sin(e[1])*sin(e[2]) + sin(e[0])*cos(e[2]);
  rm[6]=sin(e[1]);
  rm[7]=-sin(e[0])*cos(e[1]);
  rm[8]=cos(e[0])*cos(e[1]);

  rewind (points);
  return;
}

/*****************************************************************************
    SVD_compute  (singular value decomposition to solve linear equations)
    January 15, 1992
*****************************************************************************/
void  SVD_compute (double A[][NP], double B[], double *XX, int m, int n)
{
int     i,j,k,l,ITS,NM,way,jj,ii;
double  U[MP][NP],W[NP],V[NP][NP];
double  TMP[NMAX],RV1[NMAX];
double  X,Y,Z;
double  WMAX,WMIN,G,SCALE,ANORM,S,F,H,C,SIGN;
```

```
/*using SVD to solve linear equations*/
for (i = 1;i < = m;i + + )
 {
 for (j = 1;j < = n;j + + )
  {
  U[i][j] = A[i][j];
 }}
 /*SVD procedure*/
 if(m < n)
  {
  printf("\n You must augment A with extra row zero rows !!!");
  exit(0);
  }
 /*Householder reduction to bidiagonal form*/
 G = 0.0;
 SCALE = 0.0;
 ANORM = 0.0;
 for (i = 1;i < = n;i + + )
  {
  l = i + 1;
  RV1[i] = SCALE*G;
  G = 0.0;
  S = 0.0;
  SCALE = 0.0;
  if (i < = m)
   {
   for (k = i;k < = m;k + + )
   SCALE + = fabs(U[k][i]);
   if (SCALE != 0.0)
    {
    for (k = i;k < = m;k + + )
     {
     U[k][i] = U[k][i]/SCALE;
     S + = U[k][i]*U[k][i];
     }
    F = U[i][i];
    if (F < 0.0)   G = sqrt(S);
    else          G = -sqrt(S);
    H = F*G-S;
    U[i][i] = F-G;
    if (i != n)
     {
     for (j = 1;j < = n;j + + )
      {
      S = 0.0;
      for (k = i;k < = m;k + + )
      S + = U[k][i]*U[k][j];
      F = S/H;
      for (k = i;k < = m;k + + )
      U[k][j] + = F*U[k][i];
     }}
    for (k = i;k < = m;k + + )
    U[k][i] = SCALE*U[k][i];
    W[i] = SCALE*G;
    G = 0.0;
```

```
S = 0.0;
SCALE = 0.0;
if (i < = m && i! = n)
 {
 for (k = l;k < = n;k + + )
 SCALE + = fabs(U[i][k]);
 if (SCALE ! = 0.0)
  {
  for (k = l;k < = n;k + + )
   {
   U[i][k] = U[i][k]/SCALE;
   S + = U[i][k]*U[i][k];
   }
  F = U[i][l];
  if (F < 0.0)   G = sqrt(S);
  else          G = -sqrt(S);
  H = F*G-S;
  U[i][l] = F-G;
  for (k = l;k < = n;k + + )
  RV1[k] = U[i][k]/H;
  if (i ! = m)
   {
   for (j = l;j < = m;j + + )
    {
    S = 0.0;
    for (k = l;k < = n;k + + )
    S + = U[j][k]*U[i][k];
    for (k = l;k < = n;k + + )
    U[j][k] + = S*RV1[k];
   }}
  for (k = l;k < = n;k + + )
  U[i][k] = SCALE*U[i][k];
 }}
ANORM = max(ANORM,(fabs(W[i]) + fabs(RV1[i])));
}
/*Accumulation of right-hand transformations*/
for (i = n;i > = l;i--)
 {
 if (i < n)
  {
  if (G! = 0.0)
   {
   for (j = l;j < = n;j + + )
   V[j][i] = (U[i][j]/U[i][l])/G;
   for (j = l;j < = n;j + + )
    {
    S = 0.0;
    for (k = l;k < = n;k + + )
    S + = U[i][k]*V[k][j];
    for (k = l;k < = n;k + + )
    V[k][j] + = S*V[k][i];
   }}
  for (j = l;j < = n;j + + )
   {
   V[i][j] = 0.0;
```

```
    V[j][i] = 0.0;
   }}
  V[i][i] = 1.0;
  G = RV1[i];
  l = i;
  }
 /*Accumulation of left-hand transformations*/
 for (i = n;i > = 1;i--)
  {
  l = i + 1;
  G = W[i];
  if (i < n)
   {
   for (j = l;j < = n;j + + )
   U[i][j] = 0.0;
   }
  if (G! = 0.0)
   {
   G = 1.0/G;
   if (i! = n)
    {
    for (j = l;j < = n;j + + )
     {
     S = 0.0;
     for (k = l;k < = m;k + + )
     S + = U[k][i]*U[k][j];
     F = (S/U[i][i])*G;
     for (k = i;k < = m;k + + )
     U[k][j] + = F*U[k][i];
    }}
   for (j = i;j < = m;j + + )
   U[j][i] = U[j][i]*G;
   }
  else
   {
   for (j = i;j < = m;j + + )
   U[j][i] = 0.0;
   }
  U[i][i] + = 1.0;
  }
 /*Diagonalization of the bidiagonal form*/
 for (k = n;k > = 1;k--)
  {
  for (ITS = 1;ITS < = 30;ITS + + )
   {
   for (l = k;l > = 1;l--)
    {
    NM = l-1;
    way = 0;
    if ((fabs(RV1[l]) + ANORM) = = ANORM)
     {
     way = 1;
     break;
     }
    if ((fabs(W[NM]) + ANORM) = = ANORM)
```

```
  break;
 }
if (way! = 1)
 {
 C = 0.0;
 S = 1.0;
 for (i = l;i < = k;i + + )
  {
  F = S*RV1[i];
  RV1[i] = C*RV1[i];
  if ((fabs(F) + ANORM) = = ANORM)   break;
  G = W[i];
  H = sqrt(F*F + G*G);
  W[i] = H;
  H = 1.0/H;
  C =  (G*H);
  S = -(F*H);
  for (j = 1;j < = m;j + + )
   {
   Y = U[j][NM];
   Z = U[j][i];
   U[j][NM] = (Y*C) + (Z*S);
   U[j][i] = -(Y*S) + (Z*C);
 }}}
Z = W[k];
if (l = = k)
 {
 if (Z < 0.0)
  {
  W[k] = -Z;
  for (j = 1;j < = n;j + + )
  V[j][k] = -V[j][k];
  }
 break;
 }
if (ITS = = 30)
 {
 printf("\n No convergence in 30 iterations !!!");
 exit(0);
 }
X = W[l];
NM = k-1;
Y = W[NM];
G = RV1[NM];
H = RV1[k];
F = ((Y-Z)*(Y + Z) + (G-H)*(G + H))/(2.0*H*Y);
G = sqrt(F*F + 1.0);
if (F < 0) SIGN = -G;
else     SIGN = G;
F = ((X-Z)*(X + Z) + H*((Y/(F + SIGN))-H))/X;
C = 1.0;   /*next QR transformation*/
S = 1.0;
for (j = l;j < = NM;j + + )
 {
 i = j + 1;
```

```
    G = RV1[i];
    Y = W[i];
    H = S*G;
    G = C*G;
    Z = sqrt(F*F + H*H);
    RV1[j] = Z;
    C = F/Z;
    S = H/Z;
    F =  (X*C) + (G*S);
    G = -(X*S) + (G*C);
    H = Y*S;
    Y = Y*C;
    for (jj = 1;jj < = n;jj + + )
     {
     X = V[jj][j];
     Z = V[jj][i];
     V[jj][j] =  (X*C) + (Z*S);
     V[jj][i] = -(X*S) + (Z*C);
     }
    Z = sqrt(F*F + H*H);
    W[j] = Z;
    if (Z! = 0.0)
     {
     Z = 1.0/Z;
     C = F*Z;
     S = H*Z;
     }
    F =  (C*G) + (S*Y);
    X = -(S*G) + (C*Y);
    for (jj = 1;jj < = m;jj + + )
     {
     Y = U[jj][j];
     Z = U[jj][i];
     U[jj][j] =  (Y*C) + (Z*S);
     U[jj][i] = -(Y*S) + (Z*C);
    }}
   RV1[l] = 0.0;
   RV1[k] = F;
   W[k] = X;
}}
WMAX = 0.0;
for (j = 1;j < = n;j + + )
if (W[j] > WMAX) WMAX = W[j];
WMIN = WMAX*0.000000000001;
for (j = 1;j < = n;j + + )
if (W[j] < WMIN) W[j] = 0.0;
/*Calculate transpose of U*/
for (j = 1;j < = n;j + + )
 {
 S = 0.0;
 if (W[j]! = 0.0)
  {
  for (i = 1;i < = m;i + + )
  S + = U[i][j]*B[i];
  S = S/W[j];
```

```
        }
        TMP[j] = S;
        }
       for (j = 1;j < = n;j + + )
        {
        S = 0.0;
        for (jj = 1;jj < = n;jj + + )
        S + = V[j][jj]*TMP[jj];
        XX[j] = S;
        }

    return;
}
/*****************************************************************************
    DEM_interpolation  (interpolate the desired portion of DEM)
    January 26, 1992
*****************************************************************************/
void DEM_interpolation (char *fname6, char *fname66, float *pointer[])
{
FILE    *image;                 /*file pointer used to call subfunction*/
int     REPEAT = 1;               /*the number of rows repeated in reading*/
long    read_row;               /*the number of DEM rows can be read once*/
float   *pointer1;              /*pointer used to store interpolated data*/
int     i,j;
long    n,m,r,c,row_N,k,*offset;
double  in_x,in_y,xdir,ydir,dd,S,d0,d1,d2,d3,dist[4];
float   cell[4],cellf;

/*          j = 1 to image          j = 2 to DEM                    */

void    read_image (FILE *image, int j, long row_N, float *pointer[],
                long  read_row, int REPEAT, long *offset);
void    write_image (FILE *image, int j, float *pointer1);
void    write_docum (FILE *image, int j);


    clrscr ();
    flushall ();
    gotoxy (5,6);
    printf ("DEM interpolation for image correction");

    gotoxy (2,10);
    printf("INPUT THE FILE NAME FOR INTERPOLATED DEM (no extension) - > ");
    scanf ("%s",fname6);
    strcpy(fname66,fname6);
    strcat(fname6,".img\0");
    strcat(fname66,".doc\0");

    if ((in_DEM1 = fopen(fname66,"w")) = = NULL)
     {
     clrscr ();
     gotoxy (5,12);
     printf ("Error in opening DEM document. to be interpolated.");
     gotoxy (5,14);
     printf ("The program was terminated !");
```

```
 exit (0);
 }

if (filetype[2] = = 'a')
{
 if ((in_DEM = fopen(fname6,"w")) = = NULL)
 {
 gotoxy (5,12);
 printf ("Error in opening DEM image to be interpolated.");
 gotoxy (5,14);
 printf ("The program was terminated !");
 exit (0);
}}
else
{
 if ((in_DEM = fopen(fname6,"wb")) = = NULL)
 {
 gotoxy (5,12);
 printf ("Error in opening DEM image to be interpolated.");
 gotoxy (5,14);
 printf ("The program was terminated !");
 exit (0);
}}

/*allocate memory to store manipulated DEM for one row*/
if ((pointer1 = (float *) calloc(in_col[1],sizeof(float))) = = NULL)
 {
 gotoxy(5,12);
 printf("NULL in allocating memo. for pointer1 in DEM_interpolation");
 gotoxy (5,14);
 printf ("Program was terminated in DEM_interpolation function !!");
 exit (0);
 }

 /*allocate memory to store many rows of input DEM*/
 for (m = 0;m < PROW;m + + )
  {
  if ((pointer[m] = (float *) calloc(col[2] + 1,sizeof(float))) = = NULL)
   {
   if (m < 2)
    {
    gotoxy(5,12);
    printf ("NULL in allocating two rows of DEM data %ld",(col[2] + 1)*2);
    gotoxy(5,14);
    printf("Program was terminated in DEM_interpolation function !!");
    exit (0);
    }
   else
    break;
  }}
read_row = m;

/*interpolate input DEM from the UL cell to the desired resolutions*/
printf("\n  Interpolating DEM . . .");
```

```
j = 2;
out_zmin[1] = 10000.0;
out_zmax[1] = 0.0;
row_N = read_row-1;
read_image (DEMimage,j,row_N,pointer,read_row,REPEAT,offset);

for (m = 0;m < in_row[1];m + + )
 {
 in_y = DEMy[0]-DEMy[1] + in_resoly[1]*m;
 r = in_y/resoly[2];
 while (in_y > = row_N*resoly[2])
  {
  row_N + = (read_row-REPEAT);
  read_image(DEMimage,j,row_N,pointer,read_row,REPEAT,offset);
  }
 k = read_row-(row_N-r)-1;        /*row number in the array pointer*/
 ydir = r*resoly[2];
 for (n = 0;n < in_col[1];n + + )
  {
  in_x = DEMx[1]-DEMx[0] + in_resolx[1]*n;
  c = in_x/resolx[2];
  xdir = c*resolx[2];
  d0 = (in_x-xdir)*(in_x-xdir);
  d1 = (in_y-ydir)*(in_y-ydir);
  d2 = (xdir + resolx[2]-in_x)*(xdir + resolx[2]-in_x);
  d3 = (ydir + resoly[2]-in_y)*(ydir + resoly[2]-in_y);
  dist[0] = sqrt(d0 + d1);
  dist[1] = sqrt(d1 + d2);
  dist[2] = sqrt(d2 + d3);
  dist[3] = sqrt(d3 + d0);
  cell[0] = *(pointer[k] + c);
  cell[1] = *(pointer[k] + c + 1);
  cell[2] = *(pointer[k + 1] + c + 1);
  cell[3] = *(pointer[k + 1] + c);
  dd = 0.0;
  S = 0.0;
  cellf = 0.0;
  for (i = 0;i < 4;i + + )
   {
   if (dist[i]  = =  0.0)
    {
    if (cell[i] > = zmin[2])
    cellf = cell[i];
    dd = 0.0;
    break;
    }
   else if (cell[i] > = zmin[2])
    {
    if (d0 = = 0.0 && (i = = 1 || i = = 2))
    continue;
    if (d1 = = 0.0 && (i = = 2 || i = = 3))
    continue;
    S + = cell[i]*(1.0/dist[i]);
    dd + = 1.0/dist[i];
   }}
```

```
      if (dd != 0.0)   cellf = S/dd;
      if (cellf > = zmin[2])
       {
       out_zmin[1] = min(out_zmin[1],cellf);
       out_zmax[1] = max(out_zmax[1],cellf);
       }
       *(pointer1 + n) = cellf;                    /*store in a array pointer*/
      }
     write_image (in_DEM,j,pointer1);
     gotoxy(5,20);
     printf("%6.2f  percent finished",100.0*(m + 1)/in_row[1]);
     }

    zmin[2] = out_zmin[1];
    zmax[2] = out_zmax[1];
    write_docum(in_DEM1,j);

    free ((void *) pointer1);
    for (m = 0;m < read_row;m + + )
    free ((void *) pointer[m]);

    fclose (DEMimage);
    rewind (in_DEM);
    return;
}

/*****************************************************************************
     read_image  (in IDRISI format and read one row or many rows one time)
     February 4, 1992
*****************************************************************************/
void read_image (FILE *image, int j, long row_N, float *pointer[],
                 long read_row, int REPEAT, long *offset)
{
long    n,r,coln,m,k,i;
unsigned char cellb,*cellb1;
int     celli,*celli1;
float   cellf,*cellf1;

    celli1 = (int *) calloc(1,sizeof(int));
    cellf1 = (float *) calloc(1,sizeof(float));
    cellb1 = (char *) calloc(1,sizeof(char));

    if (REPEAT > = 0)
     {
     /*read many rows for DEM or image*/
     coln = col[j];
     if (row_N < = (read_row-1))
      k = 0;
     else
      {
      k = REPEAT;                  /*the repeated number when read many rows*/
      for (i = 0;i < k;i + + )
       {
       for (n = 0;n < coln;n + + )
       *(pointer[i] + n) = *(pointer[read_row-REPEAT + i] + n);
```

```
 }}
 if (row_N > (row[j]-1))
  {
  read_row = read_row-row_N + row[j]-1;
  if (j = = 2 && read_row = = REPEAT)
   {
   for (n = 0;n < coln;n + + )
    *(pointer[k] + n) = 0.0;              /*read one more row of DEM*/
}}}
else if (REPEAT < 0)
{
/*read one row for DEM or image*/
k = 0;
if (j = = 1)  coln = col[1];
if (j = = 2)
 {
 if (resolx[2] = = in_resolx[1] && resoly[2] = = in_resoly[1])
  coln = col[2];
 else
  coln = in_col[1];
 }
}

for (m = k;m < read_row;m + + )
 {
 for (n = 0;n < coln;n + + )
  {
  if (filetype[j] = = 'a')
   {
   if (datatype[j] = = 'i')
    {
    fscanf(image,"%d",&celli);
    cellf =  celli;
    }
   else if (datatype[j] = = 'r')
    fscanf(image,"%f",&cellf);
   else if (datatype[j] = = 'b')
    {
    fscanf(image,"%c",&cellb);
    celli = cellb;
    cellf = celli;
   }}
  else if (filetype[j] = = 'b')
   {
   if (datatype[j] = = 'i')
    {
    fread((void *)celli1, sizeof(int),1,image);
    cellf =  *celli1;
    }
    else if (datatype[j] = = 'r')
    {
    fread((void *)cellf1,sizeof(float),1,image);
    cellf = *cellf1;
    }
   else if (datatype[j] = = 'b')
```

```
        {
        fread((void *)cellb1,sizeof(char),1,image);
        celli = *cellb1;
        cellf = celli;
       }}
      if (REPEAT > = 0)
      *(pointer[m] + n) = cellf;        /*store in many rows*/
      else
      *(pointer[j-1] + n) = cellf;      /*store in one row*/
      }
     if (j = = 1 && REPEAT  > = 0)
      {
      r = row_N-read_row + m + 1;
      if ((*(offset + r) = ftell(image)) = = -1L)  /*store each image row position*/
      perror("ftell failed !");
     }}

    free ((void *) celli1);
    free ((void *) cellf1);
    free ((void *) cellb1);
    return;
}
/*****************************************************************************
     write_image   (in IDRISI format and write one row once)
     February 4, 1992
*****************************************************************************/
void write_image (FILE *image, int j, float *pointer1)
{
long     n;
int      celli,*celli1;
unsigned char  cellb,*cellb1;

    celli1 = (int *) calloc(1,sizeof(int));
    cellb1 = (char *) calloc(1,sizeof(char));

    if (filetype[j] = = 'a')
     {
     for (n = 0;n < in_col[1];n + + )
      {
      if (datatype[j] = = 'i')
       {
       celli = *(pointer1 + n);
       fprintf(image,"%d\n",celli);
       }
      else if(datatype[j] = = 'r')
       fprintf(image,"%f\n",*(pointer1 + n));
      else if(datatype[j] = = 'b')
       {
       celli = *(pointer1 + n);
       cellb = celli;
       fprintf(image,"%c\n",cellb);
     }}}
    else if (filetype[j] = = 'b')
     {
     for (n = 0;n < in_col[1];n + + )
```

```
    {
    if (datatype[j]==='i')
     {
     *celli1 = *(pointer1 + n);
     fwrite((void *)celli1,sizeof(int),1,image);
     }
    else if(datatype[j]==='r')
     fwrite((void *)(pointer1 + n),sizeof(float),1,image);
    else if(datatype[j]==='b')
     {
     celli = *(pointer1 + n);
     *cellb1 = celli;
     fwrite((void *)cellb1,sizeof(char),1,image);
    }}}

   free ((void *) celli1);
   free ((void *) cellb1);
   return;
}

/*****************************************************************************
    map_to_image  (from DEM to image transformation using space resection)
    February 6, 1992
*****************************************************************************/
void map_to_image (float *pointer[])
{
FILE    *image;              /*file pointer used to call subfunction*/
long    *offset;            /*store image row offset from the head in byte*/
int     REPEAT;              /*the repeated rows when read image data*/
long    read_row;           /*the number of image rows can be read once*/
float   *pointer1,*pointer2[3];/*pointers to store one row image or DEM data*/
int     j;
double  x,y,X,Y,Z,DX,DY,DZ,fq,xdir,ydir;
long    r,c,m,n,k,c1,r1,row_N,r_offset;
float   cellf;

/*          j = 1 to image          j = 2 to DEM                    */

void    read_image (FILE *image, int j, long row_N, float *pointer[],
                long read_row, int REPEAT, long *offset);
void    write_image (FILE *image, int j, float *pointer1);
void    write_docum (FILE *image, int j);


   clrscr ();
   gotoxy (5,8);
   printf("Coordinates transformation from the DEM to image.");

   /*allocate memory for a row of manipulated image data*/
   if ((pointer1 = (float *) calloc(in_col[1],sizeof(float)))==NULL)
    {
    gotoxy(5,12);
    printf("NULL in allocating memo. for pointer1 in map_to_image");
    gotoxy (5,14);
    printf ("The program was terminated in map_to_image function !!");
```

```
 exit (0);
 }

/*allocate memory for a row of read image data*/
if ((pointer2[0] = (float *) calloc(col[1],sizeof(float))) = = NULL)
 {
 gotoxy(5,12);
 printf("NULL in allocating memo. for pointer2[0] in map_to_image");
 gotoxy (5,14);
 printf ("The program was terminated in map_to_image function !!");
 exit (0);
 }

/*allocate memory for a row of read DEM data*/
c1 = 0;
if (resolx[2] = = in_resolx[1] && resoly[2] = = in_resoly[1])
 {
 if ((pointer2[1] = (float *) calloc(col[2],sizeof(float))) = = NULL)
  {
  gotoxy(5,12);
  printf("NULL in allocating memo. for pointer2[1] in map_to_image");
  gotoxy (5,14);
  printf ("The program was terminated in map_to_image function !!");
  exit (0);
  }
 c1 = (DEMx[1]-DEMx[0])/resolx[2];
 r1 = (DEMy[0]-DEMy[1])/resoly[2];
 for (m = 0;m < r1;m + + )
 read_image (DEMimage,2,0,pointer2,1,-1,offset);
 }
else
 {
 if ((pointer2[1] = (float *) calloc(in_col[1],sizeof(float))) = = NULL)
  {
  gotoxy(5,12);
  printf("NULL in allocating memo. for pointer2[1] in map_to_image");
  gotoxy (5,14);
  printf ("The program was terminated in map_to_image function !!");
  exit (0);
 }}

/*allocate memory to store image row offsets from image file head*/
if ((offset = (long *) calloc(row[1],sizeof(long))) = = NULL)
  {
  gotoxy(5,12);
  printf("NULL in allocating memo. for offset in map_to_image");
  gotoxy (5,14);
  printf ("The program was terminated in map_to_image function !!");
  exit (0);
  }

/*allocate memory to store many rows of input image data*/
for (m = 0;m < PROW;m + + )
 {
 if ((pointer[m] = (float *) calloc(col[1],sizeof(float))) = = NULL)
```

```
  {
  if (m = = 0)
   {
   gotoxy (5,12);
   printf ("NULL in allocating one row of pointer[] in map_to_image");
   gotoxy(5,14);
   printf("Program was terminated in map_to_image function !!");
   exit (0);
   }
  else
   break;
 }}
read_row = m;

if (read_row > 10)
 REPEAT = 5;
else if (read_row > 8 && read_row < = 10)
 REPEAT = 4;
else if (read_row > 5 && read_row < = 8)
 REPEAT = 3;
else if (read_row > = 4 && read_row < = 5)
 REPEAT = 2;
else if (read_row > = 2 && read_row < = 3)
 REPEAT = 1;
else
 REPEAT = 0;

printf("\n\n   Correcting image using DEM . . .");

j = 1;
r_offset = -1;
out_zmin[1] = 10000.0;
out_zmax[1] = 0.0;
row_N = read_row-1;
read_image (inimage,j,row_N,pointer,read_row,REPEAT,offset);

for (m = 0;m < in_row[1];m + + )
 {
 Y = DEMy[1]-in_resoly[1]*m;
 if (resolx[2] = = in_resolx[1] && resoly[2] = = in_resoly[1])
  read_image (DEMimage,2,0,pointer2,1,-1,offset);
 else
  read_image (in_DEM,2,0,pointer2,1,-1,offset);
 for (n = 0;n < in_col[1];n + + )
  {
  X = DEMx[1] + in_resolx[1]*n;
  Z = *(pointer2[1] + c1 + n);
  cellf = 0.0;
  if (Z  > =  zmin[2])
   {
   Z = Z;
   DX = X-e[3];
   DY = Y-e[4];
   DZ = Z-e[5];
   fq = f/(rm[6]*DX + rm[7]*DY + rm[8]*DZ);
```

```
      x = -fq*(rm[0]*DX + rm[1]*DY + rm[2]*DZ);
      y = -fq*(rm[3]*DX + rm[4]*DY + rm[5]*DZ);
      c = affine[2][0] + x*affine[2][1] + y*affine[2][2] + 0.5;
      r = affine[3][0] + x*affine[3][1] + y*affine[3][2] + 0.5;
      if (r > = 0 && r < row[1] && c > = 0 && c < col[1])
       {
       while (r > row_N)
        {
        row_N + = (read_row-REPEAT);
        read_image (inimage,j,row_N,pointer,read_row,REPEAT,offset);
        }
       k = read_row-(row_N-r)-1; /*row number in pointer array of read image*/
       if (k < 0)
        {
        if (r_offset! = r)
         {
         /*outside the read data, then read one row data for point (r,c)*/
         if (r = = 0)
          rewind (inimage);
         else
          {
          if (fseek(inimage,*(offset + r-1),SEEK_SET)! = 0)
          perror("fseek failed !");
          }
         read_image(inimage,j,0,pointer2,1,-1,offset);
         r_offset = r;
         if (fseek(inimage,*(offset + row_N),SEEK_SET)! = 0)
         perror("fseek failed !");
         }
        cellf = *(pointer2[0] + c);
        }
       else
        cellf = *(pointer[k] + c);
      }}
     out_zmin[1] = min(out_zmin[1],cellf);
     out_zmax[1] = max(out_zmax[1],cellf);
     *(pointer1 + n) = cellf;        /*store corrected data in a pointer array*/
     }
    write_image(outimage,j,pointer1);
    gotoxy(5,20);
    printf("%6.2f  percent finished",100.0*(m + 1)/in_row[1]);
    }

   write_docum(outdocum,j);
   free ((void *) pointer1);
   free ((void *) pointer2[0]);
   free ((void *) pointer2[1]);
   free ((void *) offset);
   for (m = 0;m < read_row;m + + )
   free ((void *) pointer[m]);
   return;
}

/*****************************************************************************
    write_docum  (write image documentataion file in IDRISI format)
```

```
    February 4, 1992
*****************************************************************************/
void write_docum (FILE *image, int j)
{
char    doc_char[14];
int     k,legend = 0;
char    buffer[COLUMN1 + 1],buffer1[COLUMN1 + 1];

   clrscr ();
   gotoxy(5,8);
   printf("Writing the documentation for output file");
   gotoxy(5,10);

   for(k = 0;k < 10;k + + )
    {
    if (j = = 2)   fgets(buffer,COLUMN1,DEMdocum);
    else        fgets(buffer,COLUMN1,indocum);
    strcpy (buffer1,buffer);
    strncpy (doc_char,buffer,14*sizeof(char));
    doc_char[14] = '\0';
    if (k = = 0)
     {
     if (j = = 2)
      fprintf(image,"%sinterpolated DEM\n",doc_char);
     else
      fprintf(image,"%srectified image\n",doc_char);
     }
    else if (k = = 3)
     fprintf(image,"%s%ld\n",doc_char,in_row[1]);
    else if (k = = 4)
     fprintf(image,"%s%ld\n",doc_char,in_col[1]);
    else if (k = = 5)
     fprintf(image,"%s %17.11E\n",doc_char,out_zmin[1]);
    else if (k = = 6)
     fprintf(image,"%s %17.11E\n",doc_char,out_zmax[1]);
    else if (k = = 7)
     fprintf(image,"%s %17.11E\n",doc_char,in_resolx[1]);
    else if (k = = 8)
     fprintf(image,"%s %17.11E\n",doc_char,in_resoly[1]);
    else if (k = = 9)
     fprintf(image,"%s%d\n",doc_char,legend);
    else
     fprintf(image,"%s",buffer1);
    }

   fclose (image);

   return;
}

/*****************************************************************************
   Write_info (write transformation information in a file)
   February 13, 1992
*****************************************************************************/
void write_info ()
```

```
{
int     i,n,np;
double  xa,ya,x,y,X,Y,Z,DX,DY,DZ,fq;

    clrscr ();
    gotoxy(5,8);
    printf ("Writing all information in files ...");

    fprintf(info1,"the UTM coordinates of upper left cell in image\n");
    fprintf(info1,"X  %lf        Y  %lf\n",DEMx[1],DEMy[1]);
    fprintf(info1,"six orientation elements\n");
    fprintf(info1,"%lf  %lf  %lf  %lf  %lf  %lf\n",
              e[0],e[1],e[2],e[3],e[4],e[5]);
    fprintf(info1,"rotation matrix\n");
    fprintf(info1,"%lf  %lf  %lf\n",rm[0],rm[1],rm[2]);
    fprintf(info1,"%lf  %lf  %lf\n",rm[3],rm[4],rm[5]);
    fprintf(info1,"%lf  %lf  %lf\n",rm[6],rm[7],rm[8]);
    fprintf (info1,"the coefficients of affine transformation from c,r to x,y\n");
    fprintf(info1,"%lf  %lf  %lf\n",affine[0][0],affine[0][1],affine[0][2]);
    fprintf(info1,"%lf  %lf  %lf\n",affine[1][0],affine[1][1],affine[1][2]);
    fprintf (info1,"the coefficients of affine transformation from x,y to c,r\n");
    fprintf(info1,"%lf  %lf  %lf\n",affine[2][0],affine[2][1],affine[2][2]);
    fprintf(info1,"%lf  %lf  %lf\n",affine[3][0],affine[3][1],affine[3][2]);

    fclose (info1);
    return;
}
/*****************************************************************************
     another (another image manipulation selection)
     December 12, 1992
*****************************************************************************/
char another ()
{
char  yn;

    clrscr ();
    do
     {
     gotoxy (10,15);
     printf ("Do you want to process another image file (Y/N) ?  ");
     scanf ("%c",&yn);
     if (yn! = 'Y' && yn! = 'y' && yn! = 'n' && yn! = 'N')
      {
      clrscr ();
      gotoxy (10,13);
      printf ("Please enter either Y or N.");
     }}
    while (yn! = 'y' && yn! = 'n' && yn! = 'Y' && yn! = 'N');
    return (yn);
}

/*****************************************************************************/   .fo on
```

Vita

Limei Ran was born December 3, 1963 in Yunnan Province, China. After her graduation from Huaping High School in China in 1979, she studied in the Department of Cartography at Wuhan Technical University of Surveying and Mapping, Wuhan, China, for 4 years and graduated in Engineering in July, 1985.

After the graduation from the B.S. program, she worked in the Division of Cartography at the Research Institute of Surveying and Mapping of China, Beijing, as an assistant engineer for 5 years. During the working years, she was involved in three research and application projects. She was fortunate to work on designing and compiling Mountain Map of China, establishing a digital elevation model using the FORTRAN computer language on a VAX11/785 computer, and designing and codifying a land-use geographic information system using ARC/INFO software on the VMS/VAX computer. Her master's program focused on geographic information systems and remote sensing. She intents to focus on technical aspects of GIS and RS and applications of GIS and RS in physical geography for her Ph.D program.